The Optimisation of Steam Turbine Design

Guy Richard Wakeley

Submitted as a Thesis for the degree of Doctor of Philosophy

Engineering Design Centre

University of Newcastle upon Tyne

September 1997

Table of Contents

Abstract

The world market-place for steam turbine products is becoming increasingly competitive, and manufacturers must routinely produce designs which are extensively optimised whilst working within demanding tender and contract lead-times. The objective of the research work has been to develop a methodology whereby established turbomachinery analysis methods can be integrated within a framework of optimising algorithms. A rule-base, numerical optimisation, fuzzy logic, and genetic algorithms are used to optimise bladepath configurations, with particular emphasis on the minimisation of life-cycle operating costs. Significantly, automation of the design process is increased, design lead-times can be reduced, and performance improvements are predicted. The optimisation procedure relies on a sequential approach, with much emphasis placed on the iterative running of simple design codes.

Simplified design methods are often reliant on correlated loss data to predict turbine performance, and in some cases this data is inaccurate or incomplete. An example of this is in the design of partially-admitted control stages, where little published data is available. It is suggested that CFD methods can, in some cases, be applied to derive new performance correlations or re-assess the validity of existing models. The application of an unsteady CFD solver to typical control stage geometries is presented in detail, and the approach is extended to include the development of a new control stage optimisation method.

Acknowledgment

The research work described in this Thesis has been performed within the Engineering Design Centre of the University of Newcastle upon Tyne, under the sponsorship of Parsons Power Generation Systems Ltd. Many people both within the University and industry have contributed to interesting discussions on a variety of turbomachinery and optimisation issues. In particular the author is indebted to Dr. Ian Potts of the department of Mechanical Materials and Manufacturing Engineering and Dr. Ian Ritchey of Rolls-Royce Industrial Power who have creatively and attentively supervised the progress of the work. Thanks are also due to Professor Bill Hills, Professor Pratyush Sen, Professor John Grant, and Mr. Geoff Horseman for providing strong management support and a forum for lively review meetings. Much has been learned from discussions with engineers at Parsons, in particular Don Borthwick, Neil Burnell, John Grant, Geoff Horseman, and Andy Russell whose input is gratefully acknowledged. Additionally Professor John Denton of the University of Cambridge and Dr. Li He of the University of Durham are thanked for providing access to their CFD codes. Finally Nigel Smith and Raj Subramani of the EDC are thanked for providing guidance on a number of optimisation and programming matters.

Key to symbols

A	area of section
C_o	isentropic jet speed
C_x	axial chord
D	diameter
h_o	specific enthalpy
I_{ww}	second moment of area, weak axis
I_{ss}	second moment of area, strong axis
Re	Reynolds Number
U	blade speed
V	velocity
x	axial coordinate
μ	dynamic viscosity
η	isentropic efficiency
ψ	stage loading
ϕ	flow coefficient
ρ	density

Chapter One

The Thermodynamic Design of Axial Flow Steam Turbines.

Synopsis. The development of the steam turbine over the last century has provided society with a seemingly endless supply of electrical power and become a cornerstone of the modern technological world. In this chapter the inception and subsequent development of the steam turbine are briefly summarised, and the evolution of steam turbine design methods is discussed. Finally the objectives of the current research work are stated.

1.1 A brief history of the steam turbine.

The steam turbine was first suggested some 2000 years ago by Hero of Alexandria (Parsons [1911a]). Hero's turbine (figure1.1) comprised a rotating spherical vessel and two diametrically opposed jets. Water within the central vessel was heated by naked flame, and the subsequent discharge of steam through the jets applied a reactive torque to the body. No means of extracting shaft work from the arrangement was proposed, and the first reports of the use of a steam turbine as a source of mechanical power originate much later in the early 19th century.

FIGURE 1.1. Hero's Steam Reaction Wheel

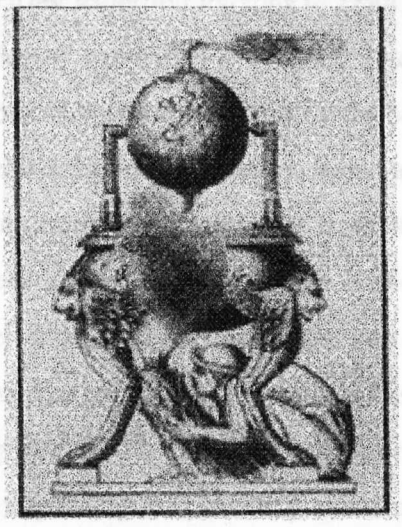

During the industrial revolution there was renewed interest in the application of reaction steam turbines as an alternative to reciprocating engines as sources of mechanical

drive. Around 1840 Avery (working in the USA) devised a reaction turbine to drive circular saws, and at the same time Wilson (working in Scotland) independently implemented a reaction turbine as a mechanical drive in a cotton mill. Both turbines had much in common with the arrangement proposed by Hero and were extremely inefficient in practice, largely because the kinetic energy of the steam jets is rejected to the operating atmosphere. The principle behind Hero's turbine was extended and improved by De Laval, working in Stockholm in 1888 (Parsons [1900], Richardson [1911]). Recognising that the extraction of shaft power through flow reaction alone was impractical De Laval designed and implemented a series of tangentially admitted impulse turbines. In such a device steam was expanded through an orifice to form a jet which struck a row of curved buckets arranged circumferentially around the periphery of a wheel. The steam speed was contemporaneously described as approximately half that of a cannon projectile (around 4000 feet per second) causing rotational speeds of between 10000 and 30000 revolutions per minute (rpm). Such large angular velocities inevitably led to considerable centrifugal stresses in the rotating element which limited the wheel peripheral diameter and shaft power output to relatively modest levels. Notwithstanding the obvious mechanical limitations of these devices, the de Laval turbine was widely used in a variety of industrial drive applications of up to 400 horse-power throughout mainland Europe.

The first practical steam turbine generator for the continuous production of electrical power was patented by Sir Charles Algernon Parsons in 1884 (British Patents 6734 and 6735 [1884]). Through a series of experiments Parsons determined that single stage turbines of the type later proposed by de Laval could only be expected to deliver low levels of power output with relatively poor efficiency. Since all the power is developed by critical expansion in a single stage increasingly large wheel diameters must be employed to obtain large power output, and the design is constrained by the material properties of the turbine wheel. Additionally, both steam and wheel velocities are high which causes considerable loss due to windage effects. In the patents of 1884 Parsons proposed the division of the pressure drop available to the turbine into smaller steps thereby performing the steam expansion successively over a number of stages of axial flow blading. In this construction the steam flow was turned towards the tangential direction by a row of stationary blading, and the tangential component of momentum was converted to shaft work in the following rotating bladerow. The blades were sim-

ply manufactured from flat strip, and arranged to give approximately equal enthalpy drop over both fixed and moving rows. The equal division of enthalpy drop between stator and rotor has become known as 50% reaction blading or pressure-velocity compounded blading (Kearton [1922]). By performing the expansion in small steps the steam velocities could be kept relatively low: Parsons knew that small controlled expansions were conducive to increased efficiency (he also later claimed that he was attracted to the concept since the calculations could be performed in terms of small expansions alone without the use of any integral expressions! (Lord Rayleigh [1933])).

FIGURE 1.2. Parsons' Turbine of 1884.

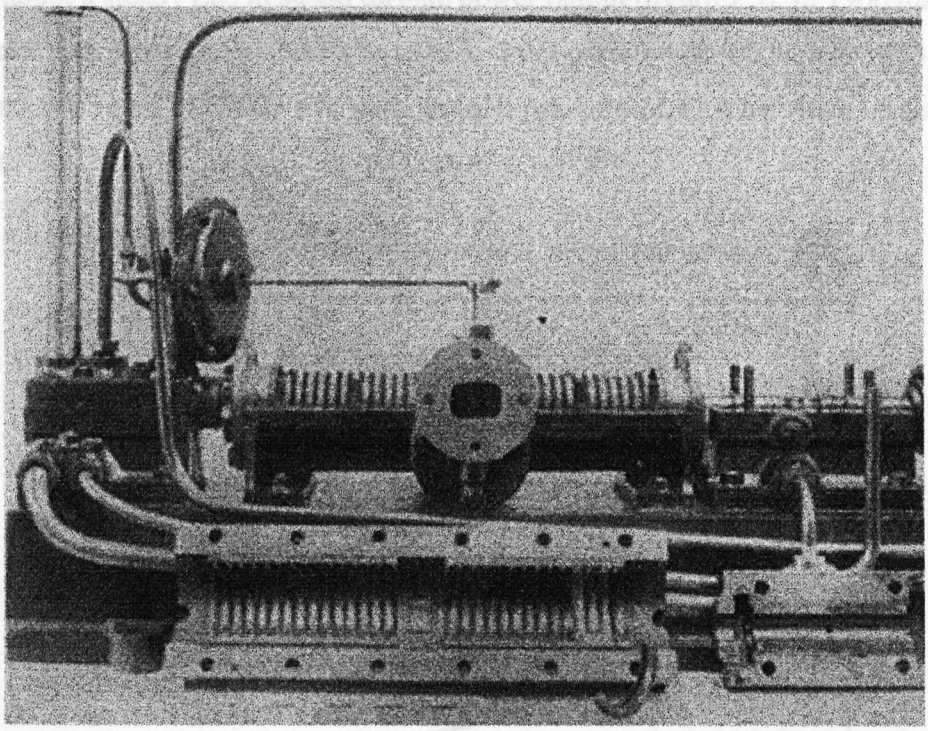

The turbine of 1884,shown in figure 1.2, produced 10 horsepower (7.5 kW) at 18000 revolutions per minute (rpm) directly driving a specially designed high speed dynamo. This pioneering machine shows many of the features of modern steam turbines, including labyrinth packings, forced oil bearing lubrication, flexible bearings to accommodate shaft eccentricity, and a primitive electromagnetic governor. From these early beginnings the steam turbine was to become the prime mover in a multitude of power generation, industrial drive, and marine propulsion applications.

Development work progressed rapidly, with the introduction of serrated and interleaved seals in 1887, and both curved and shrouded reaction blading in 1888. In 1889 Parsons temporarily lost control of the earlier patents and experimented with radial

flow machines. This first of these were radial inflow machines (Jumbo, patent 1120, 1890) and subsequently radial outflow variants (Mongrel, 1891). The radial outflow machines proved reliable in service, and when in 1892 such a unit was designed to exhaust to a condenser the modern steam turbine for power generation was born. A number of 'Mongrel' units rated at 32 kW were supplied to the Metropolitan Police at New Scotland Yard, and were still in satisfactory service some twenty years later (Richardson, op. cit.).

Continued design and development work along with increases in steam conditions brought about a steady rise in steam turbine power output (figure 1.3). In 1900 the largest Parsons' set was rated at 1000kW with an inlet pressure of 9.0 bar; in 1923 cross compound sets rated at 60000 kW with an inlet pressure of 41.4 bar were under construction.

FIGURE 1.3. Increase in turbogenerator output over the last century.

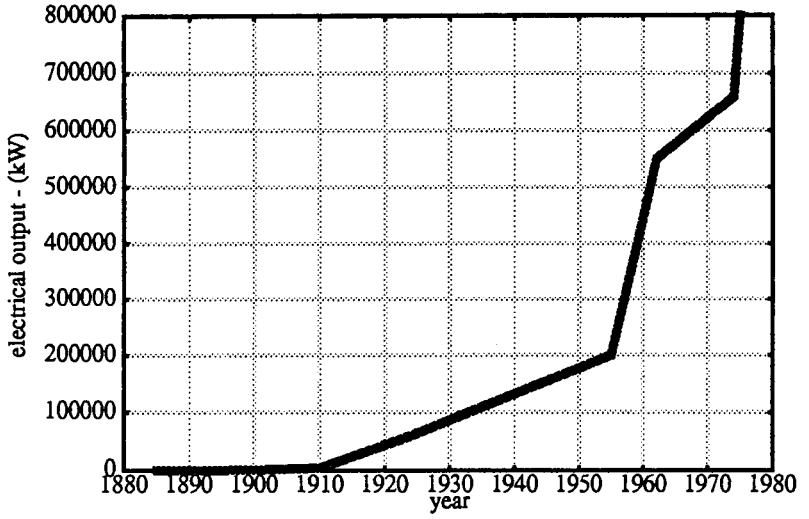

Figure 1.4, overleaf, shows a 50000 kW cross-compounded condensing turbogenerator supplied to the Chicago Edison Company in 1924 (Parsons [1924]) for installation at the Crawford Avenue Power Station. At this time increases in boiler steam temperature above 400 degrees centigrade (750 degrees Fahrenheit) were regarded as impractical for mechanical reasons. It was recognised from the laws of thermodynamics that the efficiency of a heat engine is governed by the temperature difference over which it operates, and from Carnot's principle that increased efficiency could be achieved by maximising the working temperature range. Much theoretical and experimental effort was devoted to the search for methods of increasing cycle efficiency, and two innova-

tions were devised for the Chicago Edison units: regenerative feedheating of the boiler feedwater with steam extracted from the bladepath, and reheating of the HP turbine exhaust steam. Each of these methods increases the cycle efficiency by raising the mean temperature of the steam flow. For a turbine of relatively high efficiency it can be shown that the loss of efficiency due to irreversible processes is almost proportional to the rate of entropy generation through the machine (e.g. discussion given by Denton [1993]). The amount of entropy generated in a fluid dynamic process (e.g. boundary layer growth, heat transfer) is usually inversely proportional to the local fluid temperature so if a fixed proportion of the steam dynamic enthalpy is lost at each stage of the expansion more entropy is generated as temperature falls through the turbine. Raising the cycle mean temperature therefore reduces the net generation of entropy and elevates the cycle efficiency.

FIGURE 1.4. 50000 kW cross-compound turbogenerator for the Chicago Edison Company.

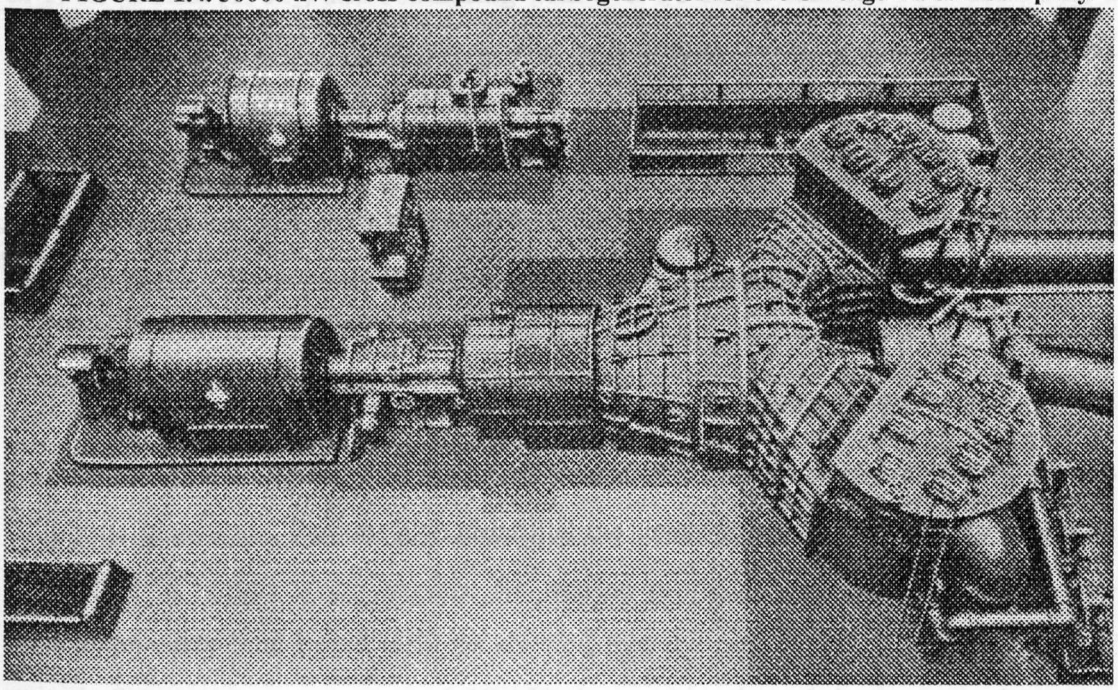

The turbine expansion is performed in three separate turbine sections, denoted high pressure (HP), intermediate pressure (IP), and low pressure (LP), arranged on three separate shafts. The HP turbine in the upper line receives steam at 41.4 bar abs. and drives a 15000 kW 1800 rpm alternator to the left of the figure. The HP exhausts to the reheater at 7 bar abs. in which the steam is superheated to 370 degrees centigrade. The IP turbine is located at the centre of the lower line, and exhausts from left to right through a conical duct into the single flow LP turbine in the ribbed housing in the right of the picture. Steam is received from the LP turbine by two vertical condensers operat-

ing with a back pressure of around 0.025 bar abs. The IP turbine drives a 30000 kW 1800 rpm alternator at the left of the set, and the LP turbine is coupled to a third alternator, rated at 5000 kW 720 rpm located between the condensers.

Such turbine arrangements offered enhanced cycle efficiency, but a greatly increased component cost since the unit comprises three turbine cylinders and three alternators. In the following years accumulated operating experience in conjunction with further technological developments allowed much larger power units to be manufactured. In the 1950s and 1960s metallurgical advances allowed the development of boiler materials and rotor forgings suitable for steam inlet temperatures of 565 degrees centigrade, and units were designed for inlet pressures as high as 160 bar abs. In 1961 a 500 MW cross compound unit was installed in the USA, and a series of nominally 500 MW units were constructed for the UK market, beginning with a 550 MW cross compounded set in 1962 (Dollin [1962]) and continuing with over 50 single line 500 MW units over a period of approximately fifteen years. The largest units currently operating in the UK are rated at nominally 660 MW, and low speed units rated at 1200 MW are now installed in France. This rapid advancement in steam turbine technology is the result of a considerable body of work performed by many manufacturers both individually and in conjunction with generating utilities, government research bodies, and universities (e.g. the Institution of Mechanical Engineers Steam Nozzles Research Committee founded in 1924).

As well as recognising the promise of the steam turbine as the prime mover for electrical power generation, Parsons also identified the steam turbine as particularly attractive alternative to reciprocating engines for marine propulsion applications. Trials performed on early land-based turbines showed that the rate of steam consumption per unit shaft horsepower was around 10-15% lower than that of the best contemporary steam piston engines, with a similar decrease in overall equipment mass. The principal experimental difficulty to be overcome was the design of screw propellers for use at high rotational speeds. Following a period of experimental work to deduce an appropriate hull geometry the first turbine powered vessel, Turbinia, was launched in November 1894. She was 100 feet in length, weighed 44.5 tons, and was originally fitted with two radial outward flow turbines of similar construction to the Mongrel type. Early trials showed a disappointing maximum speed which was attributed to poor propeller effi-

ciency. A series of water tank experiments showed the problem to be cavitation, a phenomenon in which low surface pressure causes the water flow to leave the propeller surface, creating a vapour filled cavity. New propellers were designed, and the original radial flow turbine replaced by three axial flow units following the recovery of the early patents. The completed vessel was tested in April 1897, and it was found that the transmitted power was doubled to around 2300 horse-power by the improvements, producing a maximum cruising speed 34 knots. The initial trials of Turbinia attracted considerable interest from both the Admiralty and many British ship builders. Several comparative studies were performed during the final years of the 19th century to assess the performance of turbine driven craft in relation to that of conventional piston driven steamers over a wide range of commercial and naval applications (e.g. trials of the Eden and Velox, discussed by Parsons [1911b]). It became accepted that turbine driven warships and turbine (or combined turbine reciprocator) driven merchant vessels offered considerable benefits in terms of economy, response, and freedom from vibration. A period of considerable naval spending encouraged the rapid development of marine turbine installations, reaching 42000 horse-power in the H.M. Invincible cruiser in 1908. The financial incentive of faster and cheaper trans-Atlantic passage created considerable commercial investment in steam turbine propulsion, with the 74000 horse-power steamers Mauretania and Lusitania launched only a decade after the Turbinia in 1907. Figure 1.5 shows the increase in marine turbine propulsive power from 1897 to 1907, and figure 1.6, overleaf, shows the relative proportions of Turbinia (44.5 tons) and Mauretania (44000 tons).

FIGURE 1.5. Increase in marine turbine shaft power during first decade of application.

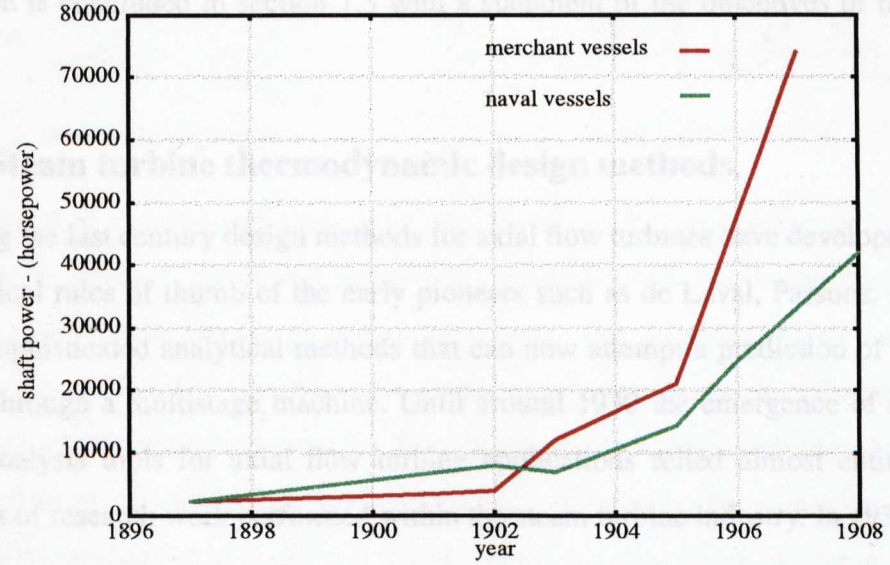

FIGURE 1.6. Turbinia (1897) and Mauretania (1907)

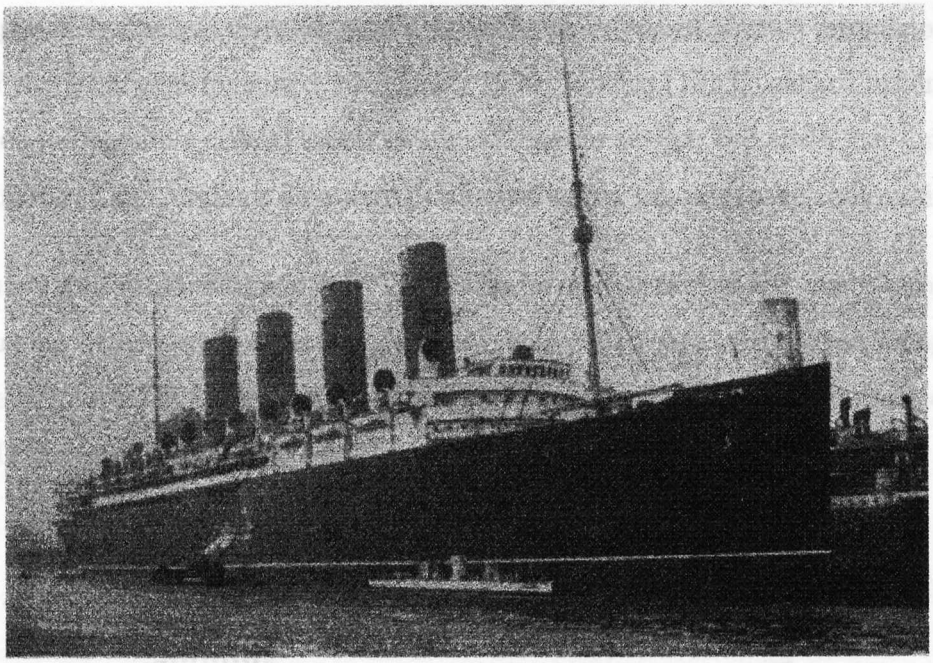

The ever increasing demand for electrical power and marine propulsion exerted a strong pull on steam turbine technology throughout the 20th century. By 1910 the total installed capacity of Parsons' land and marine turbines was around 12 million shaft horse-power (Parsons [1911a]).

Today the steam turbine has developed into a mature technology which can be applied to a considerable variety of both power generation and mechanical drive applications. Section 1.1 describes the evolution of steam turbine thermodynamic design methods, with particular reference to power station applications, and the discussion is extended in section 1.2 to cover the implementation of modular product ranges. Finally, the discussion is concluded in section 1.3 with a statement of the objectives of the research work.

1.2 Steam turbine thermodynamic design methods.

During the last century design methods for axial flow turbines have developed from the empirical rules of thumb of the early pioneers such as de Laval, Parsons, and Rateau into sophisticated analytical methods that can now attempt a prediction of the full 3D flow through a multistage machine. Until around 1930 the emergence of new design and analysis tools for axial flow turbine applications relied almost entirely on the results of research work performed within the steam turbine industry. In 1930 however,

the development of the axial flow turbine was greatly accelerated by Sir Frank Whittle's suggestion that gas turbines could be used as a means of aircraft propulsion. The birth of the jet engine (patented 16 January 1930, Whittle [1953]) caused turbine performance to become a crucial factor in aircraft engine design, and since that time new design features and methods have also originated within the aerospace community.

Very many published methods exist for the aerodynamic design and analysis of axial flow turbine bladepaths. Generally they can be grouped into one of four categories, which are, in order of increasing complexity: dimensional analyses, 1D meanline analyses, 2D meridional methods, and 2D and 3D blade to blade methods.

FIGURE 1.7. Hierarchy of bladepath analysis methods

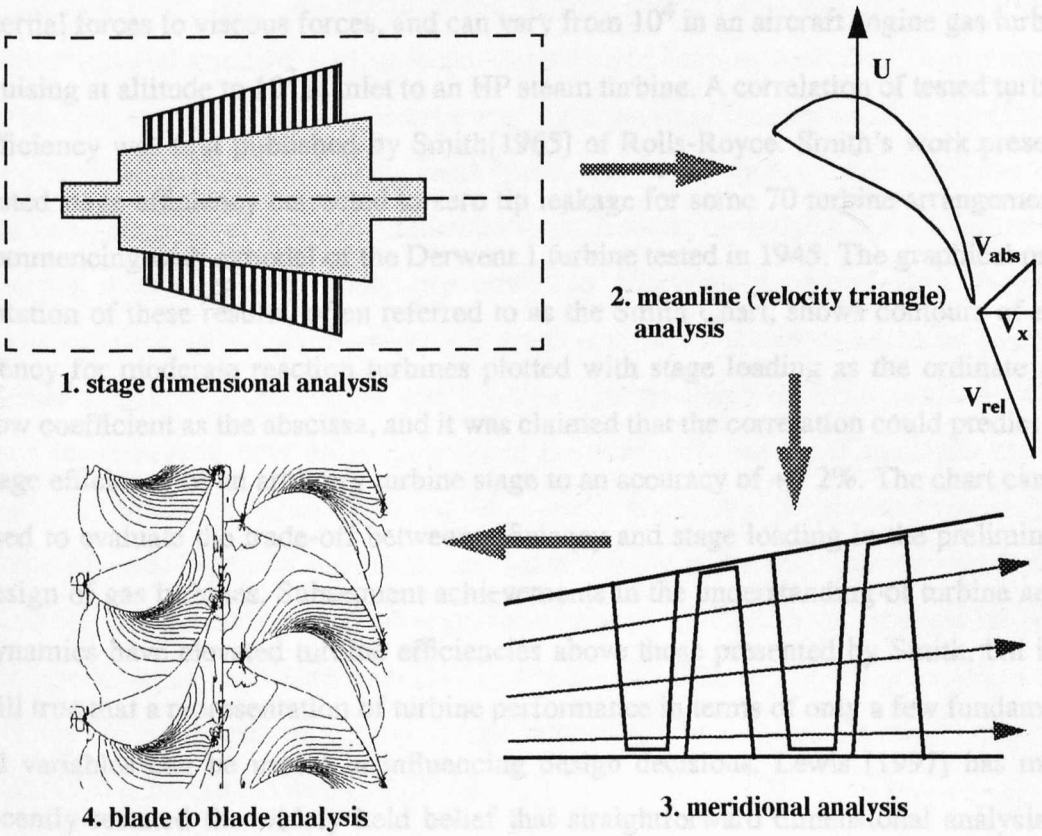

The method of dimensional analysis is used to ensure that reduced scale models and experiments retain dynamic and geometrical similarity with the design intent, and to present experimental results on a consistent basis. The flow through two turbines is dynamically similar if the machines are geometrically similar and have the same velocity triangle throughout the expansion. If these two fundamental conditions are satisfied all non-dimensional groups will be the same for both turbines. For incompressible flow (i.e. negligible changes in density) it is well known that the turbine performance can be

described by three non-dimensional groups, stage loading ψ, flow coefficient ϕ, and Reynold's number (Re) as shown below. Symbols are defined on page 5.

$$\psi = \frac{\Delta h_o}{U} \qquad \phi = \frac{V_m}{U} \qquad Re = \frac{\rho UD}{\mu}$$

For the more general problem of compressible flow Mach number must also be considered. The stage loading coefficient represents the non-dimensional heat drop per stage, and is usually in the range 1.0 to 3.0 for axial flow turbines. The flow coefficient is a non-dimensionalised axial velocity (often regarded as the 'height' of the velocity triangle), usually in the range 0.2 to 0.8. Reynold's number is interpreted as the ratio of fluid inertial forces to viscous forces, and can vary from 10^4 in an aircraft engine gas turbine cruising at altitude to 10^7 at inlet to an HP steam turbine. A correlation of tested turbine efficiency was first published by Smith[1965] of Rolls-Royce. Smith's work presents tested stage efficiency corrected to zero tip leakage for some 70 turbine arrangements, commencing with a model of the Derwent 1 turbine tested in 1945. The graphical presentation of these results, often referred to as the Smith Chart, shows contours of efficiency for moderate reaction turbines plotted with stage loading as the ordinate and flow coefficient as the abscissa, and it was claimed that the correlation could predict the stage efficiency of an arbitrary turbine stage to an accuracy of +/- 2%. The chart can be used to evaluate the trade-off between efficiency and stage loading in the preliminary design of gas turbines. Subsequent achievements in the understanding of turbine aerodynamics have elevated turbine efficiencies above those presented by Smith, but it is still true that a representation of turbine performance in terms of only a few fundamental variables can be useful in influencing design decisions. Lewis [1997] has more recently restated the widely held belief that straightforward dimensional analysis of this type is of pivotal importance in guiding concept design work, and proposes that dimensional analysis can be extended to provide a unified turbine performance analysis framework.

1D meanline (or pitchline) analysis is used to calculate the fluid velocity triangles at the exit from each bladerow. Thermodynamic properties are therefore determined at each stage, either from perfect gas relations if the fluid is air, or from steam tables (e.g. E.R.A., 1967) in the case of a steam turbine. Calculations of this type are usually per-

formed along the mean diameter of the turbine blading; the flow is assumed to be uniform in both the radial and tangential directions. Some authors describe these calculations as 2D (e.g. Horlock [1966]) presumably since tangential components of velocity are computed; the term 1D is regarded as more correct because the net displacement of the flow can be described with an axial coordinate alone.

Meanline analysis is usually the first step undertaken in the design of a steam turbine bladepath. The contract lead-time for new steam turbines is currently between one and two years between receipt of order and commissioning of the equipment, and when designing within a reduced timescale it is often not possible to design new blade profiles for each contract. Instead, most manufacturers have developed parameterised sets of blading (each with associated metal angles, chord sizes, and root and shroud geometries) and standard blading is usually preferred for new contracts. Thus if standard blading at design condition is to be employed the stage loading and flow coefficient are effectively fixed, and the rotational speed, number of stages, stage diameters and blade heights must be selected to match the swallowing capacity of the blading to the specified mass flow and turbine pressure ratio. Blade numbers and steam bending moments are usually determined at this stage, and blade chords can then be sized to achieve satisfactory centrifugal and bending stresses using standard blade profiles. Once blade chords have been determined the bladepath overall dimensions can be fixed, and layout work can begin. At this point in the design process the geometrical details of each bladerow are fixed, and an efficiency calculation can be performed, based on either published performance correlations (e.g. Soderberg, reported by Horlock[1966], Ainley and Mathieson[1951], Kacker and Okapuu [1982]) or experimental data derived from cascade work or model turbine tests (e.g. Denton et. al.[1996], Hart et. al.[1991], Tong and Gregory [1992]).

After the meanline design has been established using appropriate meanline methods the blading can be analysed in the meridional plane. Meridional (or throughflow) calculations are regarded as 2D because the bladepath is described by axial and radial coordinates, and the flow is assumed to exhibit full circumferential symmetry. For a typical fossil fuelled reheat turbine operating with an inlet temperature of 565 degrees centigrade the inlet steam density is approximately 45 kg/m^3. The volumetric flow is small and therefore blade heights are relatively short, with a typical hub to tip ratio of

0.90. For these conditions the meridional flow (i.e. in the axial-radial plane) can be regarded as cylindrical and radial components of velocity are small. Stage pressure ratio gradually increases through the expansion with significant increases in volumetric flow (and therefore blade height) in the IP and LP turbines. Under such conditions the meridional flow can no longer be assumed cylindrical, and spanwise variations of both the primary thermodynamic variables and the stage velocity triangles is inevitable. The discovery of the significance of radial variations of flow properties is commonly attributed to Whittle (Whittle [1953]), but was referred to as early as 1910 by Stodola (reviewed by Pochabradksy [1947]). Furthermore, certain manufacturers had discovered that twisted bladerows could give increased bladepath efficiency. An early example of the use of twisted blading in LP turbines is the 367 mm last stage bladerow fitted to the Parsons 6 MW Bankside units in 1919, reviewed by Smith [1970].

Meridional calculations allow a prediction of the radial distribution of the flow, and can be used to select an appropriate degree of blade twist to achieve a satisfactory vortex distribution. The full meridional streamline curvature equations are non-linear, and are generally solved by computerised numerical methods (e.g. the streamline equilibrium method of Denton [1978], or matrix methods due to Wu[1952], and Marsh [1968]). A number of simplifying assumptions can be made to allow an analytical solution of the equations, although the results are only valid for cylindrical stream surfaces with constant axial velocity; simple radial equilibrium solutions (S.R.E.) are discussed in many engineering textbooks (e.g. Cohen et. al. [1972]). The influence of appropriate vortex design on throughflow performance and stage efficiency is presented in more detail in chapters 4 and 5.

Two further calculation methods (S1-S2 stream-surface calculation, and actuator disc theory) have been applied to the 2D analysis problem. In the former (e.g. Potts [1987]) the flow is computed on several blade-wise (S1) and blade-to-blade (S2) stream surfaces. The latter models the influence of the bladerow as a step change in flow properties over an idealised disc (Horlock [1978]). These methods have found application in the design of axial flow compressors and are not generally prevalent within the turbine design community. Currently the use of fully 3D solvers is preferred.

After the 2D meridional design phase is complete the blade angles are specified at a number of spanwise positions. Appropriate blade shapes must then be chosen and

stacked to create the final aerofoils, either from libraries of standard or parameterised profiles, or designed to suit the application. The selection of suitable blade profiles has a strong influence on the overall efficiency of the machine and detailed investigations are required to determine the blade performance over a range of operating conditions. Several approximate methods for the calculation of 2D cascade flow-fields were proposed in the late 1950s (e.g. Stanitz, Kraft, reviewed by Horlock [1966]) using a variety of conformal transformations to map known potential flow solutions onto generalised aerofoil geometries. The application of such methods was not widespread in the steam turbine industry, where blade profiles were usually developed on a largely experimental basis until the mid 1970s. Around this time increases in computing power permitted research into more general methods for computing 2D and 3D blade to blade flows (e.g. Denton [1975]) resulting in the introduction of a range of time-marching methods for turbomachinery flows. These codes discretise fluid equations of motion onto a calculation grid, and have developed from simple 2D Euler methods to sophisticated multi-row Navier Stokes solvers which can compute the viscous flow through an arbitrary turbomachine with engineering accuracy. Time-marching methods solve the 'direct' or 'initial value' problem, that is boundary conditions are applied to the computational domain (usually from a 2D throughflow calculation) and the flow field is calculated using an iterative relaxation scheme. Further methods have been developed to solve the 'inverse' or 'design' problem, in which the blade mach number distribution is specified and an appropriate profile is calculated (e.g. Hart and Whitehead [1987]). Turbomachinery computational fluid dynamics (C.F.D.) remains an area of intensive research with particular emphasis currently on accurate representations of turbulence and transition to enable more accurate loss predictions, and calculation of unsteady effects such as rotor-stator interaction.

1.3 Modular design.

Orders for the design and manufacture of steam turbine generators are usually won through a process of competitive tendering, during which the purchasing utility imposes many constraints on the turbine design problem. Such constraints might include boiler steam conditions, cooling water temperature, grid frequency, operating cycle, and preferred layout of turbine cylinders and plant items. These constraints vary

around the world, due to electricity demand, fuel price, climatic conditions, and customer preference.

Cycle pressures, temperatures, and flow rates often vary from one contract to the next, and if the blading is to operate at or near to design conditions the bladepath must be sized to suit the application. Steam turbines are not a high-volume product, and in the increasingly competitive world market-place manufacturers must routinely produce designs which are extensively optimised to the local conditions whilst adhering to demanding tender and contract lead-times. The search for strategies for the reduction of design time, and the increase of bladepath performance is now a crucial part of most manufacturers' businesses.

If contract design lead-times are to be significantly reduced it follows that a significant proportion of the work must be performed as up-front development prior to the award of a contract. Turbine development work is often concerned with the design of two classes of standard products: size ranges and modular product ranges. Product standardisation is described in general terms by Pahl and Beitz [1988] and has been shown to confer competitive advantage in a number of industries. Improvements in performance have been identified in the following areas:

- previous design work can be applied to many applications.
- design time per contract can be reduced.
- production methods can be standardised and batch sizes increased with associated increases in product quality.
- delivery times can be reduced.
- generic product configuration can be used (e.g. in Ertas [1996]).

Size ranges involve the rationalisation of certain components into preferred, discretised sizes. Everyday examples of this are the standardisation of thread forms into metric sizes or sheet metal into gauge sizes (Shigley [1989]). In the steam turbine industry LP turbine final stage blades have a relatively long development cycle and cannot realistically be developed during a reduced contract lead-time. Instead a standard range of blades is often used (Mitchell [1979]) and selected for each contract on the basis of reduced exhaust loading and leaving loss.

The process of modularisation divides a complete engineering product into a series of modules or building-blocks which can be assembled into a number of possible configu-

rations. Thus a complete turbine island can be assembled from a modular range of turbines, steam chests, generators, and plant to match the duty of the specification. Additonally each modular element can be further rationalised into sub-modules, for instance the construction of turbines using modular pedestals, shaft ends, glands, and bearings.

The process of modularisation has been adopted by many manufacturers over the last twenty or so years (e.g. Bolter and Grant [1990], Oeynhausen et. al.[1997], Kalderon [1979], Ryzkov [1979]).The approach exerts a strong influence on product cost and creates a coherent, geometrically similar product range throughout which good design features are perpetuated.

However if the bladepath is to be optimised to suit the particular cycle requirements then much of the design work must still be performed during the contract stage and this activity is often a bottle-neck in the production process. It is clear that a reduction in bladepath design time would cause a reduction in time to market, and if additional design optimisation could be performed within a reduced time-scale then the cost-effectiveness of the complete turbine product could be significantly enhanced. These joint aims are the objective of the current research work.

1.4 Objectives of research work.

The primary objective of this project is to optimise the blading design of axial flow steam turbines, motivated by a strong business need for increased turbine performance with reduced product lead time. The programme of research falls naturally into two bodies of work: optimisation, and modelling. Firstly it is acknowledged that the application of formal optimising methods to axial flow turbine design is in relative infancy and there is a potential for significant competitive advantage if this area can be exploited. Secondly, although many turbine aerodynamic design methods now offer a sophisticated and comprehensive approach to the modelling of loss there are still certain aspects which are not well understood or represented only by out-dated design correlations. It is recognised that modern CFD methods can be applied as a useful experimental tool in areas for which our understanding is incomplete.

The objectives of the optimisation work and the CFD analyses are stated in sections 1.4.1 and 1.4.2.

1.4.1 Bladepath optimisation.

Steam turbine bladepaths are usually designed in four phases: steam cycle optimisation, meanline calculation, throughflow calculation, and blade detail design. In general the phases are executed sequentially and there are many design iterations within each design phase and relatively few iterations between them. The steam cycle optimisation determines an ideal duty for each turbine cylinder, meanline design is used to size the blading, throughflow methods determine the vortex, and blade detail design is necessary to finally specify the individual aerofoils.

The sequential design approach is intuitive, since fundamental bladepath design issues (e.g. how many stages?) are resolved using relatively simple methods which describe the design with relatively few variables and have run-times of the order of seconds. Only when these fundamental issues are resolved is attention turned to more detailed representations of the design problem. A bladepath throughflow analysis would typically represent a bladepath with around ten variables per stage with run-times of the order of minutes. Thus, for a fixed amount of design time many more iterations can be performed with simple design tools than with more complex ones.

The current work concerns the optimisation of meanline design and throughflow design, as these are the two activities that must be performed during each tender and contract design phase. In this context the word optimisation is understood to mean the selection of a design solution that offers the best compromise between opposing tendencies. The aim of the work has been to produce computer software that will manage the iterative running of existing design programs and the exchange of data between them with the overall aim of increasing the degree of optimisation of both meanline and throughflow design. Software has been written which will produce entirely viable meanline and throughflow designs in a completely automated fashion, using established and fully validated turbine design methods. The development, implementation and testing of this software is described in chapters 2, 3, 4 and 5, and summarised schematically in figure 1.8 overleaf.

FIGURE 1.8. Hierarchical bladepath optimisation software.

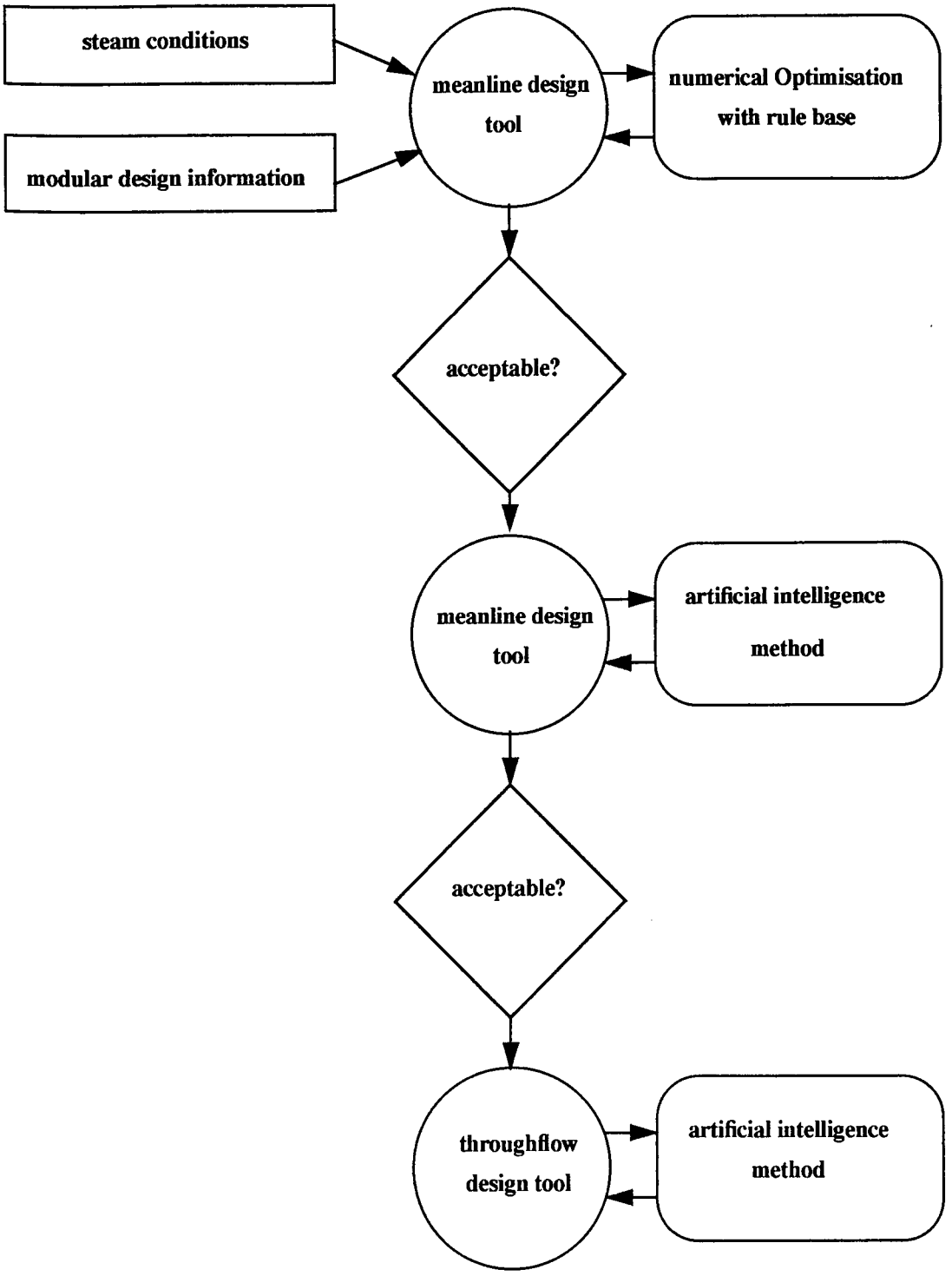

Such a software framework was perceived to offer three distinct benefits, each of increasing significance in terms of value to a steam turbine business:

1. The automation of data exchange between meanline and throughflow methods relieves the engineer of the laborious task of preparing data files and examining and post-processing results by hand. Therefore even if the software was to be proved

incapable of reducing lead-times or producing increased design performance the utilisation of engineering resources would be somewhat reduced releasing engineers for other work, or allowing additional contracts to be progressed in parallel.

2. A systematic evaluation of the design space for a certain configuration can be completed much more rapidly if all the iterative calculations and data exchange are managed by the computer with minimal human intervention. It is later shown that the duration of certain aspects of the design work can be reduced by an order of magnitude.

3. It appeared probable that the hierarchical application of a sequence of formal optimising strategies would allow new areas of the design space to be explored and solutions with improved performance to be identified. This was shown to be the case, and performance gains are demonstrated for almost all cases attempted.

1.4.2 C.F.D. analyses.

Meanline and throughflow analysis methods are based on a relatively simple representation of the bladepath geometry, and design correlations and experimental data are often incorporated to model physical flow features which are not accurately predicted by the calculation. Correlations for profile loss, secondary loss, tip leakage, diffusion effects, and partial admission are often included in such methods. Such correlated data is often incomplete, based on a few specific test cases, or not applicable to a wide range of design conditions. Additionally many correlations originate from experimental work performed during the rapid developments in axial flow turbine technology in the early post-war years, and are often not directly applicable to modern turbines.

If relatively simple design methods are to be evaluated iteratively within an optimisation framework the quality of an optimised solution is very much dependent on the accuracy of the design correlations at that particular operating point. Equally there are certain flow phenomena which are not adequately represented by any design correlations, for instance a number of unsteady effects including partial admission. Naturally these deficiencies are being continually assessed by many manufacturers and research establishments and turbine aerodynamics remains an area of detailed experimental research.

In the context of this research however certain areas of the turbine bladepath were regarded as inadequately represented by published design correlations, in particular unsteady partial admission effects in HP turbine control stages.

In the current work C.F.D. codes have been used as an experimental facility to gain some physical insight into these flow phenomena and derive design rules and correlations for subsequent inclusion into meanline design methods.

1.4.3 Three cautionary notes.

With the advent of increasingly sophisticated analysis methods less emphasis is often placed on more straightforward calculations. It is all too easy for the designer to become deeply involved in the subtleties of complex C.F.D. calculations and temporarily lose sight of the overall design objective. Conversely, highly optimised designs are unlikely to be found by over-reliance on aging design correlations and the custom and practice of previous generations. A well managed design or development project should make a balanced use of established methods and practice whilst openly embracing state-of-the-art technologies as appropriate. The following quotations reinforce the need for a systematic yet open-minded approach to the design of axial flow turbines:

1. Referring to the accuracy of loss correlations, Denton [1992] states that *success sometimes lead to a view that the predictions were based on a sound understanding of the flow physics... this is seldom the case and the success of these methods has lead to an excessive reliance on them and a reluctance to query their basic principles and assumptions.*

2. Baines [1994] stressed the necessity of continual re-evaluation of design methods: *computers do not create new knowledge, they simply rearrange existing knowledge... ultimately new knowledge comes from the direct study of turbomachines in carefully designed experiments.*

3. During the design of the first experimental jet engine in 1937 Sir Frank Whittle [1953] was astonished that the British Thompson-Houston engineers did not appear to make any allowance for the effects of vortex flow in the calculation of blade twist: *It may seem a very strange thing that specialists on turbine design had overlooked a phenomenon which I had more or less taken for granted. I heard somebody once*

define a practical man as one who puts into practice the errors of his forefathers... and how, if habits of thought become deeply rooted, errors may persist from generation to generation.

Throughout this research work every effort has been made to view practical design problems from a scientific perspective, without doctrinaire adherence to the methods of any one manufacturer.

Chapter Two

Meanline Design of Steam Turbine Reaction Bladepaths.
Part 1: An Expert Systems Approach.

Synopsis. A review of published axial flow turbine design methods is presented, including procedures for both performance prediction and design optimisation. The development of a generic software framework is described which uses a rule base and numerical optimisation to produce optimised meanline designs using existing analysis methods. Significantly the influence of component cost and heat-rate are included in the evaluation of the meanline design space.

2.0 Meanline design methods for axial flow turbines.

The first step in the bladepath design process is the determination of an appropriate meanline design. Prior optimisation of the steam cycle specifies the turbine inlet mass flow, pressure, enthalpy, and the outlet pressure. The designer must then determine an optimum combination of stage number and meanline diameter for the expansion. Some workers (e.g. Tong and Gregory [1992]) have suggested that the design of turbines *should* be easy - the fluid is in a natural state of expansion - and at first inspection the meanline design task might appear to be a straightforward problem. All the designer must do is select a meanline diameter and number of stages such that the blading operates close to the design stage loading. In reality of course the problem is more complicated: all non-trivial design problems involve the identification of an appropriate compromise solution between conflicting tendencies. When a power generating utility assesses tenders for steam turbine plant it would be unusual to rank the solutions on the basis of performance alone. Instead it would be more usual to assess the effectiveness of a design on an economic basis (Oplatka [1972]) and compare tenders on the basis of a throughlife cost evaluation. This calculation might include turbine efficiency, purchase price, size of major components, testing tolerance, and maintenance requirements. Naturally the relative importance of, say, efficiency and purchase price will differ from utility to utility. In developed countries with high fuel costs and stringent emission regulations throughlife efficiency is of crucial importance, whereas in developing countries lower purchase and maintenance costs could be dominant. Therefore the selection of the optimal meanline design depends not only on the turbine cycle con-

ditions, but also on the circumstances of the purchasing utility. It is therefore essential that the turbine design process is fully sensitized to these customer requirements if cost-effective, marketable machines are to be produced.

A number of axial flow turbine design methods have been published, and can in general be grouped into one of two categories as follows:

1. Performance prediction methods which solve the direct (analysis) problem. For given meanline stage velocity triangles a number of aerodynamic losses are predicted usually from correlated data. The influence of flow features away from the meanline such as secondary flows and tip leakage at the endwall can also be included.
2. Design methods which attempt to improve the effectiveness or quality of a design by varying blade heights, angles or mean diameters. Such calculations usually optimise on the basis of efficiency alone, but can also include mechanical requirements such as overall length or aerofoil stress.

2.1 Meanline performance prediction methods.

Table 2.1 compares five well-known meanline performance prediction methods, arranged in chronological order. To be valuable in meanline design studies these methods should be able to fulfil the following three basic functions:

1. prediction of the design point performance with engineering accuracy[1].
2. prediction of the performance of a reasonable number of similar designs to demonstrate the sensitivity of the method and to ensure that the chosen configuration is optimum.
3. prediction of the performance of the chosen design over a range of operating conditions to ensure that off-design performance degradation is acceptable.

Correlations of this type are used in the meanline and throughflow calculations of most steam turbine manufacturers, usually with 'in-house' modifications to tune the correlations to match site test data or experimental results. Each correlation is produced from contemporary tests so can only reflect the best design practice of that period. Thus

1. engineering accuracy in this context means that the estimated error in the performance prediction should be less the turbine testing tolerance.

there is a need to regularly re-evaluate such methods in the light of current design practice.

In general the more recent correlations include a greater number of independent variables and are derived from a larger body of test data. For instance the Soderberg correlations are not sensitive to pitch to chord ratio and assume that the blading lift has been fixed to achieve optimum Zwiefel coefficient (Zwiefel [1945]), whereas Dunham and Came [1970] include the effect of lift in the estimation of both profile and secondary losses. Several comparative studies of performance prediction methods exist in the literature (e.g. Horlock [1966], Denton [1973]). The method proposed by Ainley and Mathieson has been directly extended and re-validated by Dunham and Came, and again more recently by Kacker and Okapuu [1982]. A mature method that has been progressively refined over a period of some three decades might be expected to be reasonably accurate, and it is indeed the case that these methods are often sufficiently sensitive to usefully rank candidate solutions at the concept design phase. Meanline correlations however do not give an accurate absolute prediction of turbine efficiency for an arbitrary machine; Kacker and Okapuu, for instance, report an accuracy of +/- 1.50% which could be of considerable economic significance. Recent tenders for fossil fuelled plant have been evaluated at approximately one million pounds per 100 MW output per percentage point of turbine generator heat-rate. For a typical fossil fired unit a one point reduction in HP turbine efficiency would cause a 0.2 point increase in heat rate. If a 500 MW set was considered then a 1.50 point error in the prediction of HP turbine cylinder efficiency would influence the evaluation by 1.50 x 0.20 x 1000000 x 5 = one and a half million pounds which is likely to be a significant proportion of the purchase price.

2.2 Meanline optimisation methods.

Many standard text-books describe the meanline design of an axial flow turbine in some detail (e.g. Horlock [1966], Cohen et. al. [1972], Dixon [1978]). In general an analysis rather than a design problem is attempted, and the selection of an optimum design configuration is left to the judgement of the engineer.

Much less has been published on the subject of turbomachinery design optimisation, probably because viable methods have developed with recent increases in computing

TABLE 2.1 Comparison of published meanline performance prediction methods for axial flow turbines.

authors(s)	organisation	correlated loss component dependencies						reported accuracy
		profile	incidence	secondary	tip leakage	trailing edge	outlet Mach	
Soderberg [1949]	M.I.T.	gas deflection, thickness/ chord	incidence angle, thick-ness/chord	aspect ratio only	not included	not included	not included	+/- 3%
Ainley and Mathieson [1951]	N.G.T.E.	outlet angle, stagger, pitch/ chord, thick-ness / chord	incidence angle, stalling angle, pitch/ chord	lift coeffi-cient, pitch/ chord	lift coeffi-cient, pitch/ chord, clear-ance	trailing edge thickness / pitch	not included	+/- 2%
Dunham and Came [1970]	N.G.T.E.	outlet angle, stagger, pitch/ chord, thick ness / chord	incidence angle, stalling angle, pitch/ chord	lift coeffi-cient, pitch/ chord, aspect ratio	lift coeffi-cient, pitch/ chord, clear-ance, number of seals	trailing edge thickness/pitch	outlet mach number, pro-file loss	+/- 2%
Craig and Cox [1971]	G.E.C.	lift coefficient, contraction ratio, pitch / camberline	incidence angle, stalling angle, pitch/ camberline	aspect ratio, velocity ratio	clearance, number of seals, lap	trailing edge thickness/pitch outlet angle	outlet mach number, pitch / camberline	+/- 1.25%
Kacker and Okapuu[1982]	Pratt & Whitney	outlet angle, stagger, pitch/ chord, thick ness / chord	incidence angle, stalling angle, pitch/ chord	lift coefficient, pitch/ chord, aspect ratio	lift coefficient, pitch/ chord, clear-ance, number of seals	trailing edge thickness/ pitch, stagger	inlet mach number, out-let mach number	+/- 1.50%

power, and also since methods developed within the industry are much less likely to be reported. Table 2.2 reviews the major published work.

Balje and Binsley [1968] constructed simplified profile loss correlations based upon an estimation of boundary layer thickness for cascades with optimum Zwiefel coefficient. This correlation was shown to agree reasonably well with other published correlations (e.g. Ainley-Mathieson) and was integrated within a meanline velocity triangle calculation. A numerical optimisation procedure was employed which varied non-dimensional groups constructed from the turbine stage geometric parameters with the objective of maximising efficiency. Constraints could be applied to restrict the search space. Improvements in stage efficiency of between 5% and 15% are reported, but is not possible to judge the significance of these improvements as the datum point is not described. Additionally, some problems associated with the generation of non-feasible designs is reported.

Rao and Gupta [1980] acknowledged that a maximisation of stage efficiency alone would be unlikely to produce an optimum design, and for any practical machine some mechanical considerations should be considered. Rao's work extends Balje's analysis to perform a multiobjective optimisation which attempts to maximise stage efficiency and reduce stage mass, which is more representative of the objectives of an aircraft engine gas turbine stage design. The objective function is posed as a fixed weighted combination of efficiency and mass, and is also used to determine the sensitivity of the design point to small changes in stage geometrical parameters. An increase of stage efficiency of 2.48% is reported, with an associated reduction in stage mass of around 80%, most of which is from a reduction in stage diameter. In this case the design became constrained by large blade bending stresses with increased blade height. It was reported that the final trade-off between mass and efficiency is controlled by the choice of weighting factors in the objective function. This of course is an inherent weakness of a penalty function approach and is discussed in more detail in chapter 5.

Macchi and Perdichizzi [1981] investigated the thermodynamic performance of gas turbine cycles using non-conventional fluids. Their 'black-box' representation of the turbine required a simple means of estimating turbine efficiency without performing a stage-by-stage meanline analysis. This was achieved by correlating turbine efficiency with volumetric flow ratio, specific speed, and a geometrical parameter, using the cor-

relations of Craig and Cox. The aim of this work was primarily to develop a simple turbine performance model for use within cycle optimisation work, and the simplicity of the model appears to preclude its use as a meanline design method.

Massardo and Satta [1990a] integrated established turbine meanline design methods within a numerical minimisation procedure. The design codes used a discrete range of master blade profiles developed by the sponsoring manufacturers (Fincantieri and Ansaldo) and the numerical optimisation procedure used penalty functions to apply constraints such as blade aerofoil bending stress. This method appears much more closely aligned to the needs of a steam turbine manufacturer for whom the usual design problem would involve selecting an optimum meanline design using an established in-house code and a preferred range of blade profiles. The method was applied to a ten stage 80MW HP turbine, for which an increase in turbine efficiency of around 1.7% is reported. In this case the volumetric flow was small and the performance was dominated by secondary losses and tip leakage effects. Gains appear to be realised from adjusting the stage angles to increase blade heights (and therefore aspect ratio) and reducing tip reaction which dominates the rotor blade over-tip leakage flow.

The steam turbine work has been extended by Massardo and Satta [1990b] to create a axial flow compressor meanline optimisation method. A multivariable numerical minimisation scheme is reported, with the objective of maximising efficiency and stall margin whilst reducing overall compressor mass. It is shown that the final value of each parameter can be improved from the datum point: efficiency is increased from 87.5% to 89.1%, mass is reduced by 9.1% (expressed as a reduction in inlet area) and stall margin is improved from 0.535 to 0.577 (as defined by Koch [1981]). The realisation of such benefits however was found to be dependent on an appropriate choice of weighting coefficients in the objective function. These coefficients are strongly problem specific, and some further iteration was required to reach a true optimum.

The most extensive turbine meanline optimisation procedure reported is the *Engenious* system developed by General Electric (Tong and Gregory [1992]). This system is a general purpose software package into which an arbitrary design or analysis method can be integrated. Three optimisation techniques are employed to search the design space. Firstly, a expert system is used to exploit simple trade-offs using known design rules. When the expert system is unable to find further improvements a numerical opti-

misation procedure is used to investigate the local design space in the vicinity of the expert system end-point. Further gains are reported from the application of a genetic algorithm - an artificial intelligence technique which represents design parameters as chromosomes and applies a series of operators analogous to genetic reproduction to produce a population of candidate designs. The fitness of each member of the daughter generation is then judged using the objective function, and it is this selection pressure that ensures the survival of fit designs. Tong and Gregory report the improvement of a aircraft engine gas turbine design, with the objective of increasing the efficiency by 0.50% through adjustment of the annulus boundaries. The *Engenious* software was configured to run a General Electric meanline analysis code (TDOD) and yielded a 0.92% improvement in efficiency with one week of run time, which compared favourably with an improvement of 0.50% in ten weeks achieved by an experienced design engineer.

The methods of Massardo and Satta, and Tong and Gregory are of most relevance to the current research as they have both been formulated for direct application to practical design problems using existing industrial methods. Massardo demonstrated a viable numerical optimisation procedure which utilised an established design code and preferred libraries of blade profiles. Tong described a more generic approach, and has developed software which will 'wrap around' an existing design method. The combined use of a rule-base and numerical optimisation is intuitive and likely to converge upon optimum or near optimum solutions more rapidly than numerical methods alone, since the early search is guided by design knowledge. Both methods can include geometric constraints such that, for instance, the diameter of the bladepath can be restricted. Equally mechanical limitations could be imposed to constrain bladepath mass or aerofoil stress.

An aspect of meanline design not considered in any of the published work is the overriding significance of bladepath cost. Engineers might feel disposed to evaluate solutions in terms of component mass or aerodynamic performance, but a consequence of trading in a competitive market place is that purchasers will inevitably rank tenders on the basis of cost. This assessment is usually performed as a calculation of throughlife operating cost for the plant, or extended to include the time value of the plant revenue and assets over a fixed operating period.

In the design of steam turbines for power generation the optimum design (at least in terms of marketability) must be determined on the basis of cost-effectiveness. This overall cost includes many components most significant amongst which are throughlife operating cost and purchase price. It is intuitive, therefore, to include a calculation of these factors within the design evaluation to sensitize the design process to the market forces, and the absence of this feature is perceived as a weakness of the published methods.

TABLE 2.2 Comparison of published turbomachinery meanline optimisation methods.

author(s)	organisation	description of code				objective function		
		machine configuration	analysis method	loss prediction method	optimisation method	efficiency	mechanical constraints	cost effectiveness
Balje and Binsley [1968]	Rocketdyne	multistage gas turbine	velocity triangles	approximate analytical method using boundary layer thickness	numerical	maximise	not included	not included
Rao and Gupta [1980]	Indian Institute of Technology	single stage gas turbine	velocity triangles	Ainley-Mathieson, Dunham and Came	numerical (multivariable)	maximise	reduce weight	not included
Macchi and Perdichizzi [1981]	Milan Polytechnic	'black box' gas turbine with turbine cycle	velocity triangles	Craig and Cox	numerical	maximise	not included	not included
Massardo and Satta [1990a]	University of Genoa	multistage gas or steam turbine	proprietary meanline code from *Ansaldo*	in-house results from standard profiles	numerical (multivariable)	maximise (design and off-design cases)	bending stress	not included
Massardo and Satta [1990b]	University of Genoa	multistage compressor	not reported	various compressor correlations	numerical (multivariable)	maximise (design and off-design cases)	reduce weight	not included
Tong and Gregory [1992]	General Electric	multistage gas or steam turbine	proprietary meanline code TDOD	in-house results (assumed)	numerical, expert system, heuristic	maximise	length, diameter, + others	not included

2.3 Development of meanline optimisation software.

In this section the development of a meanline optimisation method is described. The method is based around the meanline design and analysis code *Sigma* used within Parsons (Dollin and Brown [1937]). This method contains a library of preferred blade profiles for application in HP and IP turbines and is based around a discrete range of chord sizes and blade outlet angles. A comprehensive meanline performance prediction correlation is included based upon cascade and model turbine testing of representative production blading over a wide range of stage loading, aspect ratio, and tip seal geometries. In addition the method contains details of standard root and shroud geometries, such that bladepath length can be assessed, and calculations of aerofoil stresses performed.

2.3.1 Statement of design problem.

It is standard practice in the steam turbine industry to assemble the turbine island from a standard range of modular components that have been devised to span a wide range of possible operating conditions. Since steam conditions vary from contract to contract it is necessary to optimise the bladepath to suit each application. Thus during the meanline design phase the engineer must select the number of stages of blading and meanline diameters using, where possible, preferred blade profiles with a discrete range of outlet angles and chord sizes. The objective is to maximise the cost evaluation of the turbine bladepath within the geometric constraints imposed by the modular product range. In particular, each modular turbine cylinder design has an associated maximum and minimum bladepath diameter and rotor length to suit available patterns and castings. Additionally rotors of small diameter are often constrained by rotor-dynamic considerations, since as hub diameter is reduced flexibility increases with an associated fall in flexural critical speed and an increase in shaft deflection and susceptibility to steam whirl. Furthermore, large bladepath diameter can become constrained by horizontal joint bolting or flange design, for as diameters rise (at the same overall turbine pressure ratio) casing hoop stress and bolt stress increase.

After careful consideration of current turbine design practice and a review of other published design and optimisation methods a preliminary software specification was compiled:

1. Established design codes should be used such that the calculation can determine turbine efficiency consistently and with known accuracy. Accumulated experience with the existing code is therefore carried forward into the new method without the need for further validation.
2. The optimisation procedure must be capable of ranking designs using a realistic financial evaluation.
3. The software should have a generic structure to allow the integration of alternative design tools as they become available.
4. Aerofoil bending and centrifugal loadings should be considered to ensure that bladepath mechanical integrity is maintained.
5. The sensitivity of the design space to variations in the dependent variables should be assessed to ensure the robustness of the method.
6. The method should be automated such that no hand-editing of datafiles is required.
7. Run-time should be short in comparison with the manual design time.
8. The software should be compatible with the standard 50% reaction blading manufactured by the sponsoring Company, yet the approach should be sufficiently generic to allow other types of blading to be considered as required.

2.4 Description of the meanline search tool.

A meanline search tool was developed in accordance with the program specification. The software architecture is shown schematically in figure 2.1.

The software was written using the ANSI-*C* programming language for use on UNIX workstations, and comprised five separate elements, the functions of which are described below:

1. The **search manager** is the software frontend. The user is prompted for the turbine steam conditions and evaluation coefficients, and selects either an HP or IP turbine cylinder type. The search manager initiates the search through the design space, post-processes the results to show the topology of the evaluation surface, and manages the interfaces with other design programs.

FIGURE 2.1.Structure of meanline search software.

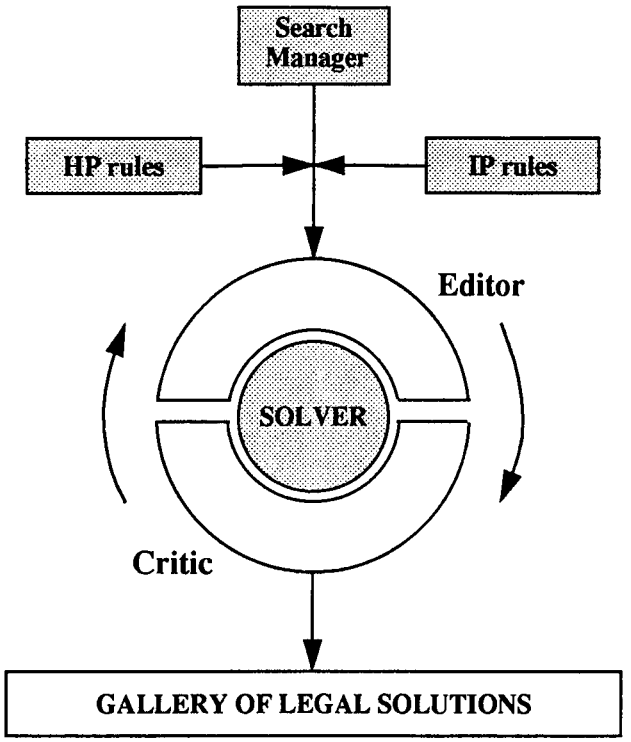

2. The **rule base** contains elementary rules used to create a first guess from which the search can proceed. The design of a turbine bladepath is a complicated problem and it is not practical to describe it fully with a set of design rules that are applicable to all cases. Instead designers rely on their accumulated knowledge and experience to make decisions. Therefore only a small number of simple rules have been included, of the form 'if stage loading is low add more stages' or 'if length exceeds constraint reduce blade chords or stage number'. These rules have sufficient generality to profitably guide the early progress of the search without becoming restrictive later on, and are therefore a useful aid to convergence.

3. The **editor** function prepares data for the design solver. Turbine bladepaths are made up of stages, diameters, blade angles, blade heights etc. and the editor assembles combinations of these data in a form readable by the design program.

4. The **critic** function inspects the design program output and uses a gradient based method to increase performance by adjusting stage number, blade heights, and smoothing the annulus boundary. Additionally the critic can identify unacceptable features of the candidate design and suggest to the editor how they might be cor-

rected. For instance, blade aerofoil stresses, root serration stresses, and bladepath dimensions are checked, and the approach could be extended to include vibration characteristics, etc.

5. When the editor and critic have iteratively produced a viable candidate design, which exhibits near optimum performance without violating any constraints or design rules, the solution is stored in a **gallery of legal designs**. The software then varies the bladepath inlet or outlet diameter and explores another region of the design space. By storing a range of legal solutions the software allows the designer to review trends within the design space, and instead of obtaining only one solution he or she is free to inspect a gallery of possible solutions, each of which is broadly representative of best design practice. In this way transparency is added to the optimisation process: trade-offs between conflicting factors can be identified and the designer himself can select his/her preferred solution. This transparency, along with the opportunity for human intervention, is necessary if users are to have confidence in the robustness of the method.

After the search is complete the gallery of legal solutions is displayed in tabular form, and various plots are displayed using the public domain plotting utility *GNUPLOT*. The search manager will also generate data for a mechanical calculation which includes a prediction of shaft length, shaft mass, critical speeds, and shaft deflection, using standard journals, couplings, and glands from the modular range. It was intended to integrate the critical speed calculation within the main search; however the finite element method used had a run-time longer than the meanline design solver so this was not practical. Instead the software has been configured such that solutions can be picked from the gallery and the mechanical calculations performed at the end of the run.

Figure 2.2, overleaf, shows a screen snapshot of the software running on a Silicon Graphics workstation.

FIGURE 2.2. Screen-dump of meanline optimisation calculation.

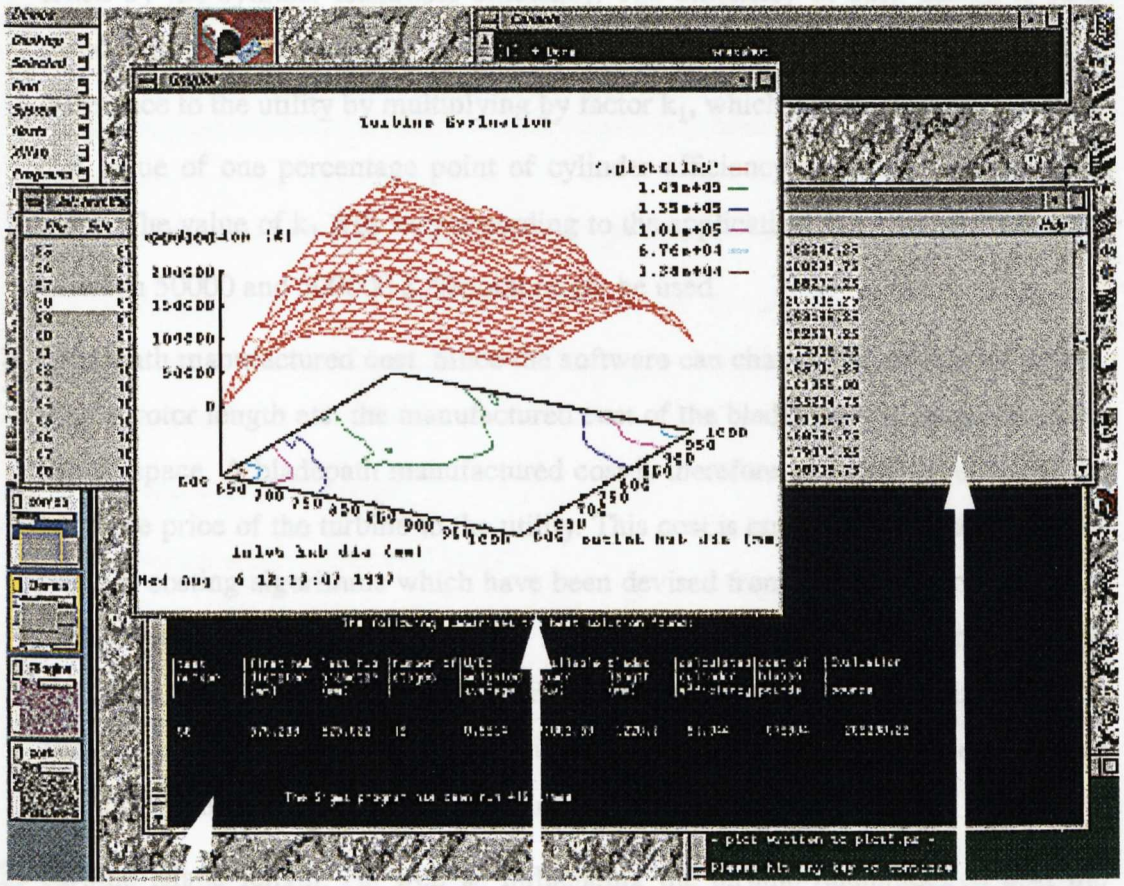

2.5 Calculation of design evaluation.

Candidate meanline designs are compared using a cost-effectiveness evaluation based on the requirements of the utility's tender specification. For each candidate design, an evaluation is calculated relative to the first design considered, according to the following formula:

$$evaluation_i = k_1 \cdot (\eta_0 - \eta_i) - k_2 \cdot (Cost_0 - Cost_i) - k_3 \cdot (length_0 - length_i)$$

The evaluation is based on the assumption that the turbine lifetime cost to the utility can be calculated as a linear function of three cost components. These are:

1. Throughlife operating cost. For a fixed steam cycle the turbine operating cost is governed by the cylinder isentropic efficiency. The efficiency of each design is compared with that of a datum design, and the difference is converted into a cost difference to the utility by multiplying by factor k_1, which is a measure of the financial value of one percentage point of cylinder efficiency over the lifetime of the plant. The value of k_1 will vary according to the application, but typically values of between 50000 and 500000 £ /%point might be used.

2. Bladepath manufactured cost. Since the software can change the number of blades, stages, rotor length etc. the manufactured cost of the bladepath will vary across the design space. A bladepath manufactured cost is therefore included to represent the purchase price of the turbine to the utility. This cost is computed from a set of proprietary costing algorithms which have been devised from a review of many recent turbine projects. They include rotor length, blade height, blade number, stage number, and allowances for both material costs and the amount of machining work. The cost is expressed as a financial value, to which a coefficient could be applied to account for the effects of inflation or subcontracted manufacture.

3. Turbine island length. As well as influencing the turbine manufactured cost the bladepath length also effects the project civil engineering costs. In general a longer turbine generator set will require larger supporting foundations, with a possible increase in structural steelwork and turbine hall dimensions. The length of each design is compared with that of the datum, and a factor is applied to convert the length difference into relative cost to the utility. Such costs are often difficult to quantify, but values of around 25 £ / mm are typical.

It is acknowledged that this costing basis is greatly simplified. For instance, throughlife cost is assumed to be a factor of efficiency alone, and no interdependencies are assumed between the three cost terms. For the purpose of preliminary design studies this approach is perceived as adequate, since in general all bladepaths of a certain modular type will have effectively identical maintenance requirements and availability, and would be constructed from standardised components for which the manufactured cost is known with some certainty.

An obvious criticism of this approach is that the identification of a near optimum design relies on the choice of coefficients in the evaluation expression. This degree of

approximation is regarded as inevitable in preliminary design studies. A significant advantage of this approach is that the coefficients can be varied: thus the sensitivity of the optimum design to the costing algorithm can be readily explored. A more detailed costing analysis based on the time value of money is presented in section 2.7.

2.6 Application of meanline design tool to HP turbine design.

The following sections describe the application of the meanline design tool to a typical HP turbine bladepath. Each of calculations presented applies to a 250 MW HP steam turbine operating on a standard fossil-fired reheat cycle.Three cases were considered:

1. Unconstrained optimisation.
2. Optimisation with constrained length.
3. Sensitivity of the optimum design point to efficiency evaluation.

In each case efficiency was evaluated at £150000 /%point, and the overall bladepath length at £25/mm.

2.6.1 Unconstrained optimisation.

In this case the software was free to explore a wide range of possible turbine diameters, and at each chosen set of diameters selected an appropriate number of stages, and sized the blade heights and chords. A gallery of 152 legal solutions was produced with 419 evaluations of the design solver; the run-time was approximately 20 minutes.

FIGURE 2.3. Contours of relative turbine efficiency

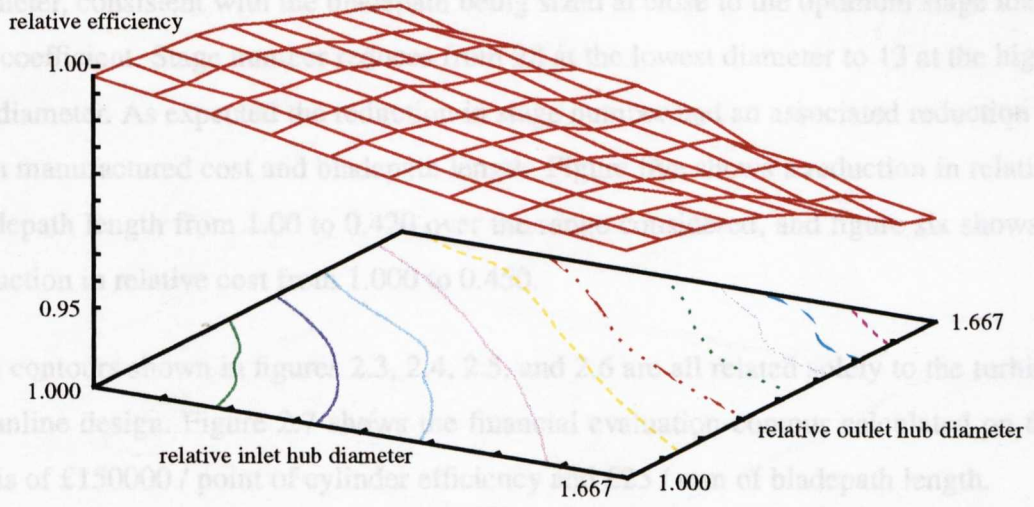

Figure 2.3 shows contours of calculated cylinder efficiency, with each point on the surface representing an optimised candidate design from the gallery of legal solutions. In this case the inlet volumetric flow was relatively low and the efficiency surface was dominated by the trade-off between diameter and aspect ratio. At low rotor diameter blade heights were increased and the improved aspect ratio reduced secondary and tip leakage losses. For this application the predicted profile, secondary, and tip leakage losses were of roughly equal magnitude in the early stages of the expansion.

FIGURE 2.4. Contours of stage number.

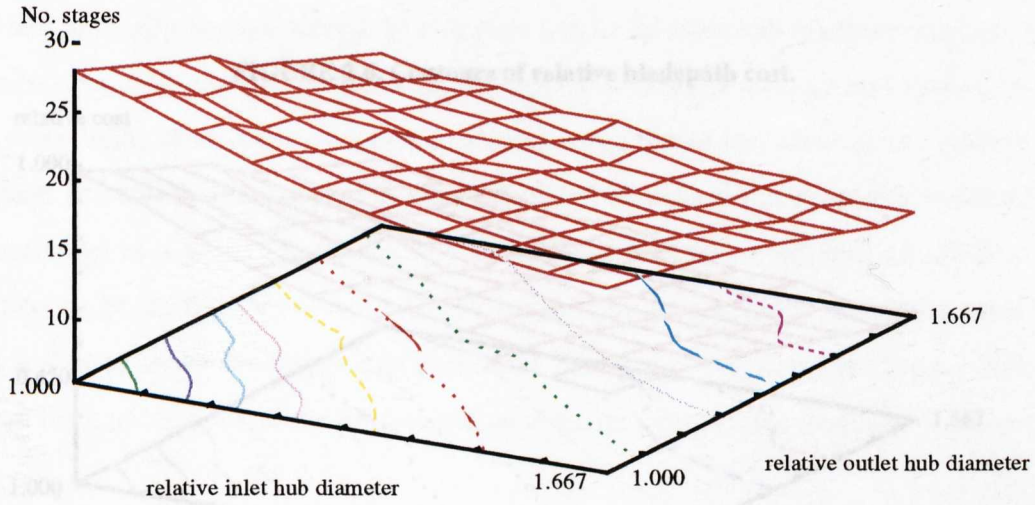

Figure 2.4 shows the expected trend of decreasing stage number with increasing hub diameter, consistent with the bladepath being sized at close to the optimum stage loading coefficient. Stage number reduces from 28 at the lowest diameter to 13 at the highest diameter. As expected the reduction in stage number had an associated reduction in both manufactured cost and bladepath length. Figure five shows a reduction in relative bladepath length from 1.00 to 0.420 over the range considered, and figure six shows a reduction in relative cost from 1.000 to 0.450.

The contours shown in figures 2.3, 2.4, 2.5, and 2.6 are all related solely to the turbine meanline design. Figure 2.7 shows the financial evaluation contour calculated on the basis of £150000 / point of cylinder efficiency and £25 / mm of bladepath length.

FIGURE 2.5. Contours of relative bladepath length.

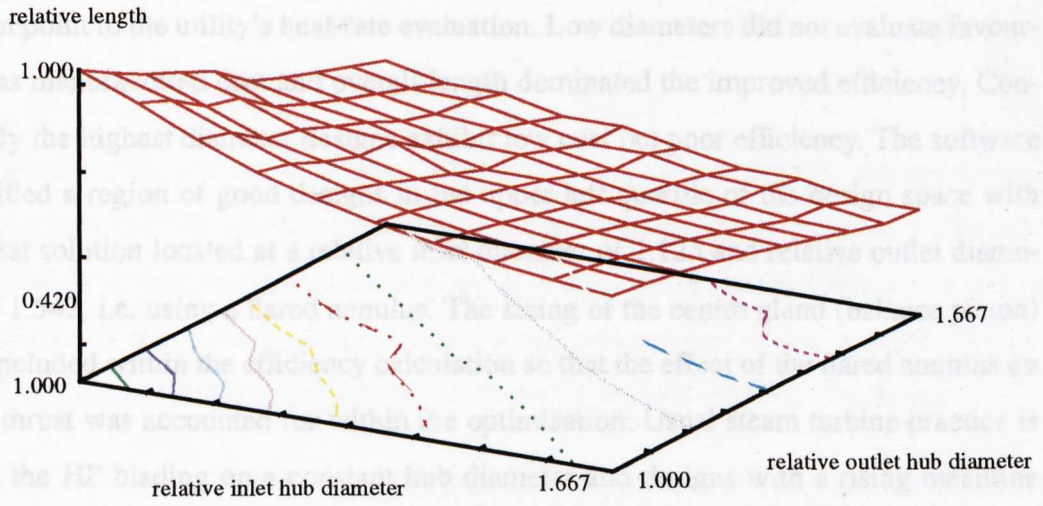

FIGURE 2.6. Contours of relative bladepath cost.

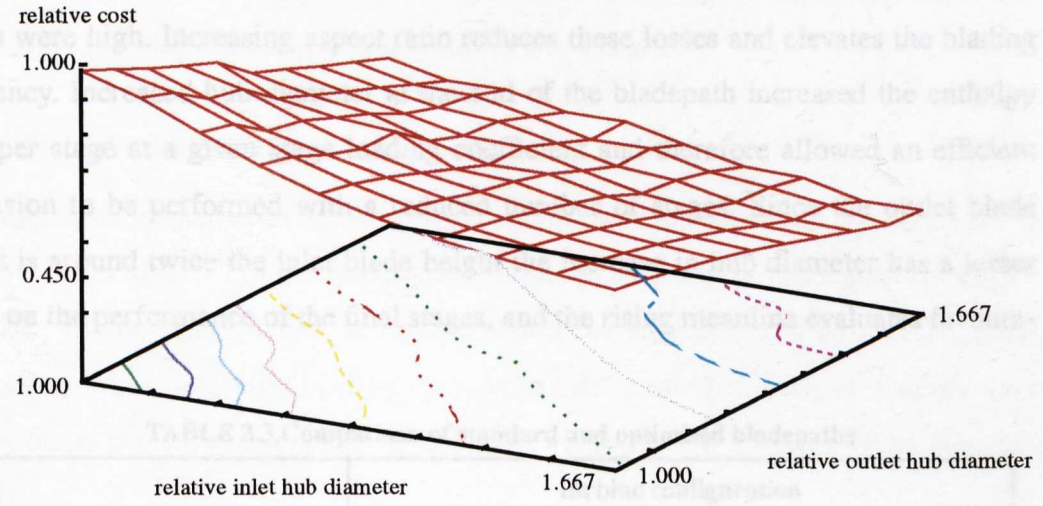

FIGURE 2.7. Contours of relative bladepath economic evaluation.

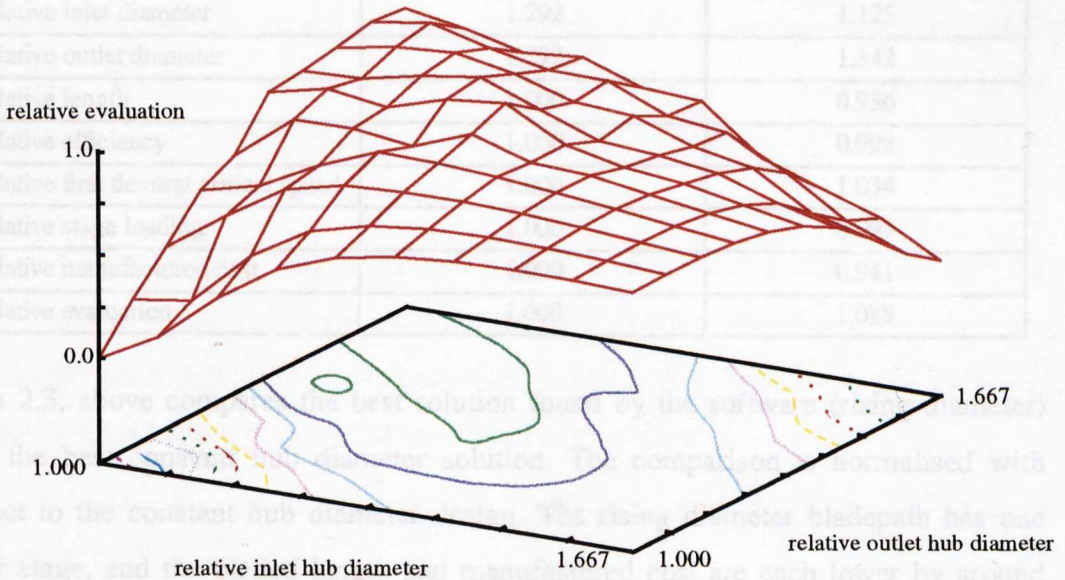

The financial evaluation surface in figure 2.7 shows the sensitivity of the meanline design point to the utility's heat-rate evaluation. Low diameters did not evaluate favourably as manufactured cost and overall length dominated the improved efficiency. Conversely the highest diameter designs exhibit low cost but poor efficiency. The software identified a region of good designs in the upper left quartile of the design space with the best solution located at a relative inlet diameter of 1.125 and relative outlet diameter of 1.542, i.e. using a flared annulus. The sizing of the centre gland (balance piston) was included within the efficiency calculation so that the effect of the flared annulus on rotor thrust was accounted for within the optimisation. Usual steam turbine practice is to set the HP blading on a constant hub diameter and designs with a rising meanline would not normally be considered. In this case a reduced inlet hub diameter increased the blade heights in the early part of the expansion where tip leakage and secondary losses were high. Increasing aspect ratio reduces these losses and elevates the blading efficiency. Increased hub diameter at the end of the bladepath increased the enthalpy drop per stage at a given stage loading coefficient and therefore allowed an efficient expansion to be performed with a reduced number of stages. Since the outlet blade height is around twice the inlet blade height the increase in hub diameter has a lesser affect on the performance of the final stages, and the rising meanline evaluates favourably.

TABLE 2.3.Comparison of standard and optimised bladepaths

	turbine configuration	
	constant diameter	**rising diameter**
number of stages	19	18
relative inlet diameter	1.292	1.125
relative outlet diameter	1.292	1.542
relative length	1.000	0.936
relative efficiency	1.000	0.998
relative first flexural critical speed	1.000	1.034
relative stage loading	1.000	0.999
relative manufactured cost	1.000	0.941
relative evaluation	1.000	1.088

Table 2.3, above compares the best solution found by the software (rising diameter) with the best constant hub diameter solution. The comparison is normalised with respect to the constant hub diameter design. The rising diameter bladepath has one fewer stage, and the bladed length and manufactured cost are each lower by around

6%. The efficiency is very slightly reduced, yet the net effect is an increase in overall turbine financial evaluation of 8.8% which is likely to be significant in the tender evaluation process.

The quality of the constant diameter design is representative of the best bladepaths produced manually. This was to be expected since the optimisation is driven by a rule base compiled from accepted design knowledge. However, a fuller exploration of this design knowledge by the software using numerical optimisation has yielded a number of rising diameter bladepaths which would not normally be considered by the designer.

It is also noteworthy that the designs which evaluate most favourably are situated on a relatively smooth surface. The method is therefore likely to be robust as the optimum design is not located in an area of severe gradients; all neighbouring designs in the gallery of legal solutions exhibit near optimum performance.

2.6.2 Optimisation with constrained length.

The optimisation attempted in the previous section was repeated with the addition of a length constraint. It is often necessary to restrict the length of the bladepath during the meanline design phase, either to remain within the envelope of a particular turbine module, or when designing blading for retrofit into existing equipment. Design work for retrofit is often more constrained than for new plant, and is discussed by Wakeley [1997].

In this example an absolute length constraint was imposed: it was mandatory that the length of each legal design was less than that of the constant section design considered in section 2.6.1. If a bladepath is too long there are only two ways of reducing the length: either using fewer stages, or reducing the axial width of the stages. The following rules were coded to guide the search:

1. If the bladepath is too long an attempt is made to reduce blade axial width. This can be achieved by increasing the blade outlet angles, thereby lowering blade height and reducing centrifugal and bending stresses. Thus it may be possible to use a blade of smaller chord size within the same reference stress level
2. If it is impossible to reduce length sufficiently by reducing blade chords, stages of blading must be removed.

FIGURE 2.8. Contours of relative bladepath efficiency.

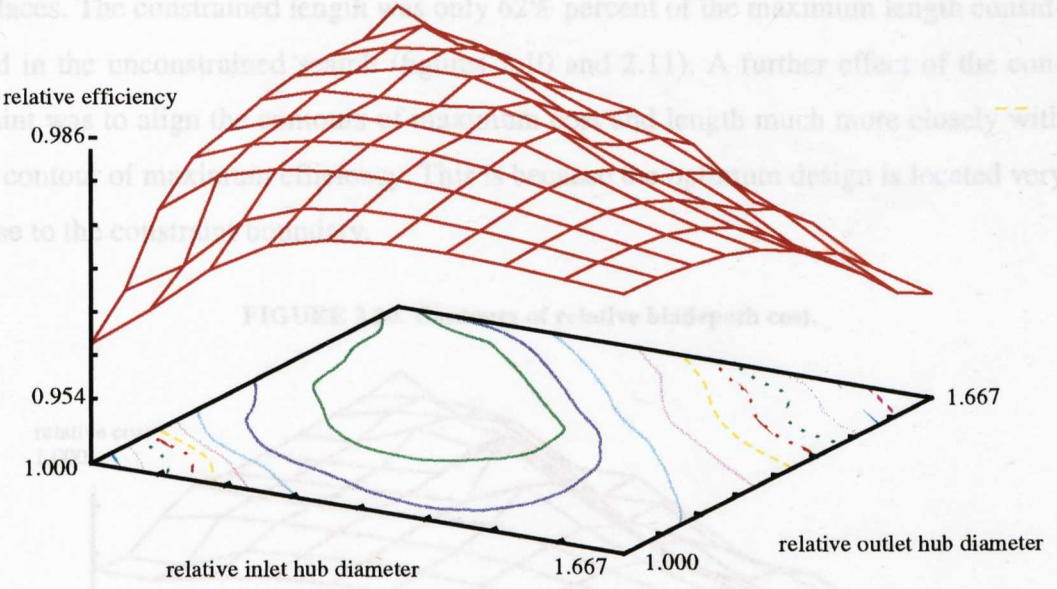

Figure 2.8 shows the contours of predicted turbine efficiency with the length constraint applied. The constraint caused the surface to be much more convex with the area of maximum efficiency located close to the unconstrained optimum design point. This is because the low diameter bladepaths are restricted to a reduced stage number by the length constraint, and it not possible to accommodate more than 18 or 19 stages over most of the design space (figure 2.9). In the unconstrained example up to 28 stages were used, and in this example the enthalpy drop per stage is increased and the blading operates significantly off-design over much of the design space.

FIGURE 2.9. Contours of stage number.

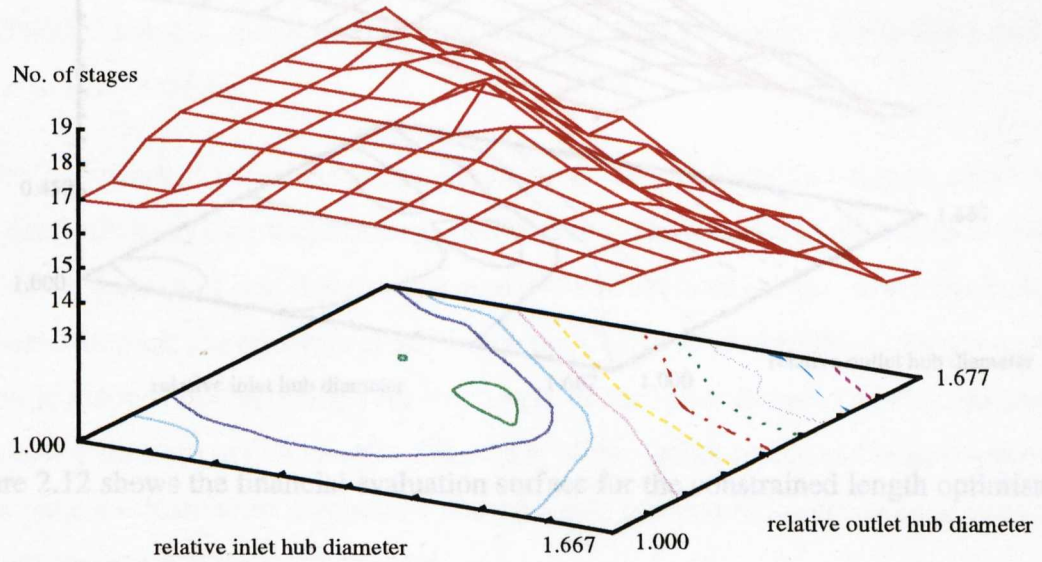

As expected, the limited stage number resulted in a flattened area in the cost and length surfaces. The constrained length was only 62% percent of the maximum length considered in the unconstrained search (figures 2.10 and 2.11). A further effect of the constraint was to align the contours of maximum cost and length much more closely with the contour of maximum efficiency. This is because the optimum design is located very close to the constraint boundary.

FIGURE 2.10. Contours of relative bladepath cost.

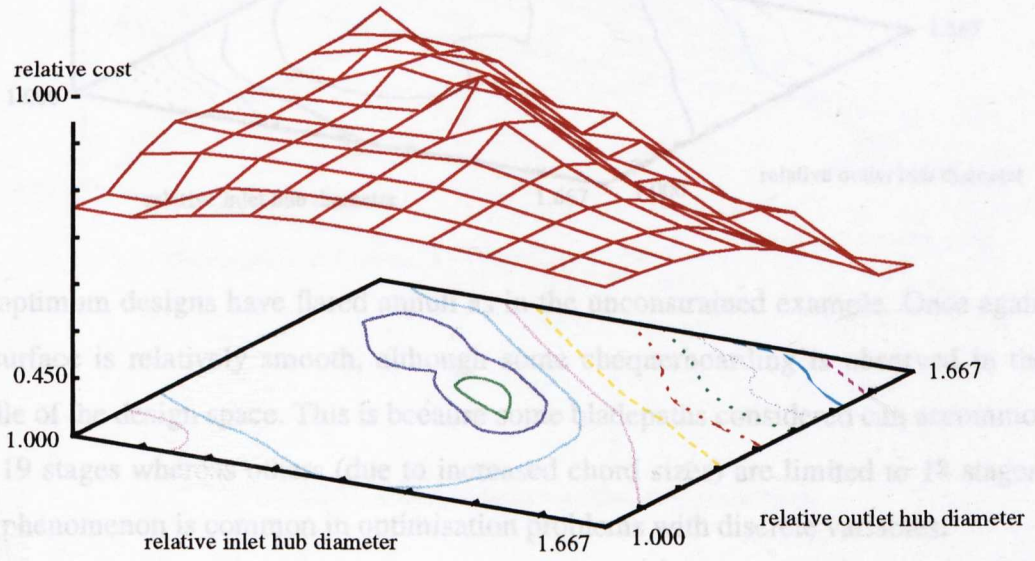

FIGURE 2.11. Contours of relative bladepath length.

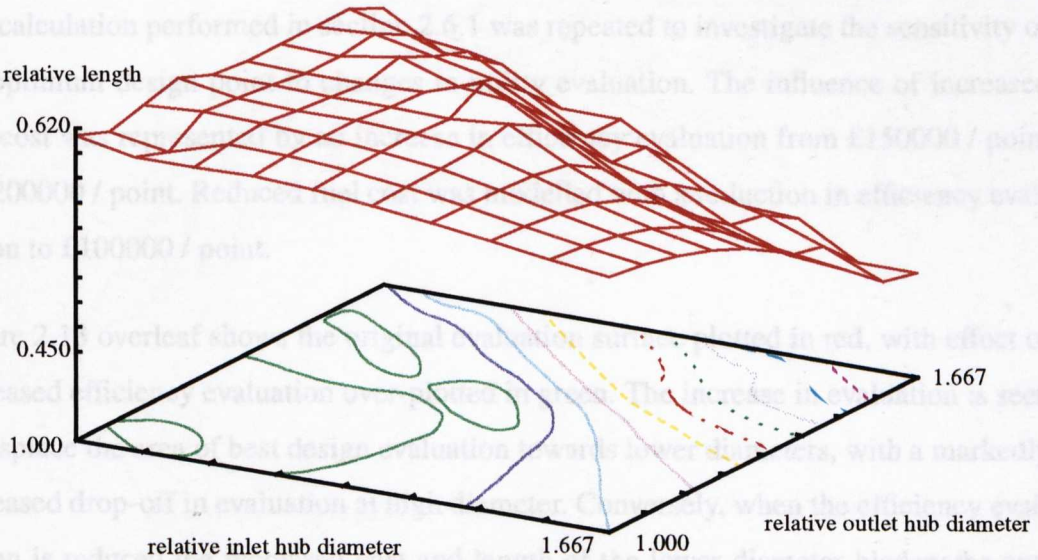

Figure 2.12 shows the financial evaluation surface for the constrained length optimisation.

FIGURE 2.12. Contours of relative bladepath economic evaluation.

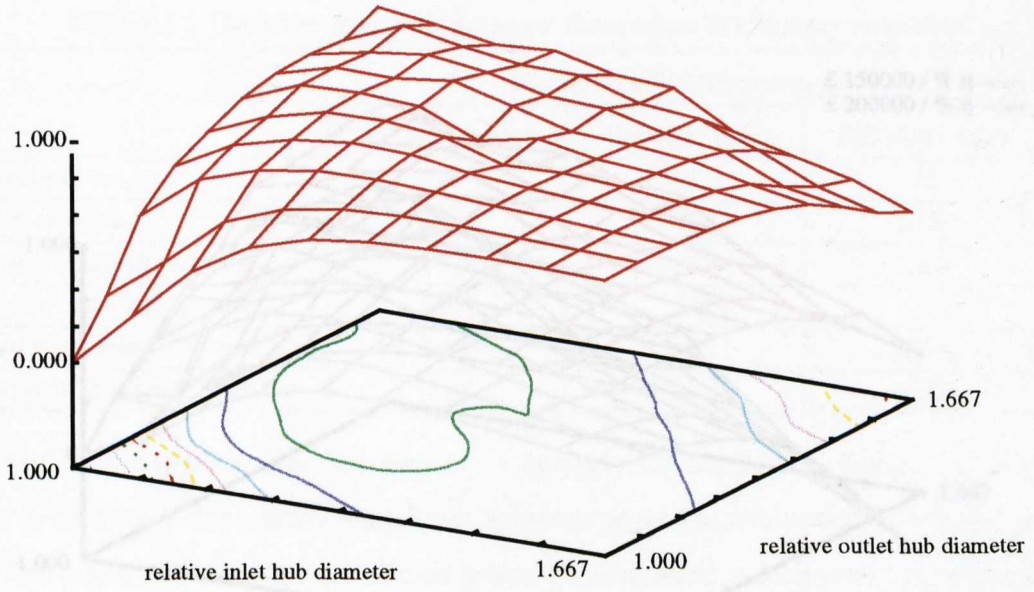

The optimum designs have flared annuli as in the unconstrained example. Once again the surface is relatively smooth, although some chequerboarding is observed in the middle of the design space. This is because some bladepaths considered can accommodate 19 stages whereas others (due to increased chord sizes) are limited to 18 stages. This phenomenon is common in optimisation problems with discrete variables.

2.6.3 Sensitivity of optimum design point to efficiency evaluation.

The calculation performed in section 2.6.1 was repeated to investigate the sensitivity of the optimum design point to changes in utility evaluation. The influence of increased fuel cost was represented by an increase in efficiency evaluation from £150000 / point to £200000 / point. Reduced fuel cost was modelled with a reduction in efficiency evaluation to £100000 / point.

Figure 2.13 overleaf shows the original evaluation surface plotted in red, with effect of increased efficiency evaluation over-plotted in green. The increase in evaluation is seen to displace the area of best design evaluation towards lower diameters, with a markedly increased drop-off in evaluation at high diameter. Conversely, when the efficiency evaluation is reduced the increased cost and length of the lower diameter bladepaths outweighs any increase in efficiency in this region of the design space, and large diameter blade paths evaluate most favourably. The optimum bladepath designs at each evaluation are compared in table 2.4 overleaf.

FIGURE 2.13. Effect of increased efficiency evaluation.

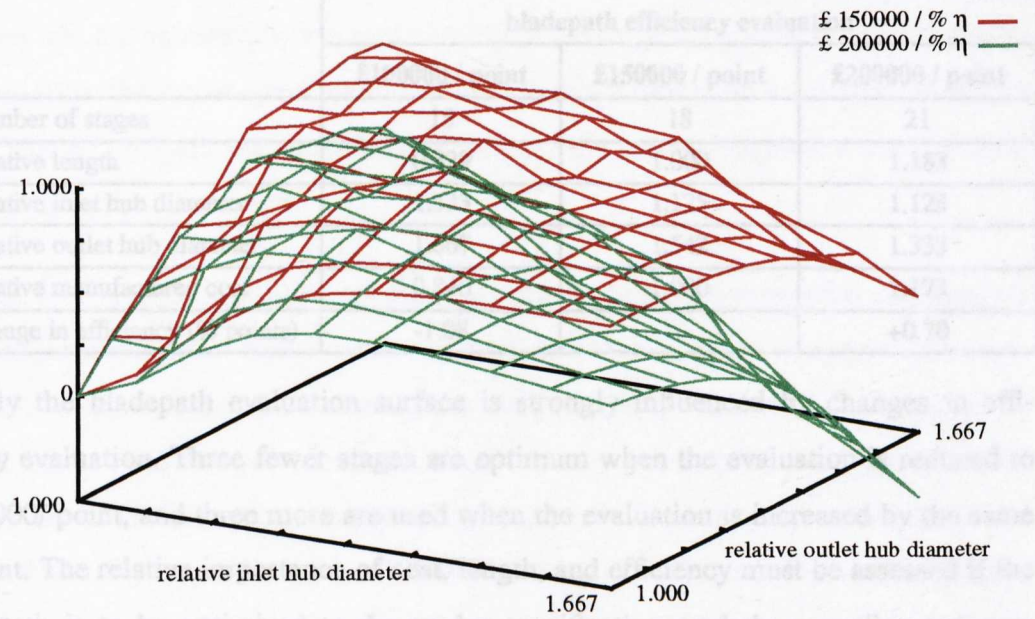

FIGURE 2.14. Effect of reduced efficiency evaluation.

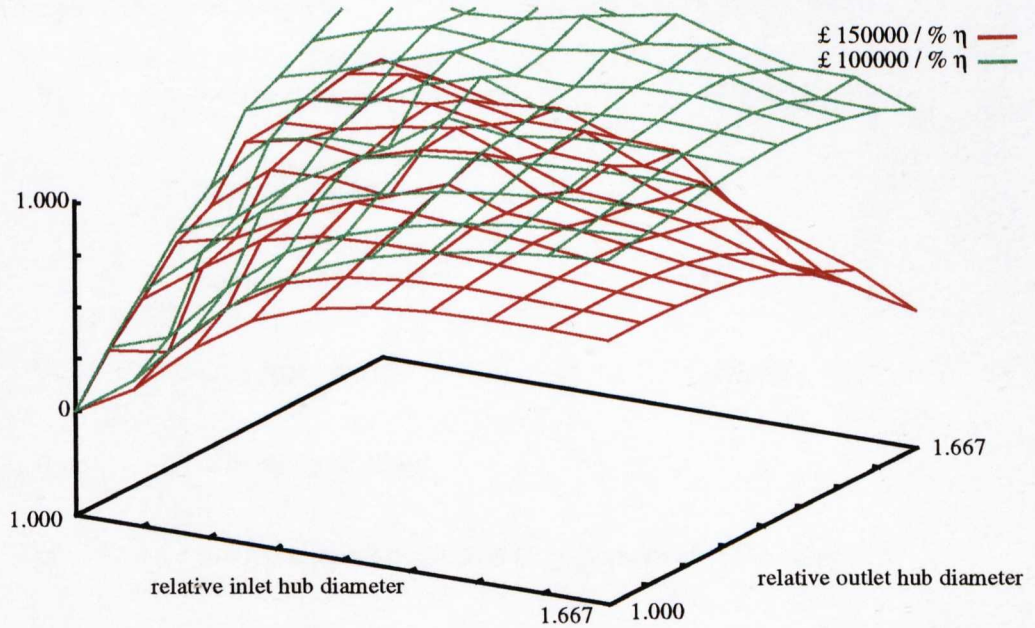

TABLE 2.4. Optimum bladepath designs at three values of efficiency evaluation.

	bladepath efficiency evaluation		
	£100000 / point	**£150000 / point**	**£200000 / point**
number of stages	15	18	21
relative length	0.829	1.000	1.183
relative inlet hub diameter	1.333	1.125	1.125
relative outlet hub diameter	1.667	1.542	1.333
relative manufactured cost	0.840	1.000	1.173
change in efficiency (% points)	-1.08	-	+0.70

Clearly the bladepath evaluation surface is strongly influenced by changes in efficiency evaluation. Three fewer stages are optimum when the evaluation is reduced to £100000/ point, and three more are used when the evaluation is increased by the same amount. The relative importance of cost, length, and efficiency must be assessed if the bladepath is to be optimised to the tender specification, and the meanline software allows the designer to perform a sensitivity analysis on the gallery of legal solutions to exploit these trade-offs fully.

2.7 Economic assessment based on unitised production cost.

The economic evaluation performed by the meanline software is relatively simple, and assumes that the monetary worth to the utility of a change in cylinder efficiency can be deduced from the tender specification. Although this information is usually available a more detailed analysis was performed to validate the software against a more general power generation cost model.

Horlock [1987] notes that all economic assessments of power generation schemes are ultimately based upon a consideration of the time value of money. A power plant has fuel costs and running costs, and a capital charge associated with the financing of the project assets. The relative economic benefit of one power plant configuration over another can be calculated by compared a unitised cost of power production, that is the cost to the utility of producing 1 kWh of electricity. The formula below, due to Horlock, expresses the unitised production cost as a function of capital cost, fuel cost, and running costs

$$Y_E = \frac{\beta \cdot C_0}{W \cdot H} + \frac{\zeta}{\eta_0} + \frac{U}{W \cdot H} + V$$

with symbols defined as follows:

Y_E	unitised production cost	(£/kWh)
β	capital charge factor	
C_0	capital cost of plant	(£)
ζ	unit cost of fuel	(£/kWh)
η_0	efficiency of plant	
U	constant operating costs (e.g. personnel)	(£/annum)
V	variable operating costs	(£/kWh)
W	plant rating	(kW)
H	plant utilisation	(hours / annum)

The capital charge factor (β) represents the cost of servicing the capital required, and can be related to the discount rate (i) and life of the plant in years (N) by the following formula:

$$\beta = \left\{ \frac{i \cdot (1+i)^N}{(1+i)^N - 1} \right\}$$

If it is assumed that a change in bladepath efficiency does not affect the fixed or variable running costs, then the associated change in unitised production cost can be expressed as follows, using subscripts 1 and 2 to denote the different design points.

$$\Delta Y_E = \left\{ \frac{\beta}{W \cdot H} \cdot ((C_0)_2 - (C_0)_1) \right\} + \left\{ \zeta \cdot \left(\frac{1}{\eta_2} - \frac{1}{\eta_1} \right) \right\}$$

In the following example the economic analysis is applied to the HP turbine for a 250 MW fossil fired reheat power plant, as discussed in section 3. Assuming a design life of 25 years and a discount rate of 12% (10% - 15% is typical) a capital charge factor of β=0.12750 is calculated. For this application a one percent increase in HP turbine efficiency reduced the turbine generator heat rate by 0.18 percent, and if a boiler efficiency of 80% is assumed, increases the overall fuel-to-terminals cycle efficiency by 0.144%. A typical plant utilisation rate of 90% was assumed giving 7884 hours of generation per annum, and a representative coal cost of £2.75/GJ was applied.

Figure 2.15 shows the variation in unitised production cost with efficiency and bladepath cost, expressed as a cost in £/kW relative to the first design in the gallery of legal solutions. The capital cost surface rises with decreasing bladepath diameter as the stage number increases, yet fuel costs are lower at reduced diameter due to increased bladepath efficiency. Figure 2.16 shows the variation in overall unitised cost which is represented by the sum of the capital cost and fuel cost surfaces. The region of lowest production cost is in the upper left region of the design space, corresponding to bladepaths with haded annuli, and coincident with the optimum design identified in section 2.6.1 using a simpler evaluation. This evaluation confirms that the optimum design has 18 stages, relative inlet and outlet hub diameters of 1.125 and 1.542, similar to that determined using the simple cost model.

FIGURE 2.15. Capital and fuel cost components of unitised electricity production price.

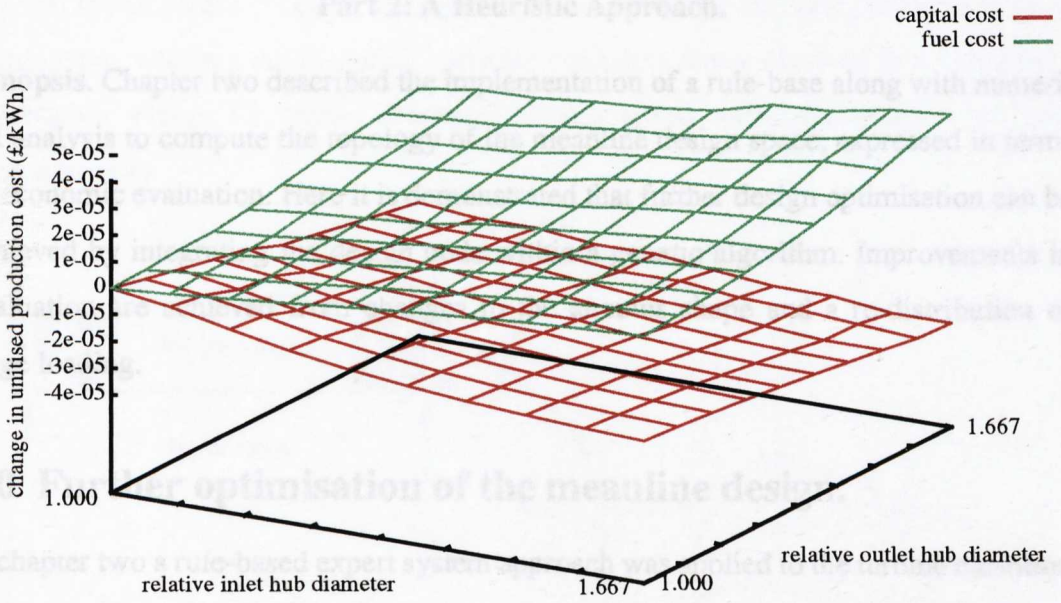

FIGURE 2.16. Variation of unitised electricity production price.

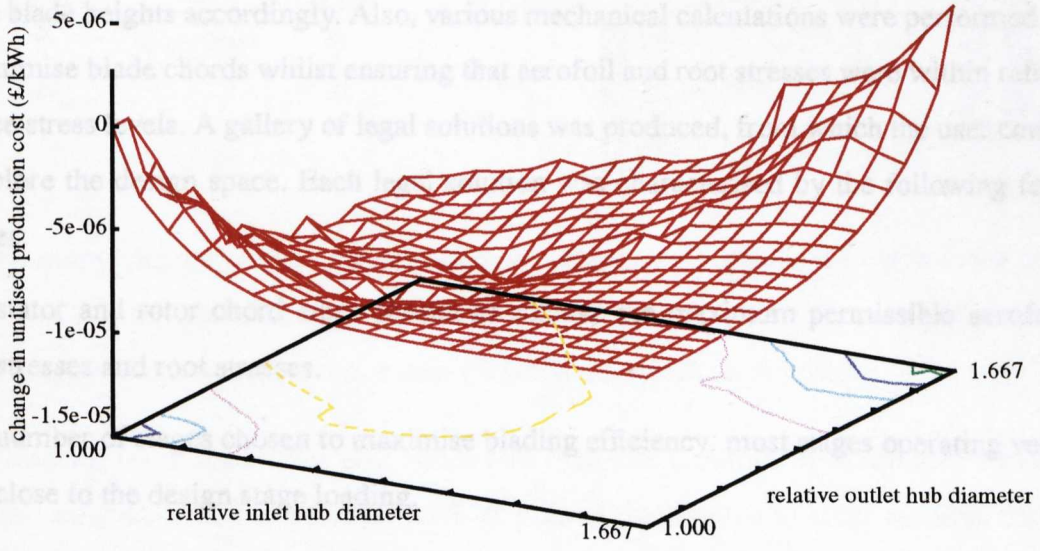

The maximum change in evaluation in figure 16 is 1.5×10^{-5} £/kWh which corresponds to a cash difference of £740000 in operating cost based upon 90% utilisation during a 25 year plant life.

Chapter Three

Meanline Design of Steam Turbine Reaction Bladepaths.
Part 2: A Heuristic Approach.

Synopsis. Chapter two described the implementation of a rule-base along with numerical analysis to compute the topology of the meanline design space, expressed in terms of economic evaluation. Here it is demonstrated that further design optimisation can be achieved by integrating the design code within a genetic algorithm. Improvements in evaluation are achieved from changes to the annulus shape and a re-distribution of stage loading.

3.0 Further optimisation of the meanline design.

In chapter two a rule-based expert system approach was applied to the turbine meanline design problem. A turbine cylinder type was chosen, and the cycle steam conditions were given as input data. The software then proceeded to traverse the meanline design space (from long, slender bladepaths with many stages to short bladepaths with few stages) and at each point in the search selected an optimum number of stages and sized the blade heights accordingly. Also, various mechanical calculations were performed to minimise blade chords whilst ensuring that aerofoil and root stresses were within reference stress levels. A gallery of legal solutions was produced, from which the user could explore the design space. Each legal solution was characterised by the following features:

- stator and rotor chord sizes chosen to achieve the maximum permissible aerofoil stresses and root stresses.
- number of stages chosen to maximise blading efficiency: most stages operating very close to the design stage loading.
- smooth and approximately linear changes in inner and outer boundary shape consistent with an even stage loading distribution.

In general each legal solution was of similar quality to that which would produced by an experienced design engineer, although the numerical optimisation often caused a slightly smoother distribution of stage loading and a slightly improved efficiency. How-

ever, significant improvements in overall economic evaluation were obtained from a fuller and more systematic exploration of the design space, during which the dominant trade-offs between efficiency and length and cost could be more fully exploited. During a usual meanline design cycle an engineer would manually evaluate perhaps five or six bladepaths, whereas the meanline software considers many hundred in a comparable time-scale. Figure 3.1, below, illustrates the rule-based optimisation of the bladepath schematically.

FIGURE 3.1. Rule-based meanline optimisation.

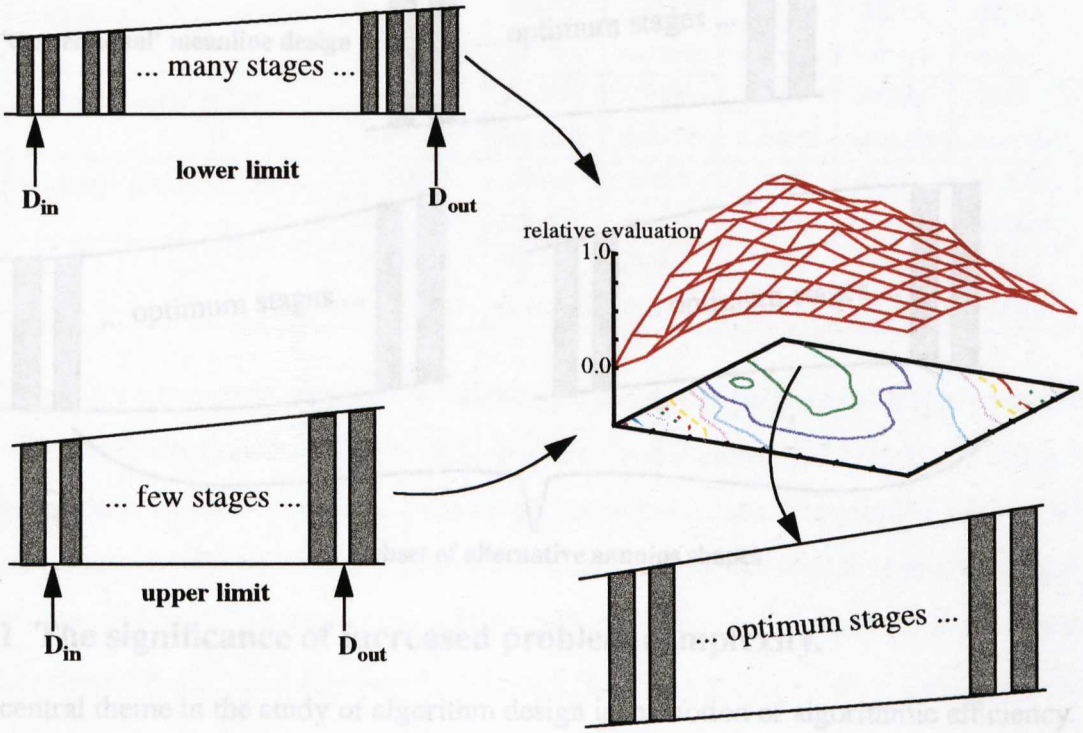

Optimum inlet and outlet hub diameters are chosen to maximise the overall cost-effectiveness of the bladepath. In each case the stage loading is almost constant from stage to stage and the meanline and annulus boundaries are close to linear.

However, for a fixed inlet and outlet hub diameter a subset of alternative meanline designs exist. These alternatives have an uneven distribution of stage loading, and are characterised by annulus shapes with inflections, as shown schematically in figure 3.2, overleaf.

If the complete range of meanline designs is be explored by varying the hub and casing shapes then many more variables must be considered and the order of the problem is increased. If a constant hub diameter is used then there is one variable per blade row,

either the blade height or the casing diameter. If both hub and casing diameter are to be changed then there are two variables per row, hub diameter and blade height. In the 250 MW test case described in chapter two the optimum bladepath had 18 stages and a rising hub diameter. For this application the evaluation would therefore be a function of 72 variables.

FIGURE 3.2. Alternative annulus shapes with same inlet and outlet hub diameter.

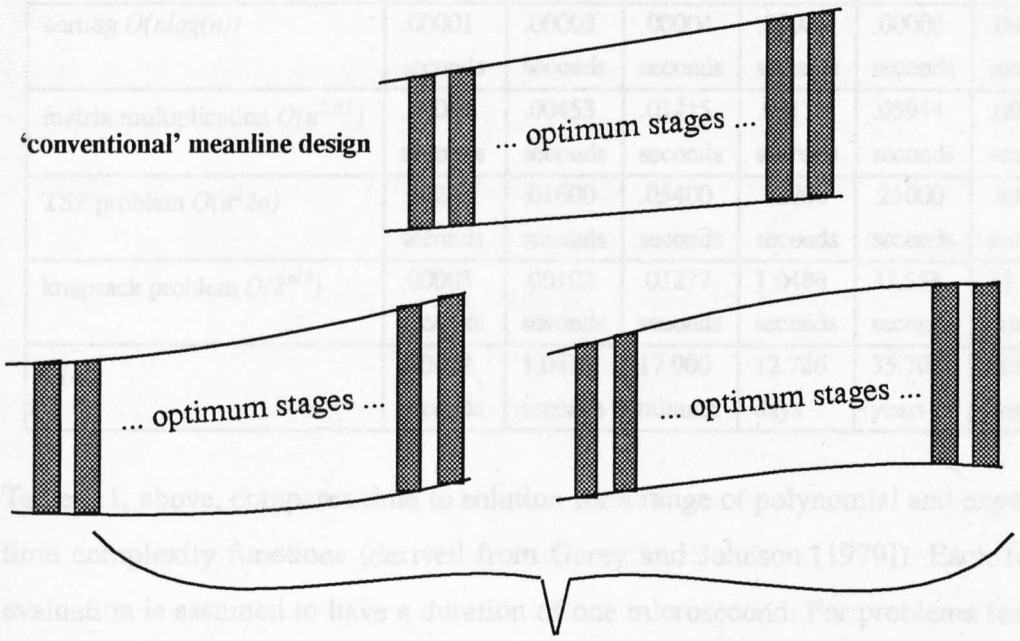

3.1 The significance of increased problem complexity.

A central theme in the study of algorithm design is the notion of algorithmic efficiency. In the broadest sense, efficiency includes all of the computational resources required to solve a problem, and can be taken to mean fastest time to solution. The relative efficiency of two algorithms can be judged by comparing the algorithmic time complexity. If $T(n)$ is the run-time for an algorithm with n inputs we can write $T(n) = O(f(n))$ defining the upper bound of computational time of the order of $f(n)$. Horowitz [1984] noted that most problems can be divided into two classes:

- solution by polynomial time algorithm, where solution time is bounded by a polynomial of small degree e.g. polynomial evaluation $O(n)$, sorting $O(n\ log(n))$, matrix multiplication $O(n^{2.81})$.
- problems for which the best known solution algorithms are non-polynomial in time, e.g. travelling salesperson problem (TSP) $O(n^2 2n)$, knapsack problem $O(2^{n/2})$.

A feature of the second class of problems, often known as NP-complete, is that the solution time rises dramatically as the number of problem variables is increased.

TABLE 3.1. Comparison of polynomial and exponential time complexity functions.

time complexity function	size of problem - n					
	10	**20**	**30**	**40**	**50**	**60**
polynomial evaluation $O(n)$	.00001 seconds	.00002 seconds	.00003 seconds	.00004 seconds	.00005 seconds	.00006 seconds
sorting $O(nlog(n))$	.00001 seconds	.00003 seconds	.00004 seconds	.00006 seconds	.00008 seconds	.00011 seconds
matrix multiplication $O(n^{2.81})$	.00065 seconds	.00453 seconds	.01415 seconds	.03175 seconds	.05944 seconds	.09922 seconds
TSP problem $O(n^2 2n)$	.00200 seconds	.01600 seconds	.05400 seconds	.12800 seconds	.25000 seconds	.43200 seconds
knapsack problem $O(2^{n/2})$	.00003 seconds	.00102 seconds	.03277 seconds	1.0486 seconds	33.554 seconds	17.900 minutes
$O(2^n)$	.00102 seconds	1.0486 seconds	17.900 minutes	12.726 days	35.702 years	365.59 centuries

Table 3.1, above, compares time to solution for a range of polynomial and exponential time complexity functions (derived from Garey and Johnson [1979]). Each function evaluation is assumed to have a duration of one microsecond. For problems for which no polynomial time solution is known and a solution in exponential time must be taken, the time to solution is seen to grow explosively as the number of variables is increased. Considering the 2^n time function for instance, doubling the number of variables from 30 to 60 increases the upper bound solution time by a factor of 10^9.

A feature of NP-complete problems is that there is no guarantee of producing a solution in polynomial time, and in fact, little chance of even coming close. A number of workers have postulated that such problems will remain perpetually intractable and have concluded that a more realistic approach is to consider the use of heuristic procedures that have reasonable run-times. The application of heuristic search methods to NP-complete problems is discussed in more detail by Cleland [1994] and Subramani [1995].

Since the bladepath meanline design optimisation process relies on repeated evaluation of an existing design code (with typically between 10 and 100 variables, and 1 second per evaluation) it is very unlikely that an exact optimum solution could be found by a

deterministic algorithm within a sensible timescale. Instead, attention was turned to faster solution methods that would produce satisfactory (rather than optimum) solutions relatively quickly.

3.2 Heuristic search techniques.

In recent years much research effort has been directed to the development of heuristic search algorithms. Such algorithms mimic physical processes observed in the natural world, and attempt to solve search problems by trial-and-error (heuristic) procedures. This approach can often have a high probability of locating satisfactory (or near optimum) solutions in a complex multimodal design space, and has been proven on a variety of large scale combinatorial optimisation problems (many of which are NP-complete). Commonly cited search techniques include Evolutionary Programming (Fogel [1966]), Genetic Algorithms (Holland [1976]), Genetic Programming (Koza [1993]), and Simulated Annealing (Kirkpatrick et. al. [1983]).

An optimisation process can be regarded as a search through a space of possible solutions. The meanline design space described in chapter two was bounded by only two variables (inlet and outlet hub diameter). It was therefore relatively straight-forward to size an optimum bladepath at each point in the design space using numerical optimisation, and perform an exhaustive search through the space of possible diameters identifying an optimum bladepath at each point. The search space was seen to be controlled by relatively few dominant trends, e.g. aspect ratio controlling efficiency. A search space defined by many variables (e.g. a full meanline annulus optimisation defined by 72 variables) is very much more complicated. Each variable (either a height or diameter) could exert a broadly equal effect on the overall efficiency, and the solution of the problem by numerical (gradient based) methods is no longer practical.

The meanline design code was integrated within a genetic algorithm to allow a full exploration of the meanline design space considering a wide range of annulus shapes. Section 3.3 outlines the operation of a simple genetic algorithm, section 3.3.1 describes the integration of the design code, and some results are discussed in section 3.4.

3.3 Application of a genetic algorithm to meanline design.

The genetic algorithm (GA) paradigm describes a large class of heuristic search techniques which are analogous to the evolution of a biological species. GA based methods have been applied to a diverse range of engineering problems in recent years and the approach has become established as robust and versatile optimising paradigm. Some reported applications include VLSI chip design (Schnecke et. al. [1996]), satellite boom design (Keane [1996]), and ship sub-division design (Subramani [1995]).

In this section the operation of a simple GA is described, and the discussion is extended to include the integration of the meanline design tool within the GA fitness function. Finally some results are presented.

3.3.1 Operation of a simple genetic algorithm.

The operation of a genetic algorithm mimics the evolution of a biological species. The problem design parameters are encoded into a binary string which represents a chromosome of genetic material. A population of many such chromosomes is created and the fitness of each member is assessed. Genetic operators (crossover and mutation) are applied to create a new population, and the search continues. This process is shown schematically below:

FIGURE 3.3. Operation of a simple genetic algorithm.

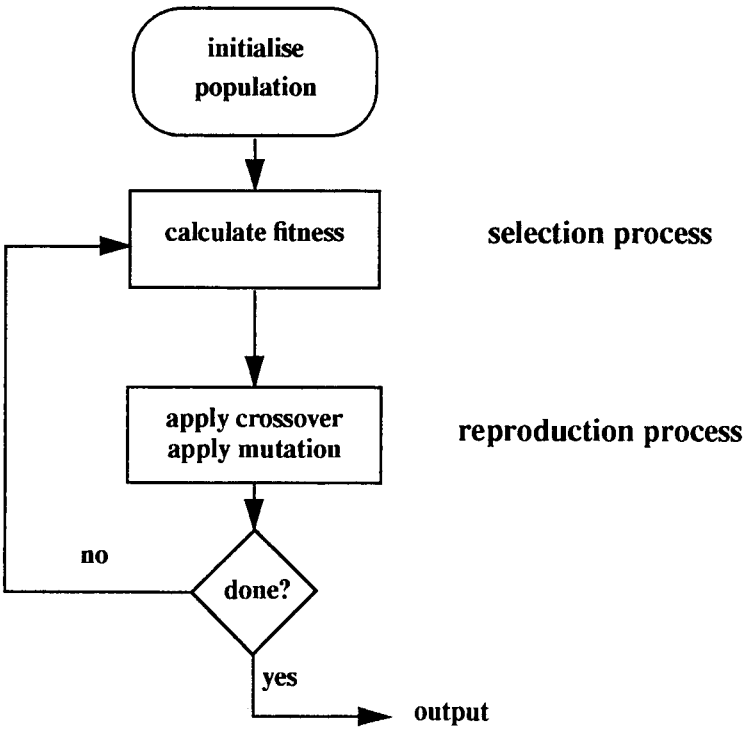

Firstly an initial population of candidate designs is created. Each member of the population is represented as a binary chromosome, which can either be created randomly or seeded from a previous calculation. This is the initialisation phase of the search.

The fitness of each member of the population is then calculated. This is performed using a fitness function (also known as an objective function) and it is this function that defines the natural selection process. For a bladepath optimisation the meanline design code would be used as a fitness function, and fitness itself might be defined as the predicted aerodynamic efficiency of the blading. A common mathematical means of representing the selection process is 'roulette wheel selection'. Other methods such as elitism and tournament selection exist but are not considered in the current work. In an implementation of roulette wheel selection each member of the population is allocated a segment of an imaginary roulette wheel in proportion to its fitness. A very fit design will have a large segment, and similarly an unfit individual will have a slender segment. The roulette wheel is then 'spun' a number of times to choose a new population. In this way natural selection will favour fitter designs, but there remains an element of chance, and it is this probabilistic feature of the search that maintains a diverse gene pool. There is always some chance that unfit designs will survive into the next generation.

Genetic operators are then applied to the population. Firstly crossover occurs, whereby chromosome lengths (genes) are swapped between members of the population starting from randomly chosen crossover sites. This is analogous to the production of a zygote from two gametes in sexual reproduction. Mutation is then applied to the daughter chromosomes; this is usually represented as a small probability that any particular bit will be 'flipped' (i.e. there is a small chance that any '0' will spontaneously become '1' and vice versa). This encourages a wide search and helps prevent premature convergence.

The process then repeats by calculating the fitness of the daughter population, and applying natural selection. An interesting feature of such heuristic methods is that the method of solution is quite independent of the nature of the fitness function. Rather than computing gradients within the search space and following these gradients to areas of good performance, the GA is free to evaluate design configurations at any point within the design space during the same generation. Thus a GA driven method is likely to be inefficient at solving problems with relatively few variables or with a

smooth and unimodal design space. However, if there are many variables or if the design space is characterised by discontinuities or pronounced multimodality the GA will be able to traverse the entire domain without becoming trapped around local optima.

In the current work the *myGENEsys* GA (Subramani [1994]) has been used. This is an ANSI-*C* version of the well-known GENEsYs algorithm developed at Dortmund University by Baeck [1992]. Proportional selection was used, with two point crossover using a crossover rate of 0.6, and simple mutation at a rate of 0.001.

Consider the solution of a relatively simple test problem of thirty variables:

minimise

$$f(x) = \sum_{i=1}^{30} x_i^2$$

subject to

$$-5.12 < x_i < 5.12$$

In this example there are 30 independent variables, and solution fitness is maximised by minimising the sum of the squares. The optimum fitness function value is 0.0 which can only be achieved if each of the variables is identically zero. Figure 3.4, overleaf, shows the convergence history for the problem using a population of 50 over 200 generations.

The initial random population is very diverse, with a best, worst, and average fitness of 171.5, 362.6, and 260.2 respectively. The diversity of the population is illustrated by the large difference between the best and worst fitnesses. A characteristic GA convergence is shown over the first 50 generations, where fit solutions rapidly emerge and there are several large step changes in the best fitness. Best and average fitness converge together rapidly as these fit solutions increasingly dominate the population. The influence of mutation is seen as the periodic 'blipping' of the worst performance, and it is this effect that prevents the best and average fitnesses from converging completely and stagnating the search. After 200 generations the best fitness is 14.5, with an average of 18.6.

Clearly such a task can be solved by inspection - each variable needs to be identically zero - and it might appear that the GA has only solved a trivial problem. This however is not the case. The GA has solved a combinatorial problem with 30 independent variables and achieves this irrespective of whether the solution is known or not. It is also noteworthy that the GA has not identified the optimum solution (fitness = 0.0) within 200 generations, instead it has produced a population of solutions each of which identifies near optimum performance. This result is typical of heuristic optimisation procedures: since the search has a probabilistic element only near optimum solutions are likely to be produced. For any general combinatorial problem for which the solution is unknown a true optimum can only be computed in exponential time.

FIGURE 3.4. GA convergence history.

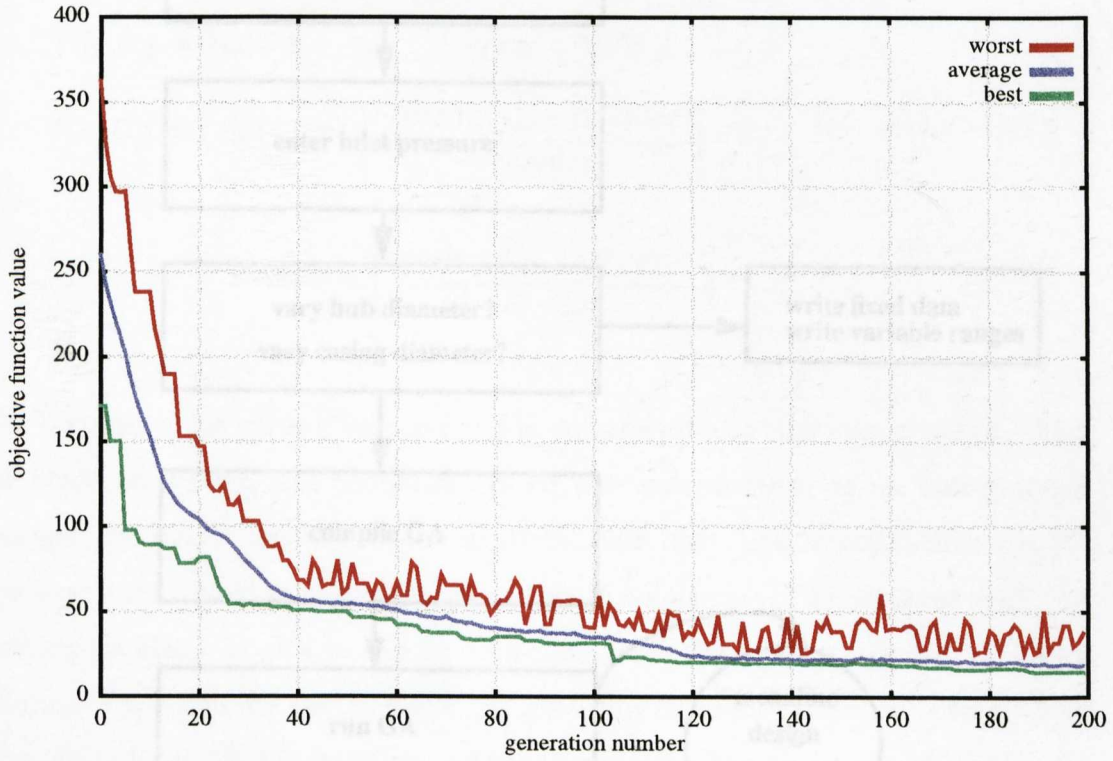

3.3.2 Integration of a meanline design tool within a genetic algorithm.

The meanline design code *SIGMA*, as used in the rule-based optimisation in chapter 2, was integrated within the *myGENEsys* genetic algorithm. The software was integrated into the rule based search manager described earlier.

When the search manager is run the user has two options. They are

- perform a rule-based optimisation to produce a gallery of legal solutions, or
- use a genetic algorithm to 'tweak' a favoured design from the gallery.

If an existing design from the gallery is chosen the search manager strips the variables from the design dataset (heights and diameters) and writes the upper and lower bounds on these variables to a file. The allowed range on both blade height and diameter is taken as +/-20% of the blade height for that row.

FIGURE 3.5. Integration of meanline design tool within GA.

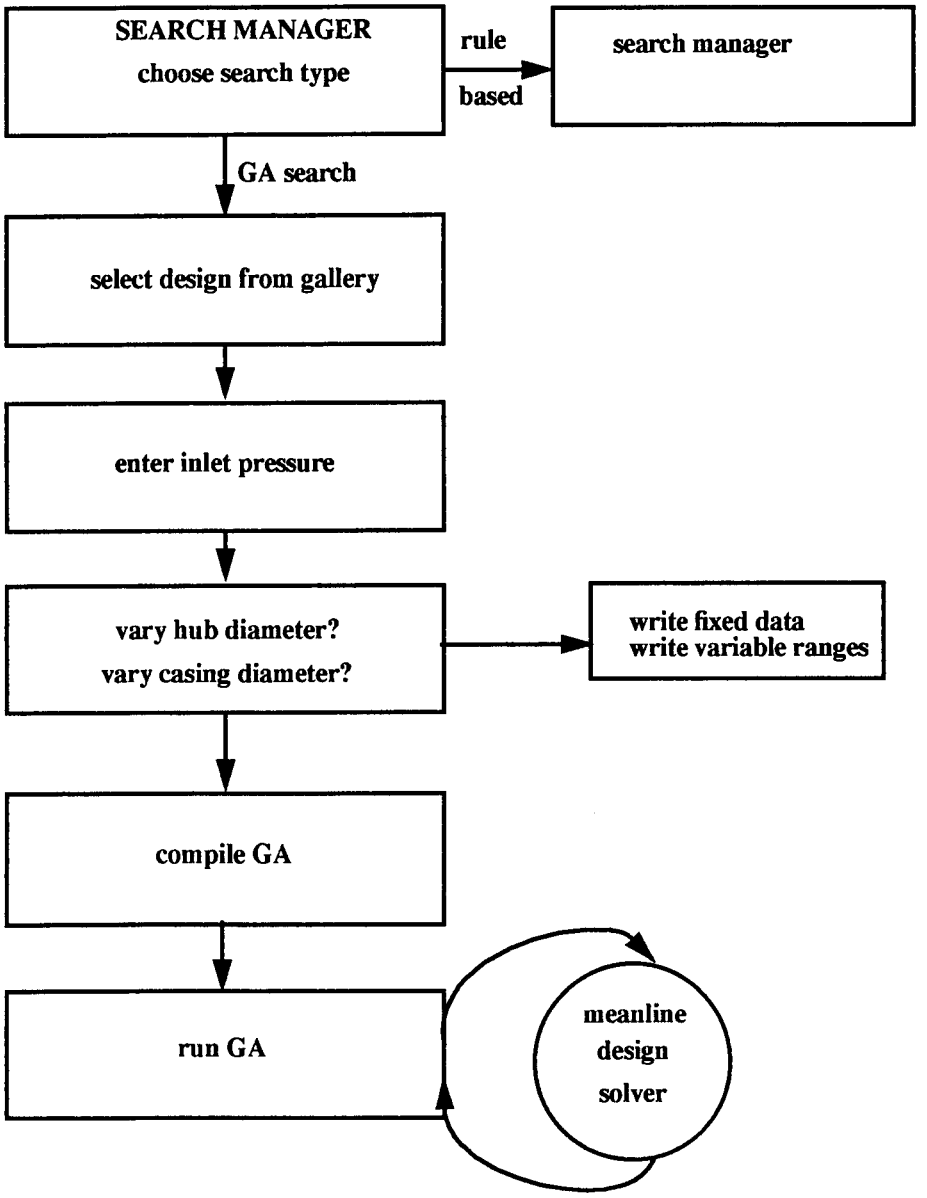

The user may then choose to vary only the casing diameter (and keep a constant hub diameter) or allow both the hub and the casing to vary. The GA software is then automatically made clean and re-compiled with the necessary configuration files, and the search commences. On the first iteration of the GA all the fixed bladepath data (e.g. cylinder type, gland details, steam conditions) is written to a memory map for rapid access. When the GA evaluates the fitness of the population each binary string is then

converted into a dataset for the meanline design solver, and the solver is run to evaluate each member of the population. After each member has been evaluated by the solver the objective function picks out the information necessary to compute fitness and the selection procedure begins.

A crucial part of any optimisation procedure is an appropriate definition of fitness. The meanline optimisation has identified the area of the design space in which the most cost effective turbine can be produced, and the logical definition of fitness would be to maximise the bladepath efficiency at this point. This definition was chosen, with the addition of a penalty term to control inlet pressure. The definition of fitness used was:

minimise:

$$f(h_i,D_i) = 100 - \eta \quad \text{for} \quad error < 0.005$$

$$f(h_i,D_i) = (100 - \eta) + \left|\frac{pressure_{calc} - pressure}{pressure}\right| \times 75 \quad \text{for} \quad error > 0.005$$

with $$error = \left|\frac{pressure_{calc} - pressure}{pressure}\right|$$

The purpose of the penalty function was to constrain the turbine inlet pressure. Since the bladepath heights and diameters can all vary independently as the casing shape changes, the swallowing capacity of the turbine can drift. This is particularly true for low aspect ratio blading, where improvements in efficiency can be achieved easily by pushing-up blade heights to reduce secondary loss. The penalty function penalises solutions for which the inlet pressure has drifted by more than 0.5%. A 1.0% error in pressure reduces the fitness of the solution by 0.75%. The modelling of constraints within genetic algorithms and the limitations of the penalty function approach are discussed in chapter 5.

3.4 Program test cases.

The genetic algorithm was tested on four meanline bladepaths. The first three were five stage HP turbine bladepaths of constant hub diameter, with first row aspect ratios of 0.328, 0.697, and 1.433. The fourth test case was the 18 stage flared HP turbine bladepath produced by the meanline rule-based software in chapter 2.

These three test cases are representative of the design of the first blading group of a typical HP turbine over a range of inlet volumetric flow conditions. In each test case the constant hub diameter was adjusted to achieve a mean diameter of around 725 mm, thus keeping the group loading coefficient constant. The group pressure ratio was 1.247 with a shaft rotational speed of 3000 rpm.

TABLE 3.2.Bladepath efficiency improvement: aspect ratio = 0.328

	blading configuration		
	smooth bladepath	GA bladepath	repeating stages
inlet blade height (mm)	11.48	10.84	12.30
inlet hub diameter (mm)	713.29	713.29	713.29
inlet aspect ratio	0.328	0.308	0.351
efficiency improvement (% points)	-	+0.099	-0.666
leaving loss (kJ/kg)	0.847	0.705	1.115

TABLE 3.3.Bladepath efficiency improvement: aspect ratio = 0.697

	blading configuration		
	smooth bladepath	GA bladepath	repeating stages
inlet blade height (mm)	24.37	23.05	26.30
inlet hub diameter (mm)	700.00	700.00	700.00
inlet aspect ratio	0.697	0.659	0.751
efficiency improvement (% points)	-	+0.148	-0.436
leaving loss (kJ/kg)	0.835	0.714	1.056

TABLE 3.4.Bladepath efficiency improvement: aspect ratio = 1.433

	blading configuration		
	smooth bladepath	GA bladepath	repeating stages
inlet blade height (mm)	50.16	48.31	53.83
inlet hub diameter (mm)	674.20	674.20	674.20
inlet aspect ratio	1.433	1.380	1.538
efficiency improvement (% points)	-	0.102	-0.404
leaving loss (kJ/kg)	0.829	0.722	1.038

A population of 50 bladepaths was used and each calculation was run for 200 generations. Good solutions were obtained after around 20 generations, with a run time of twenty to thirty minutes, and little further gain was observed throughout the rest of the run. Since the design problem is complex and heavily constrained mutations generally produce solutions that have considerably worse than average fitness. A typical convergence history is shown in figure 3.6 overleaf.

FIGURE 3.6. Typical convergence history for meanline design problem.

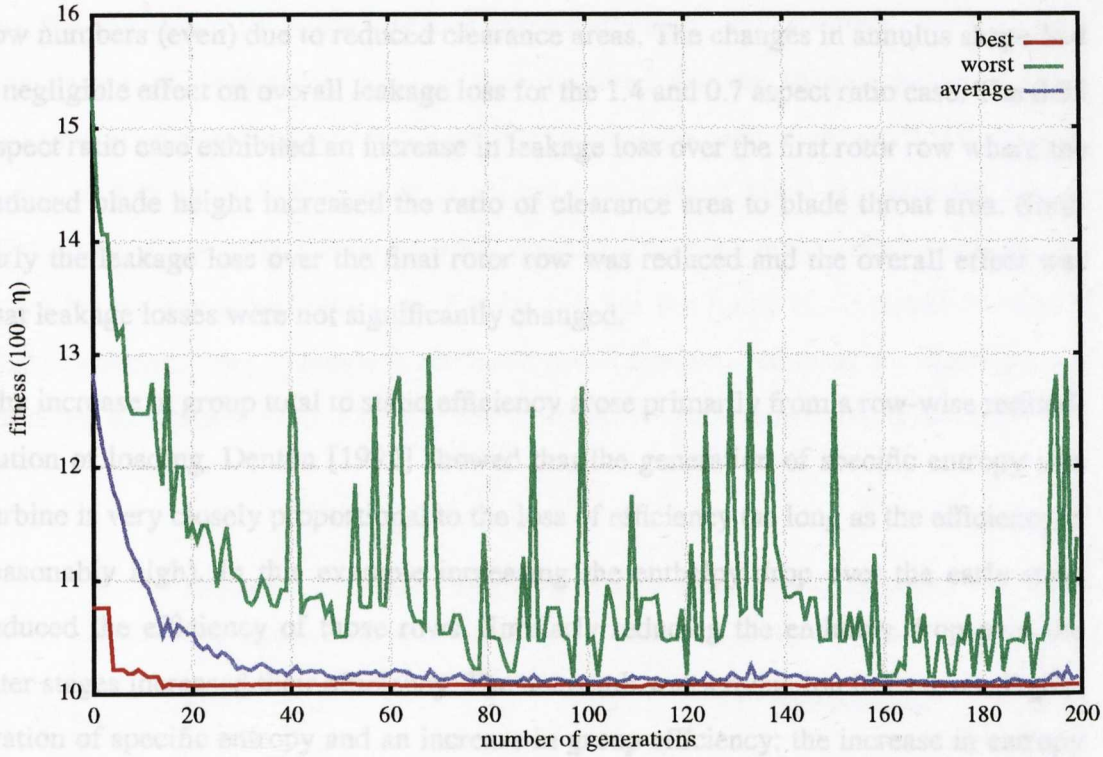

Tables 2, 3, and 4 compare the predicted bladepath efficiencies based on exhaust static conditions. Efficiency improvements of 0.099, 0.148, and 0.102 percentage points have been realised, accompanied by an additional fall in bladepath leaving loss of around 15%. Figures 3.8, 3.9, and 3.10 overleaf compare the bladepath annulus shape and the row-by-row loading, leakage loss, and efficiency.

At each of the three aspect ratios tested a similar overall annulus shape was discovered. The inlet blade height is reduced and the bladepath flare increased to create a smaller bladepath inlet area with a more steeply rising casing boundary. Flare is reduced through the mid section of the bladepath, and rises steeply again to an increased bladepath exit height.

The row-by-row loading has been plotted as a relative U/C_0, where U is the mid height blade speed and C_0 is the velocity equivalent of the row isentropic enthalpy drop. The smooth bladepath solutions created by the rule-based meanline tool have a practically constant U/C_0 distribution, typical of standard design practice. The casing boundary modifications however modify the row-wise load distribution, and in each case loading is increased on the first rows (lower than average U/C_0) and reduced on the final rows. The increased final stage blade height reduces the group leaving loss by around 15%.

Leakage losses were typically 50% lower for stator rows (odd row numbers) than rotor row numbers (even) due to reduced clearance areas. The changes in annulus shape had a negligible effect on overall leakage loss for the 1.4 and 0.7 aspect ratio case. The 0.35 aspect ratio case exhibited an increase in leakage loss over the first rotor row where the reduced blade height increased the ratio of clearance area to blade throat area. Similarly the leakage loss over the final rotor row was reduced and the overall effect was that leakage losses were not significantly changed.

The increase in group total to static efficiency arose primarily from a row-wise redistribution of loading. Denton [1992] showed that the generation of specific entropy in a turbine is very closely proportional to the loss of efficiency (as long as the efficiency is reasonably high). In this example increasing the enthalpy drop over the early rows reduced the efficiency of those rows. Similarly reducing the enthalpy drop over the later stages increased their efficiency. The net result was a reduction in the overall generation of specific entropy and an increase in group efficiency: the increase in entropy in the early rows is more than compensated for by the reduction in entropy in the final rows since the temperature is proportionally higher at inlet. This is a manifestation of the 'reheat effect'.

Reduced efficiency in the early rows traded-off against increased efficiency in the later rows was observed in each of the aspect ratio cases, but the actual distribution was dependent on both the loading distribution and the influence of leakage. At low aspect ratio leakage flow is the dominant bladepath loss and in this case the GA has configured the blading for no overall increase in leakage loss.

Figure 3.7, overleaf, compares the efficiency improvement achieved by the GA with the efficiency penalty associated with a repeating stage design. Some early 50% reaction steam turbines were built with repeating stage groups, and for a five stage group with an aspect ratio of around 1.4 the efficiency difference between a smooth bladepath and a repeating stage is around 0.40 points, approximately four times that between a smooth bladepath and an optimised bladepath produced by the GA.

The efficiency difference between smooth and repeating stage bladepaths increases with decreasing aspect ratio. This is as expected, because the absolute levels of loss are greater at low aspect ratio (due to increased leakage and secondary flow) so a larger

change is to be expected for a given redistribution of loading. From this it would follow that the GA would be able to obtain a greater efficiency improvement over the mean-line design at lower aspect ratio. It was observed that the largest change of 0.148 occurred at an aspect ratio of 0.7, with smaller changes each of around 0.100 at aspect ratios of 0.35 and 1.4. This result is not fully understood, but it is postulated that the discrepancy is an artifact of the heuristic method. There is a potentially larger improvement for the low aspect ratio case, but the GA has not found it. As stated previously, this is a shortcoming of heuristic methods; only improved solutions are identified, and there are no guarantees of finding a true optimum within a reasonable timescale.

FIGURE 3.7. Variation of efficiency improvement with aspect ratio.

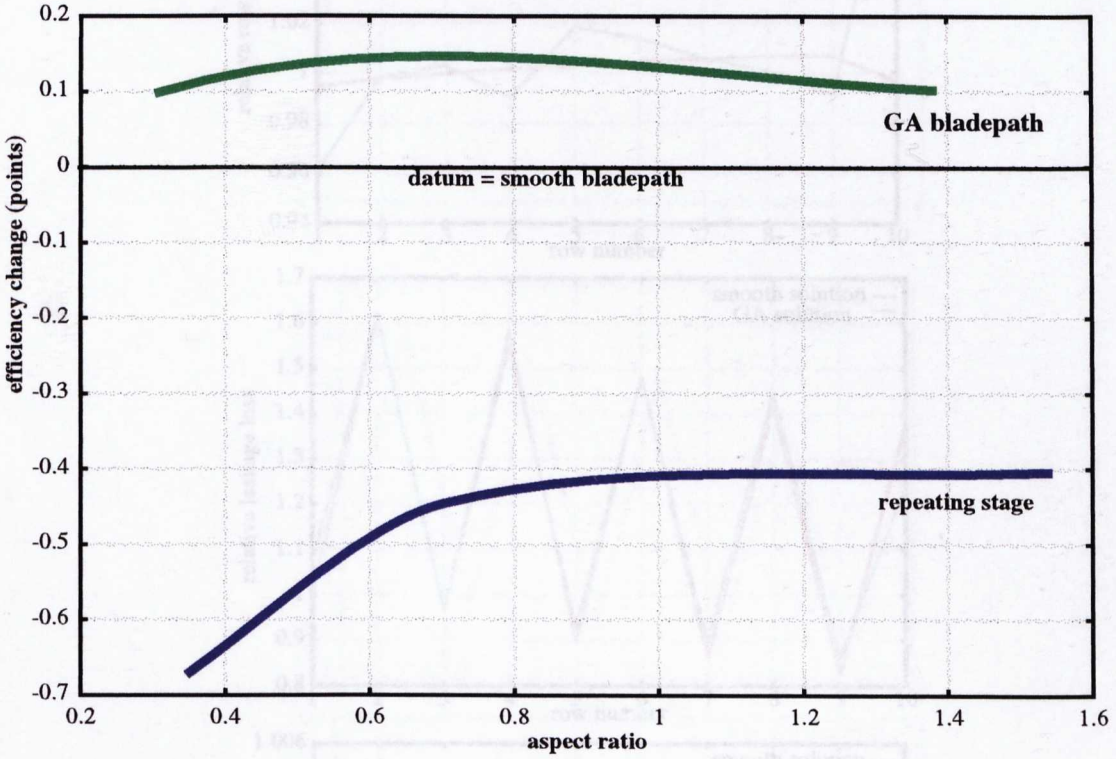

FIGURE 3.8. Five stage meanline design: aspect ratio = 1.433

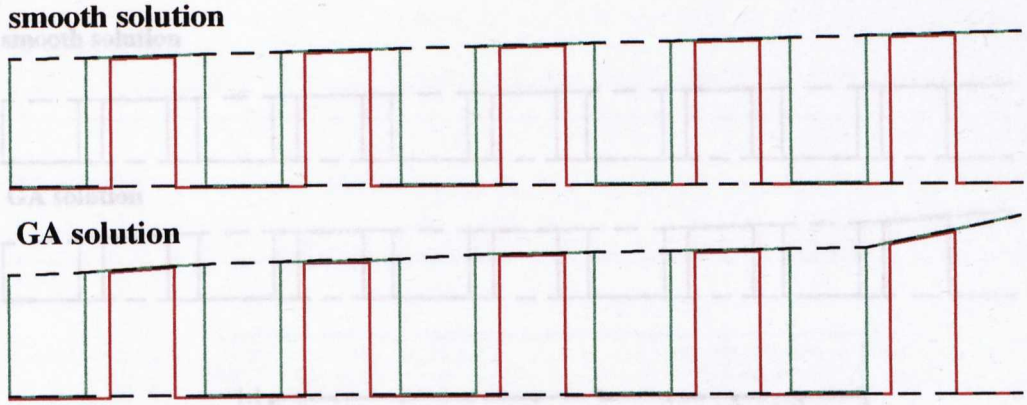

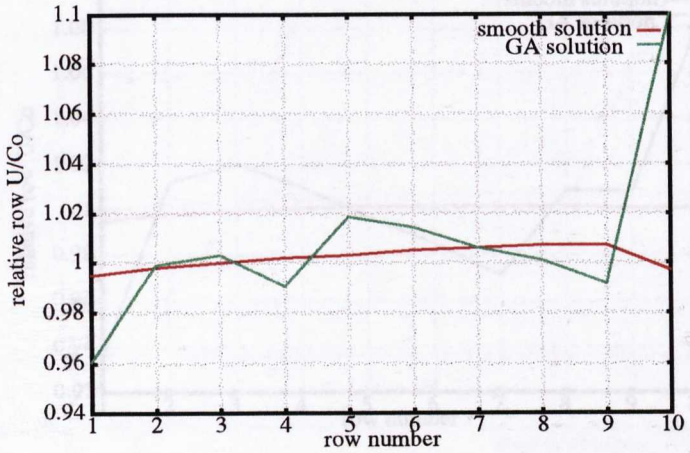

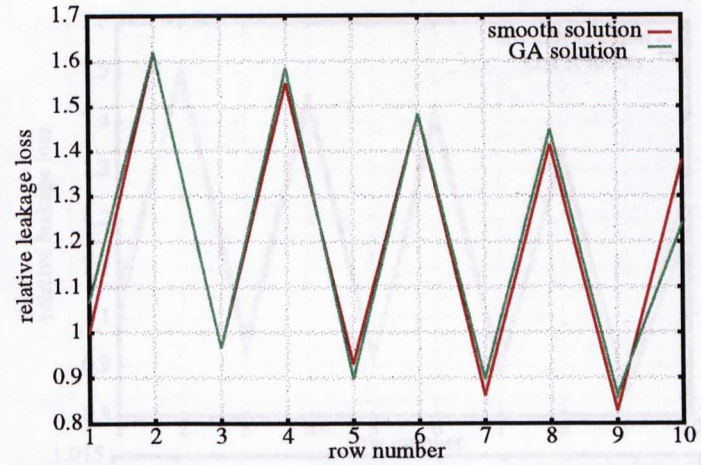

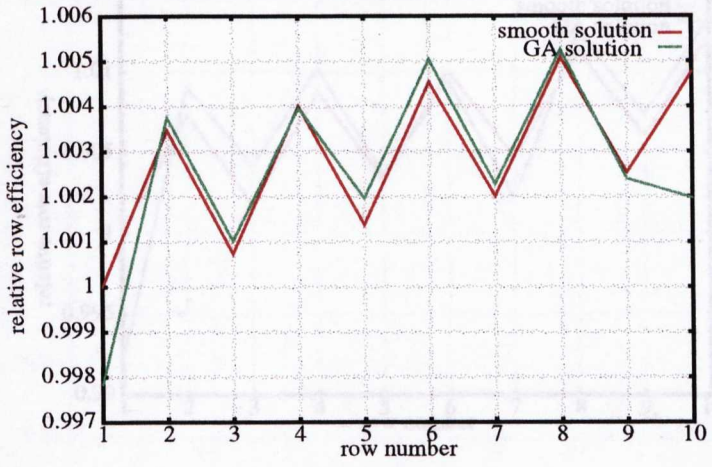

FIGURE 3.9. Five stage meanline design: aspect ratio = 0.697

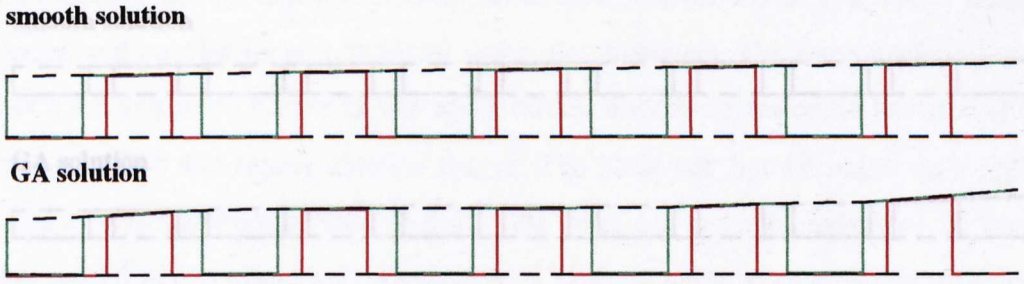

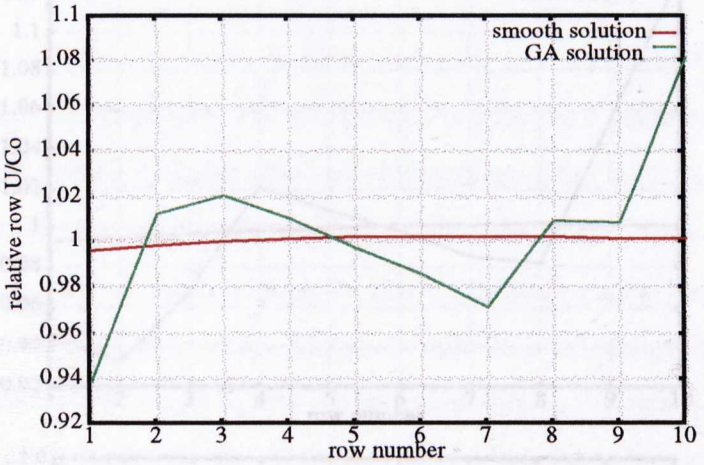

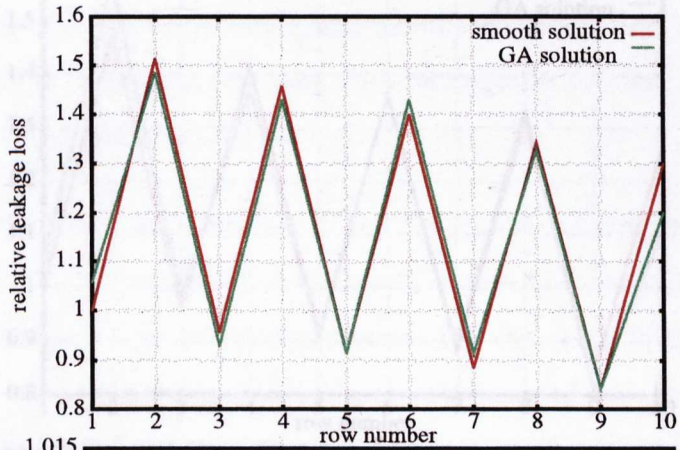

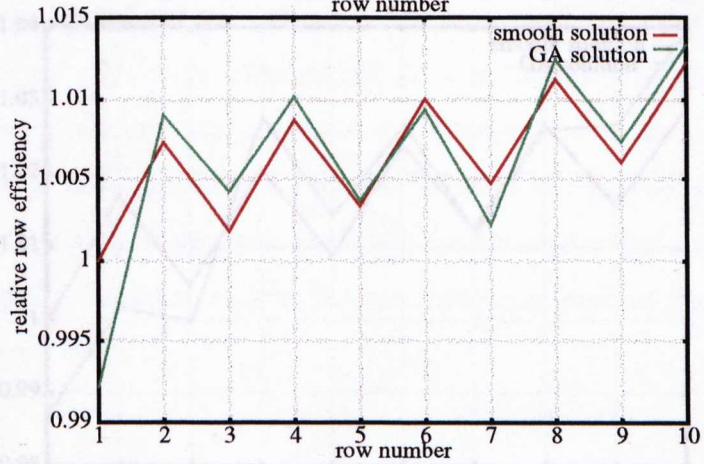

FIGURE 3.10. Five stage meanline design: aspect ratio = 0.328

smooth solution

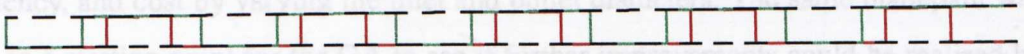

GA solution

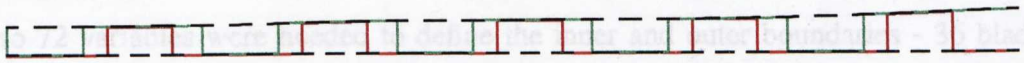

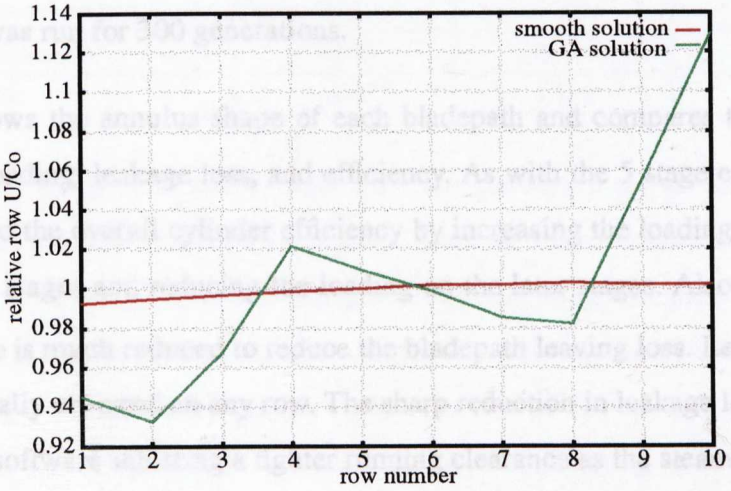

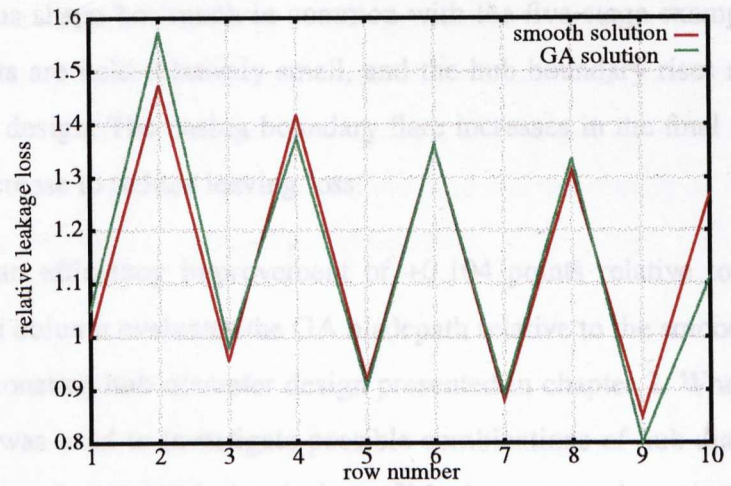

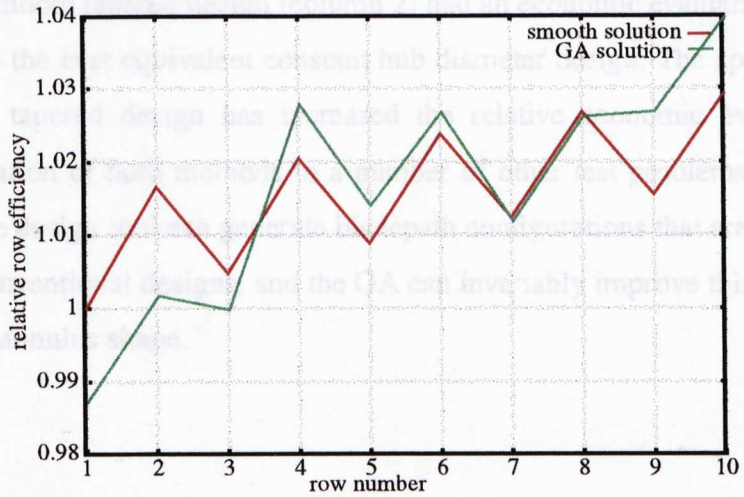

The final test case concerned the 250 MW HP turbine optimisation reported in chapter 2. The meanline design tool had determined an optimum bladepath in terms of length, efficiency, and cost by varying the inlet and outlet diameters. The same bladepath was used as a starting point for the GA to see if further improvements could be realised by adjusting the hub and casing annulus shapes. The bladepath has 18 stages on a rising hub so 72 variables were needed to define the inner and outer boundaries - 36 blade heights and 36 hub diameters. A population of 75 design configurations was used, and the calculation was run for 300 generations.

Figure 3.11, shows the annulus shape of each bladepath and compares the row-wise distribution of loading, leakage loss, and efficiency. As with the 5 stage examples, the GA has increased the overall cylinder efficiency by increasing the loading (reduced U/C_0) on the early stages and reducing the loading on the later stages. Also, the loading on the final stage is much reduced to reduce the bladepath leaving loss. Leakage losses are not substantially changed on any row. The sharp reduction in leakage loss after row 12 is due to the software selecting a tighter running clearance as the steam temperature falls. The annulus shape has much in common with the five stage example. The first few blade heights are held relatively small, and the hub boundary rises more rapidly than the smooth design. The casing boundary flare increases in the final stages as the blade heights increase to reduce leaving loss.

Table 5 shows an efficiency improvement of +0.104 points relative to the smooth design. The third column evaluates the GA bladepath relative to the smooth bladepath, and also to the constant hub diameter design presented in chapter 2. When the mean-line design tool was used to investigate possible combinations of hub diameter it was shown that the smooth tapered design (column 2) had an economic evaluation that was 8.8% better than the best equivalent constant hub diameter design. The application of the GA to this tapered design has increased the relative economic evaluation to +15.6%. Application of both methods to a number of other test problems has shown that the meanline design tool can generate bladepath configurations that are more cost-effective than conventional designs, and the GA can invariably improve this evaluation by tweaking the annulus shape.

TABLE 3.5. Bladepath efficiency improvement.

	blading configuration		
	smooth bladepath	GA bladepath	constant hub diameter
inlet aspect ratio	1.513	1.469	-
efficiency improvement (% points)	-	0.104	-
leaving loss (kJ/kg)	1.343	1.489	-
relative manufactured cost	0.941	0.945	1.000
relative bladepath length	0.936	0.936	1.000
relative evaluation	1.088	1.156	1.000

Both the meanline design tool and the meanline GA have been shown to improve the overall cost-effectiveness of reaction bladepaths. Each method produces configurations with novel features, but always at an existing level of technology. In general steam turbine efficiencies are now very high, and any further improvements in performance require increasingly costly development work - the law of diminishing returns most definitely applies. The current work demonstrates ways of obtaining more performance with existing technology, by exploring the design method more fully. The accuracy and sensitivity of such optimisations is very much dependent on the quality of the correlated data used within the meanline design method, and for this approach to have general applicability across a range of steam turbine products the validity of both cost and performance data will need to be regularly reassessed.

FIGURE 3.11. Eighteen stage meanline design optimisation.

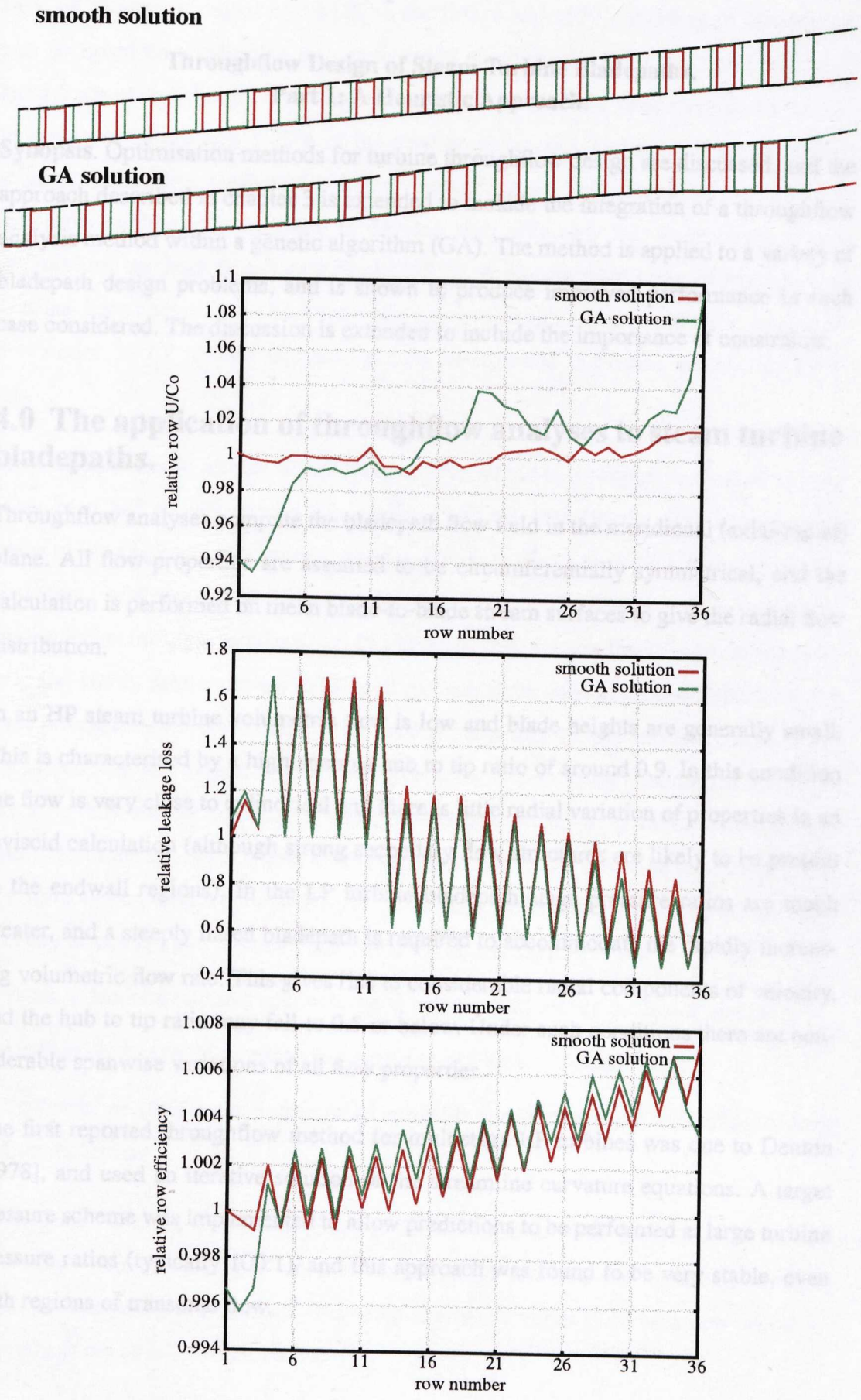

Chapter Four

Throughflow Design of Steam Turbine Bladepaths.
Part 1: A Heuristic Approach.

Synopsis. Optimisation methods for turbine throughflow design are discussed, and the approach described in chapter 3 is extended to include the integration of a throughflow analysis method within a genetic algorithm (GA). The method is applied to a variety of bladepath design problems, and is shown to produce improved performance in each case considered. The discussion is extended to include the importance of constraints.

4.0 The application of throughflow analyses to steam turbine bladepaths.

Throughflow analyses compute the bladepath flow field in the meridional (axial-radial) plane. All flow-properties are assumed to be circumferentially symmetrical, and the calculation is performed on mean blade-to-blade stream surfaces to give the radial flow distribution.

In an HP steam turbine volumetric flow is low and blade heights are generally small. This is characterised by a high annulus hub to tip ratio of around 0.9. In this condition the flow is very close to cylindrical and there is little radial variation of properties in an inviscid calculation (although strong secondary flow structures are likely to be present in the endwall regions). In the LP turbine bladepath stage pressure ratios are much greater, and a steeply flared bladepath is required to accommodate the rapidly increasing volumetric flow rate. This gives rise to considerable radial components of velocity, and the hub to tip ratio may fall to 0.5 or below. Under such conditions there are considerable spanwise variations of all flow properties.

The first reported throughflow method for multistage LP turbines was due to Denton [1978], and used an iterative solution of the streamline curvature equations. A target pressure scheme was implemented to allow predictions to be performed at large turbine pressure ratios (typically 100:1), and this approach was found to be very stable, even with regions of transonic flow.

Denton's method was used to analyse the flow-field in a number of 500 MW and 660 MW LP turbines installed in the UK in the 1960's and 1970's. Blading of this vintage was designed on a meanline or simple radial equilibrium (SRE) basis and often suffered from poor radial flow distribution and high losses. The final stage of an LP turbine may often produce 8-10% of the total power output, and improvements in final stage performance can often be extremely cost-effective. Many manufacturers and utilities have worked in partnership to develop high efficiency last stage blading using throughflow methods (e.g. Grant et al [1991]). A considerable body of experimental data has been accumulated both from site traverse work and test turbines and throughflow codes for LP turbine analysis can now be regarded as mature, established methods.

More recently steam turbine manufacturers have turned to throughflow methods for the analysis of HP and IP turbine bladepaths. Until the late 1980's most 50% reaction steam turbine builders used constant section blading throughout the HP and IP turbine bladepaths, and development work concentrated on the development of improved 2D blade profiles for these applications. Of particular interest was the strength of the aerofoil, and sturdy sections were developed that could be used at reduced chord for the same reference stress level, thereby increasing blade aspect ratio and reducing secondary losses (e.g. Bolter and Grant [1990]). It is widely accepted that further improvements in HP and IP turbine performance require the blading to be more closely optimised to the application, and more recently attention has turned to the development of families of tapered and twisted reaction blading. Denton and Wallis [1996] describe a family of tapered and twisted blades with the following properties:

- twist to produce uniform spanwise axial velocity and reduce incidence angles
- taper to control aerofoil pitch:chord ratio and optimise lift coefficient
- decreased aerofoil outlet angles at the endwalls to reduce the influence of secondary flow structures

Additionally Cofer [1996] and Singh et al [1995] have both described the use of tapered and twisted blading in low reaction HP and IP turbines, and the use of throughflow and time-marching methods to develop alternative vortex designs is now prevalent throughout the steam turbine industry.

4.1 Throughflow optimisation methods.

Relatively little has been published on the subject of optimising turbomachinery throughflow configurations. This is in part due to the increased computational expense of performing throughflow calculations. Typically, a meanline calculation for a multi-stage machine will be described by tens of variables and have a run-time of seconds. A throughflow calculation for the same machine could require in excess of one hundred variables and have a run-time of a few minutes. A natural consequence of the order of magnitude increases of both the number of variables and the code run-time is that the algorithmic time complexity function will increase by a factor of at least 10^4 and exactly optimised solutions will be extremely time consuming even for single stage calculations.

Table 4.1, summarises the published body of throughflow optimisation work. Each of the three papers originates from an academic institution; many manufacturers however have reported improvements in performance due to alternative vortex designs but only one has described a possible optimisation procedure (Wakeley and Grant [1996]).

Jenkins [1991] describes the use of simple radial equilibrium integrated within a pattern search method to optimise the vortex design of an aero-engine stage. Using a 2nd order polynomial work distribution a predicted stage efficiency of 89.9% is reported, compared to a starting point of 88.0% (free vortex). The improvement appears to originate from a tightening of the stator endwalls causing a reduced secondary loss prediction.

Massardo et al [1990c] describe the optimisation of a single axial flow compressor stage. Twenty-six variables per stage were used, and the optimisation included blade numbers, solidity, and spanwise variation of axial chord. An improvement of stage efficiency from 89.7% to 94.3% is reported, originating partly from a reduction in incidence losses and hub diffusion factor.

Cravero and Dawes [1997] coupled the Denton SLEQ program (Denton [1978]) to a NAG optimising algorithm and reported the optimisation of a single steam turbine stage. A performance improvement of around 2 points was achieved by restaggering existing blade sections. A subsequent 3D Navier-Stokes analysis of the original and

optimised configurations showed that much of the improvement originated from unloading the endwall regions and reducing the secondary losses.

Each of the reported methods considers a single stage in isolation, and Massardo et al commented that an analysis over a larger number of stages would require a prohibitive number of variables. Restricting the optimisation to a single stage precludes many commonplace design calculations, for instance:

- many manufacturers have a standard range of moving blades for use in the last two or three stages of the LP turbine. Frequently stator blades will be optimised to suit these fixed rotor blades for a certain application using a throughflow calculation for the full LP turbine.
- to minimise design work it may be necessary to design a rotor blade that will operate satisfactorily in a number of stages, for instance the first three stages of the LP turbine. If the design point varies from stage to stage a multistage calculation is required.
- hub:tip ratio gradually decreases through the HP and IP turbines and if an optimised stage by stage vortex design is sought this can only be achieved with a multistage analysis.

The following section describes the integration of a throughflow method within a genetic algorithm to produce a flexible general purpose multistage throughflow optimisation procedure. In this way the throughflow analysis code is converted into a design method. The discussion is continued to include the presentation of a number of test cases.

TABLE 4.1. Comparison of published turbomachinery throughflow optimisation methods.

		description of code					objective function	
		machine configuration	**analysis method**	**loss prediction method**	**optimisation method**	**number of variables**	**efficiency**	**constraints**
Massardo, Satta, and Marini [1990c]	University of Genoa	single stage axial flow compressor	stream function (matrix method)	Davis and Millar [1976]	Fletcher-Powell variable search	26, including inlet and outlet angles at 5 stations with a distribution of chord and solidity	maximise at design condition	rotor root stress, blade count, stall margin
Jenkins [1991]	Auburn University, Alabama	single stage axial flow gas turbine, hub:tip = 0.65	simple radial equilibrium	boundary layer method plus tip leakage loss	Hooke and Jeeves pattern search	not stated - spanwise work distribution is 2nd order polynomial	maximise at design condition	continuity satisfied through a penalty function
Cravero and Dawes [1997]	University of Cambridge, and Ansaldo	single stage axial flow steam turbine aspect ratio ~ 3.0	streamline curvature	Denton [1978]	multidimensional variable NAG E04JAF	not stated - appears to be only row inlet and outlet angles. Swirl distribution given by fourth order polynomial.	maximise at design condition	none stated

4.2 Application of a genetic algorithm to throughflow design.

In this section the integration of a throughflow solver within a genetic algorithm is presented. The solver used is a streamline curvature analysis method known as SLEQ, originally developed by Denton [1978] and subsequently by others within Parsons Power Generation Systems Ltd. The *myGENEsys* genetic algorithm (GA) as described in chapter 3 is used.

The throughflow optimisation problem is constrained by the starting point meanline design. Blade heights etc. are fixed, and the only variables are the blade inlet and outlet angles at a number of radial stations (three or five). It is assumed that the bladepath meridional coordinates will have been fixed by the meanline stress and vibration calculations, although there is usually some iteration required between the meanline and throughflow methods to achieve this. The throughflow specification of a bladerow therefore requires six or ten variables, compared to only three for the mean-line specification.

Figure 4.1 below schematically illustrates the initial generation of the starting point throughflow design. If an HP or IP bladepath is to be considered, a meanline design can be selected from the gallery of legal solutions, and processed to produce either a constant section or free-vortex throughflow dataset. Alternatively, in the case of LP design, the user may prefer to start from an existing dataset.

FIGURE 4.1. Generation of SLEQ input data.

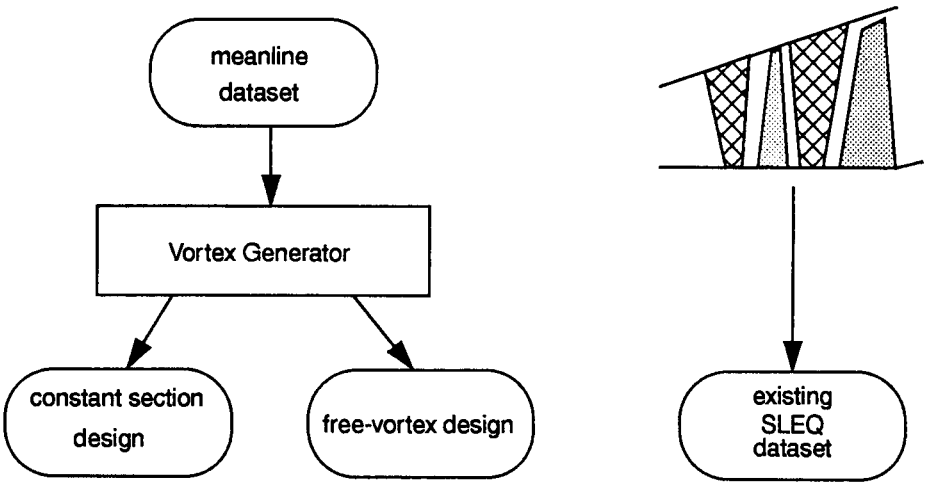

The genetic algorithm front-end combs the starting point throughflow dataset, and reads the description of the quasi-orthogonal (QO) grid upon which the calculation is performed. The user then chooses which (if any) bladerows are to remain fixed during the optimisation. In this manner one or more LP rotors can be fixed as required.

Data for the calculation can be specified on three or five radial stations as required. Three stations were generally used for HP and IP calculations with relatively large hub:tip ratios, and five stations were preferred for the low hub:tip ratios encountered in large output LP turbines. A parabolic interpolation is used to determine blade angles between those specified.

FIGURE 4.2. Generation of GA input data.

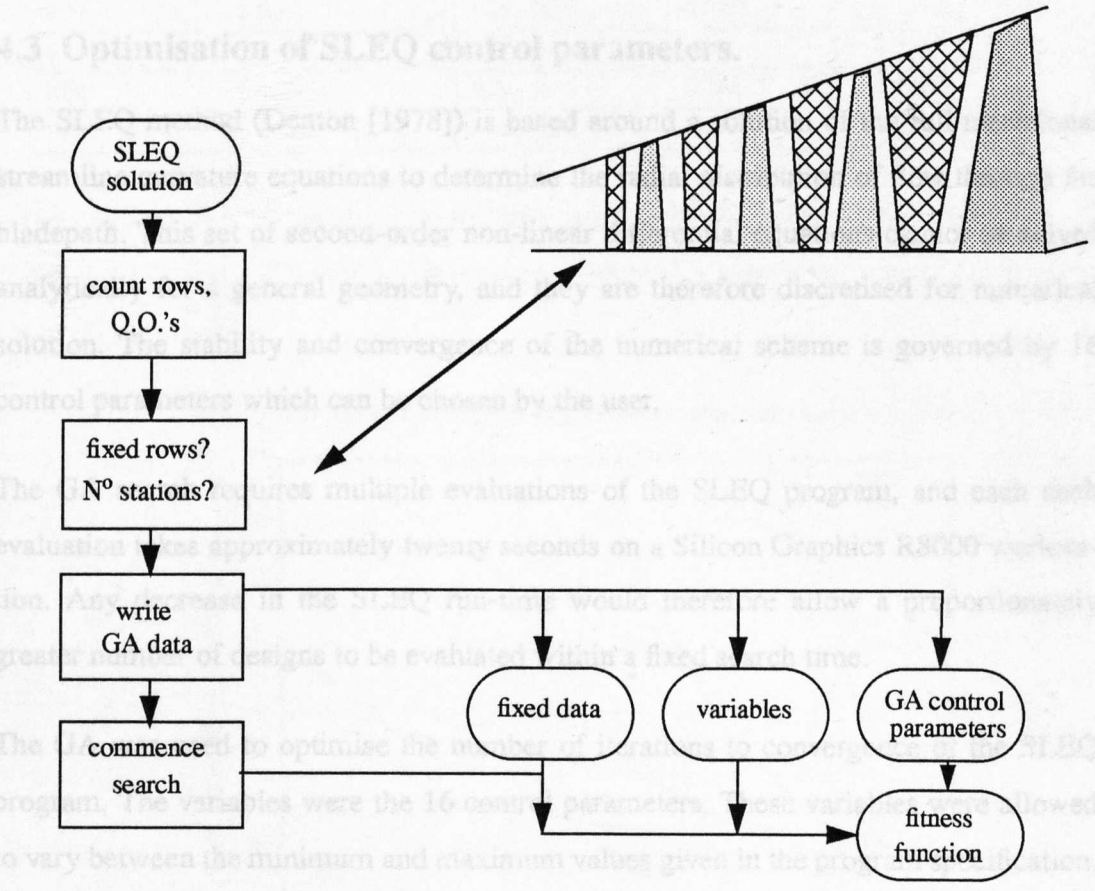

A range is required for each of the problem variables, and in general this range was centred around the starting point values. The default behaviour is to allow a range of +/-40 degrees for inlet angles and +/-10 degrees for outlet angles. When HP and IP

bladepaths are considered the midheight blade outlet angles can be held fixed if required such that the throughflow design is rigidly constrained to the meanline design.

The fixed and variable elements of the SLEQ dataset are written to separate GA initialisation files. On the first iteration of the GA the fixed data is copied into two memory maps, and the variable data read into arrays. A population of candidate designs is then generated by indexing pointers to the mapped data and inserting variable elements as required. This method allows extremely quick creation of members of the population without unnecessary file access.

The following sections summarise four test applications of the throughflow optimisation method. In the first the application of the GA to optimise the throughflow program control parameters is presented, followed by LP, IP, and HP multistage optimisations.

4.3 Optimisation of SLEQ control parameters.

The SLEQ method (Denton [1978]) is based around a solution of the full meridional streamline curvature equations to determine the radial distribution of flow through the bladepath. This set of second-order non-linear differential equations cannot be solved analytically for a general geometry, and they are therefore discretised for numerical solution. The stability and convergence of the numerical scheme is governed by 16 control parameters which can be chosen by the user.

The GA search requires multiple evaluations of the SLEQ program, and each such evaluation takes approximately twenty seconds on a Silicon Graphics R8000 workstation. Any decrease in the SLEQ run-time would therefore allow a proportionately greater number of designs to be evaluated within a fixed search time.

The GA was used to optimise the number of iterations to convergence of the SLEQ program. The variables were the 16 control parameters. These variables were allowed to vary between the minimum and maximum values given in the program specification, and where no range was given +/- 10% was used. The optimisation was performed for typical HP and LP bladepaths. Table 4.2 overleaf shows the default relaxation factors, and the results of the genetic algorithm search for a typical HP and LP bladepath.

TABLE 4.2. Optimised SLEQ control parameters

relaxation factors			GA results	
	default	range	HP turbine	LP turbine
ERF1	0.6	+/- 10%	0.545	0.594
ERF2	1.6	+/- 10%	1.500	1.540
ERF3	0.6	+/- 10%	0.599	0.577
ERF4	0.01	+/- 10%	0.00973	0.0116
ERF5	0.5	+/- 10%	0.493	0.402
ERF6	0.5	+/- 10%	0.467	0.449
RF1	0.25	0.25 - 0.50	0.324	0.334
RF2	0.25	0.25 - 0.50	0.255	0.398
RF3	0.06	0.05 - 0.08	0.0793	0.0756
RF4	0.50	0.00 - 0.50	0.230	0.252
RF5	0.001	+/- 10%	0.00107	0.00109
RF6	0.06	0.05 - 0.08	0.0664	0.0587
RF7	0.1	0.00 - 0.50	0.0245	0.0490
RF8	1.00	+/- 10%	0.975	1.05
RF9	0.25	0.20 - 0.40	0.344	0.397
RF10	0.0125	0.05 - 0.10	0.0968	0.0962

The GA was able to significantly improve the number of iterations to convergence for both the HP and LP examples attempted. Figure 4.3 shows the convergence history over 60 generations

FIGURE 4.3. Genetic algorithm convergence history.

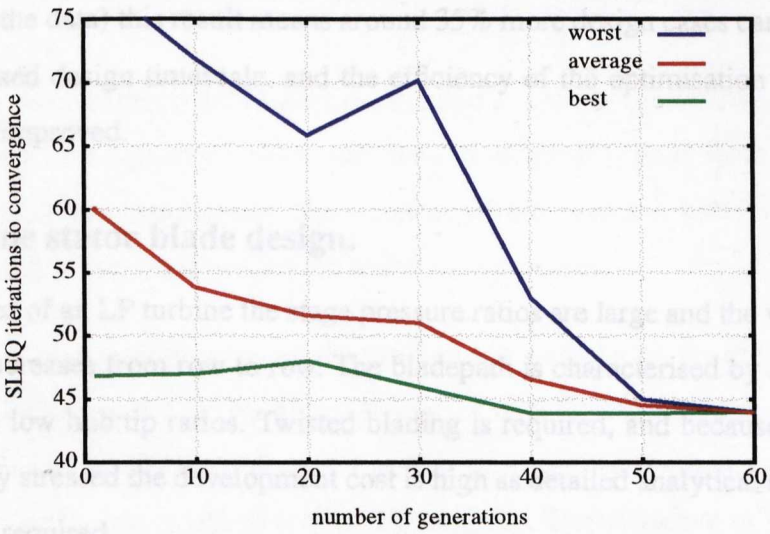

Much of the improvement has come from the initial randomisation of the control parameters. In the LP case described above the initial number of iterations to convergence was 67, and in the first generation a solution with 47 iterations has been created.

Even after 60 generations the GA has completely converged upon a solution with 44 iterations to convergence. It is noteworthy, however, that both the HP and LP cases considered resulted in very similar optimised control parameters. This is because for most applications the convergence is governed primarily by two relaxation factors, controlling meridional velocity and target pressure. For the purposes of all further calculations, the HP and LP optimised control parameters have been averaged. Table 4.3, below, shows the reduction in iterations to convergence.

TABLE 4.3.

	iterations to convergence		
	default RF's	**GA RF's**	**reduction (%)**
HP turbine	52	33	36.5
LP turbine	67	44	34.3

Wilkinson [1970] has shown that the stability and convergence of streamline curvature methods is related to the aspect ratio of the quasi-orthogonal grid, and it is probable that optimum relaxations factors could be deduced from an examination of the governing equations and geometry. However, it has not been necessary to perform such a detailed numerical analysis in the current work; the GA has determined appropriate relaxation factors that reduce the number of iterations to convergence by around 35% for both HP and LP turbines of widely different geometry. Since the SLEQ run-time is proportional to the number of iterations (excluding the overheads associated with reading and writing the data) this result means around 35% more design cases can be evaluated within a fixed design timescale, and the efficiency of the optimisation process is therefore much improved.

4.4 LP turbine stator blade design.

In the final stages of an LP turbine the stage pressure ratios are large and the volumetric flow of steam increases from row to row. The bladepath is characterised by significant casing flare and low hub:tip ratios. Twisted blading is required, and because the rotor blades are highly stressed the development cost is high as detailed analytical and experimental work is required.

For a typical LP turbine design a manufacturer will often select the final two or three stages of blading from a modular product range with the primary aim of reducing the turbine leaving energy rejected to the condenser. In such cases the meridional layout of

the bladepath is fixed, but the opportunity exists to redesign the stator blade profiles to improve the radial flow distribution, reduce rotor blade incidence, and fix interstage extraction pressures as required.

For this test case the application of a modular LP turbine to a new contract application was considered. The turbine is a standard 3000 rpm LP turbine from the standard product range of Parsons Power Generation Systems Ltd., and has four stages of 50% reaction blading followed by three stages of variable reaction blading. The final stage hub:tip ratio is 0.45. A meridional view through the bladepath is shown in figure 4.4.

FIGURE 4.4. Meridional view through modular LP turbine.

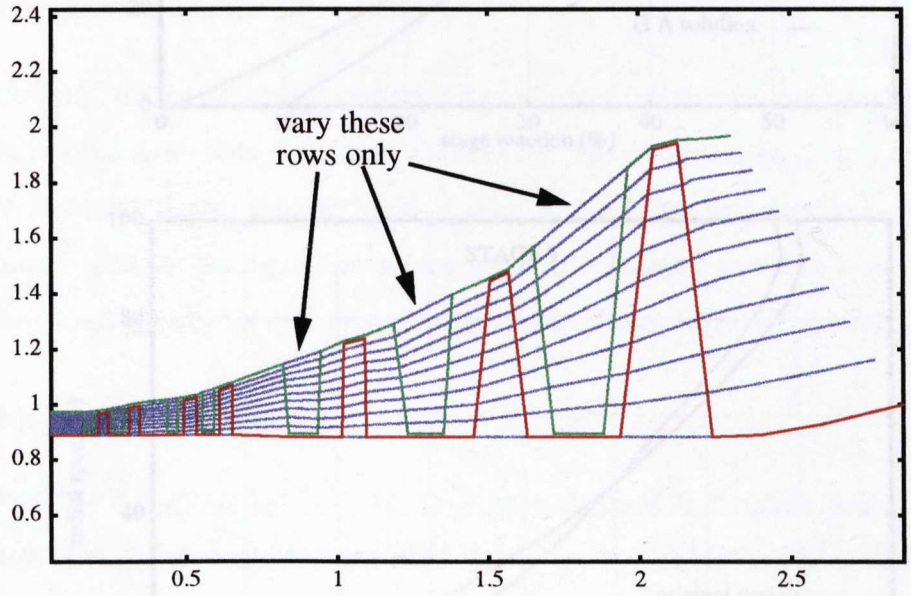

In the application considered the bladepath operated at a lower mass flow than the original design and consequently volumetric flow through the final three stages was reduced. The final and penultimate stages suffered from very low hub reaction, and it was known that this feature is associated with low efficiency.

An optimisation was performed using the throughflow calculation for the entire bladepath. Blade inlet and outlet angles were allowed to vary for the final three stator rows and every other row was held fixed. Stator angles were defined on three radial sections (hub, mid, and tip) so the problem was of 18 variables. The objective of the optimisation was to increase cylinder efficiency whilst ensuring that each stage maintained a healthy hub reaction. A population of 100 designs was considered over 100 genera-

tions, and convergence was observed after around 30 generations with an overnight run-time.

FIGURE 4.5. Radial distribution of stage reaction.

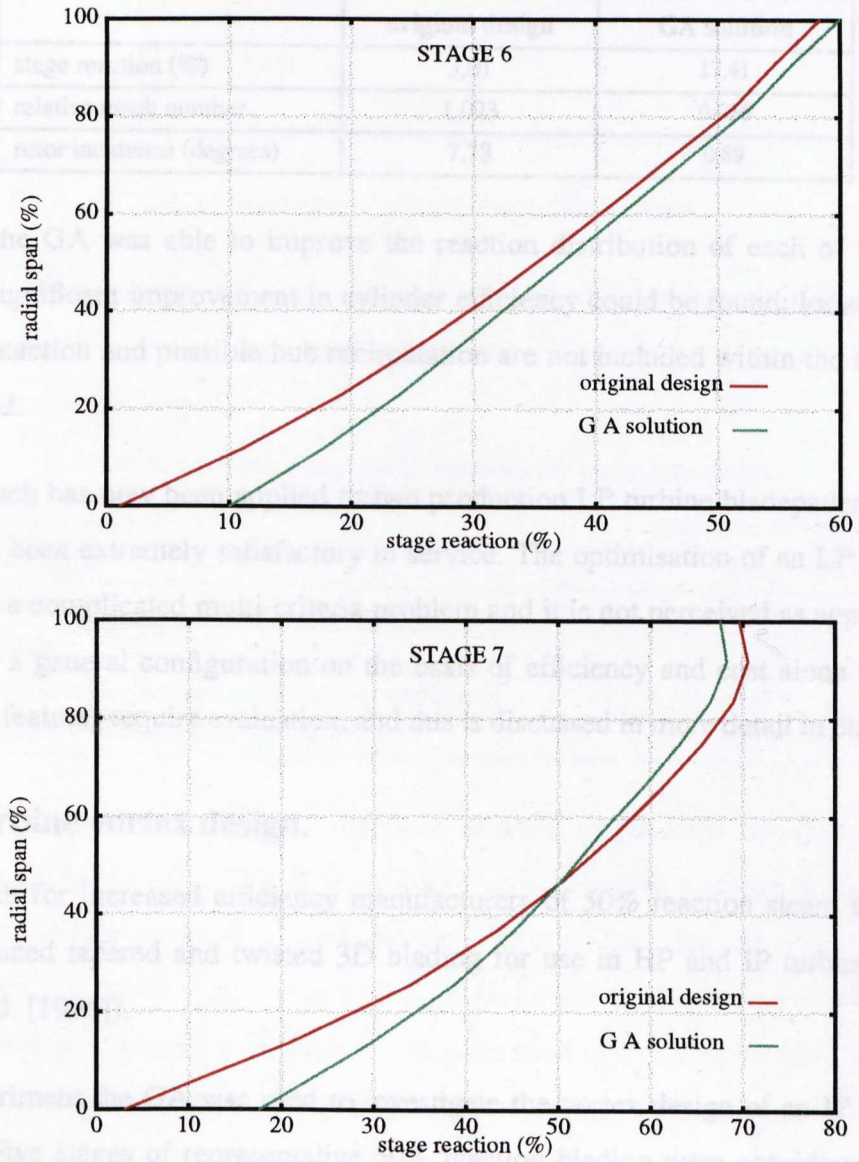

Figure 4.5, above, shows the radial distribution of stage reaction for stages 6 and 7. The GA has quickly learned that hub reaction can be increased by decreasing the stator blade hub outlet angle. This elevates the static pressure in the intra-stage gap and increases the mass flow through the rotor hub section. Considering stage 7, the GA has adjusted the radial work distribution, by decreasing the hub turning and increasing the tip turning. Additionally, stator blade incidence has been traded-off against rotor blade incidence, and the reduction in tip reaction serves to reduce leakage over the

unshrouded final stage rotor blade. Table 4.4 compares the original and optimised flow conditions at inlet to the rotor hub section.

TABLE 4.4. Conditions at stage 7 rotor hub.

	original design	GA solution
stage reaction (%)	3.01	17.41
relative mach number	1.023	0.956
rotor incidence (degrees)	7.78	0.89

Although the GA was able to improve the reaction distribution of each of the final stages no significant improvement in cylinder efficiency could be found; losses due to low stage reaction and possible hub recirculation are not included within the through-flow method.

This approach has now been applied to two production LP turbine bladepaths both of which have been extremely satisfactory in service. The optimisation of an LP turbine, however, is a complicated multi-criteria problem and it is not perceived as appropriate to optimise a general configuration on the basis of efficiency and cost alone. Instead many more features require evaluation, and this is discussed in more detail in chapter 5.

4.5 IP turbine vortex design.

In the search for increased efficiency manufacturers of 50% reaction steam turbines have introduced tapered and twisted 3D blading for use in HP and IP turbines (e.g. Denton et. al. [1996]).

In this experiment the GA was used to investigate the vortex design of an IP turbine bladepath. Five stages of representative 50% reaction blading were considered, with aspect ratio around 0.3 and hub:tip ratio of around 0.8. The blading was generated using the meanline design tool and is typical of the first bladegroup of a 250 MW IP turbine.

Each bladerow was defined by an inlet and outlet angle on three radial stations, and a polynomial interpolation was used to determine angles at intermediate heights. The meanline blade outlet angles were held fixed to constrain the solution to the meanline design. The optimisation problem was to vary the 60 blade angles to maximise the predicted cylinder efficiency.

Five separate calculations are referred to in this discussion. They are:

1. constant section design
2. free-vortex design
3. GA solution
4. GA solution with constrained streamtube smoothness
5. GA solution with constrained axial velocity

Table 4.5 below summaries the efficiency improvement achieved in each of the calculations, and figure 4.6, compares the radial distribution of stator exit yaw, axial velocity, and stage reaction for stage 3.

TABLE 4.5. Calculated SLEQ efficiency for five vortex designs.

blading configuration	calculated efficiency
(1) constant section	datum
(2) free-vortex design	+0.08%
(3) GA solution	+0.27%
(4) GA solution with constrained streamtube smoothness	+0.21%
(5) GA solution with constrained axial velocity	+0.12%

The constant section design shows a decrease in blade outlet angle as aerofoil pitch increases up the blade span. This is associated with a spanwise increase in stator exit axial velocity, and the streamlines move outwards through the rotor row. The free-vortex design has increased stator twist and is characterised by an inverse relationship between radius and tangential velocity. A consideration of the simple radial equilibrium equations shows that this condition is consistent with a constant spanwise distribution of axial velocity and no streamline shift through the blade rows (at least for incompressible flow).

It was anticipated that the GA would rapidly converge upon a free-vortex (or constant mass flux) design as such designs have been extensively used in gas turbine design for many decades. Instead, the GA optimised efficiency using a constant reaction design, which is characterised by almost constant stator outlet absolute velocity, and increased rotor swirl angles at hub and tip. This arrangement, with tighter blade settings at the endwalls, diverts flow towards the blade midheight and causes a pronounced outward streamtube shift through the rotor row. It can be seen that axial velocity is significantly

increased at midspan. This radial flow redistribution significantly reduces stator leakage flow, as the hub reaction is increased from 36% to 46% reducing the stator pressure drop. Equivalently, rotor over-tip leakage is reduced by reducing the tip reaction form 53% to 48%.

The streamtube shift associated with tightening the stators at the endwalls is shown in figure 4.7. Intuitively increased streamtube migration appears to be an undesirable effect. In an axial flow turbomachine steady work can only be extracted from the flow by the exchange of tangential momentum with the shaft, and streamtube migration is associated with increased radial velocity that must ultimately manifest itself as loss. When any flow with a radial component is turned through a blade passage components of streamwise and normal vorticity arise. The loss associated with this inviscid effect is increased by the stretching of vortex lines in the downstream bladerow.

It was postulated that the GA's preference for a constant stator absolute exit velocity could be due to an artifact of the SLEQ loss calculation method. SLEQ uses correlations to determine the bladerow profile, secondary, and tip leakage loss coefficients, and these are summed along the streamline at each blade trailing edge and applied to the exit dynamic enthalpy to calculate a specific loss. Clearly then the GA can reduce the generation of loss in one of two ways: either by adjusting blade angles to minimise the loss coefficients (e.g. by reducing incidence) or by reducing the exit dynamic head. For a given massflow and tangential momentum the exit dynamic head can be reduced by arranging the flow for constant absolute velocity.

To investigate the importance of streamtube migration two further optimisations were performed. For each of these the objective was to maximise efficiency, with a penalty function applied to changes in streamline curvature in the first case, and gradients in axial velocity in the second case. Changes in streamline curvature were computed by calculating a streamtube variation factor (SVF), which is the rate of change of streamline curvature integrated through the bladepath at each streamline-QO intersection.

$$SVF = \left(\sum_{r=0}^{N_{str}} \left\{ \sum_{i=0}^{N_{qo}} \left\{ \frac{r_{(i+1)} - 2r_i + r_{(i-1)}}{\Delta x^2} \right\} \right\} \right) \times \frac{1}{N_{qo}}$$

FIGURE 4.6. Stage 3 - radial variation of axial velocity, stator yaw, and reaction.

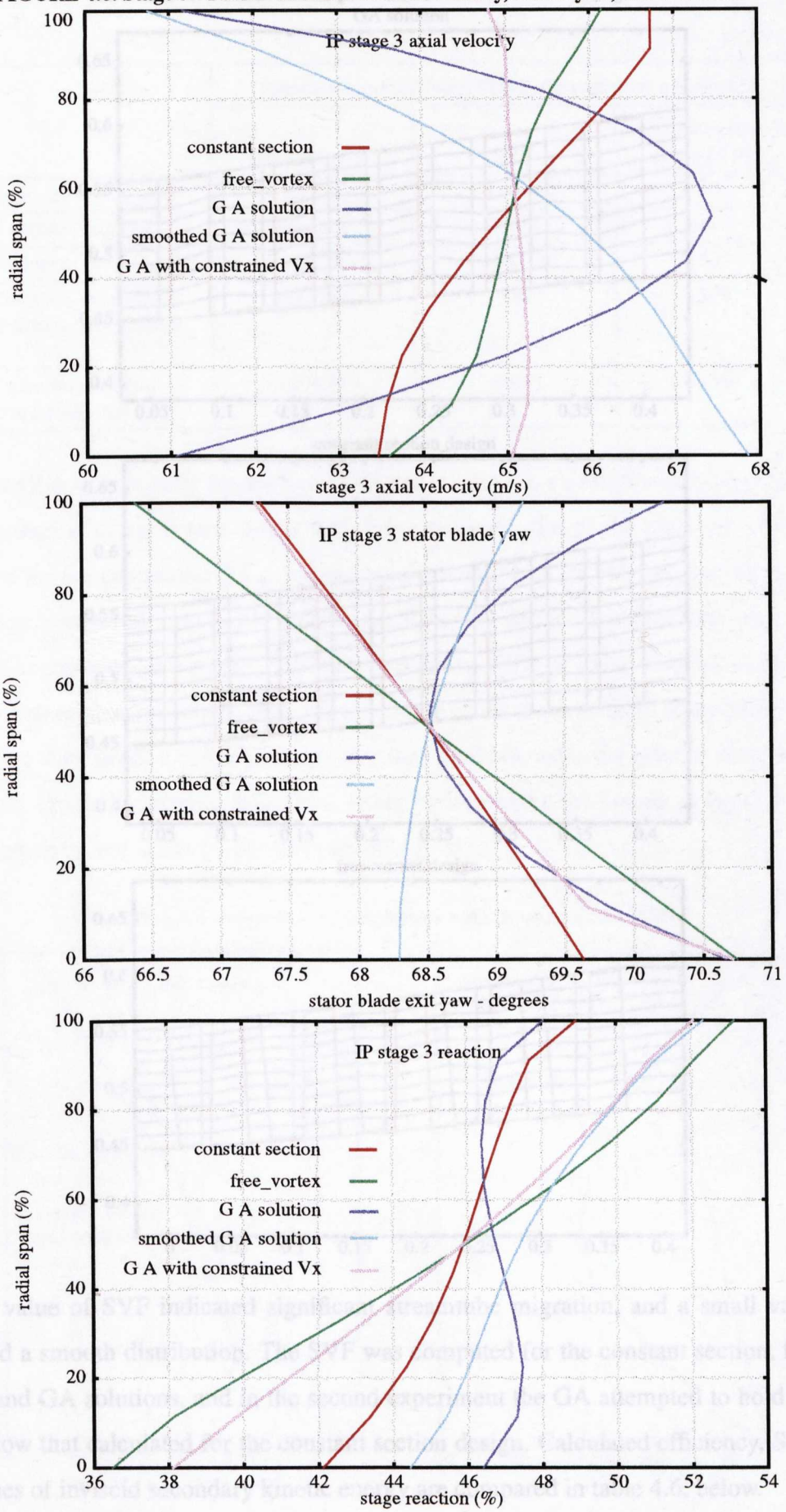

FIGURE 4.7. Streamtube positions for three vortex designs.

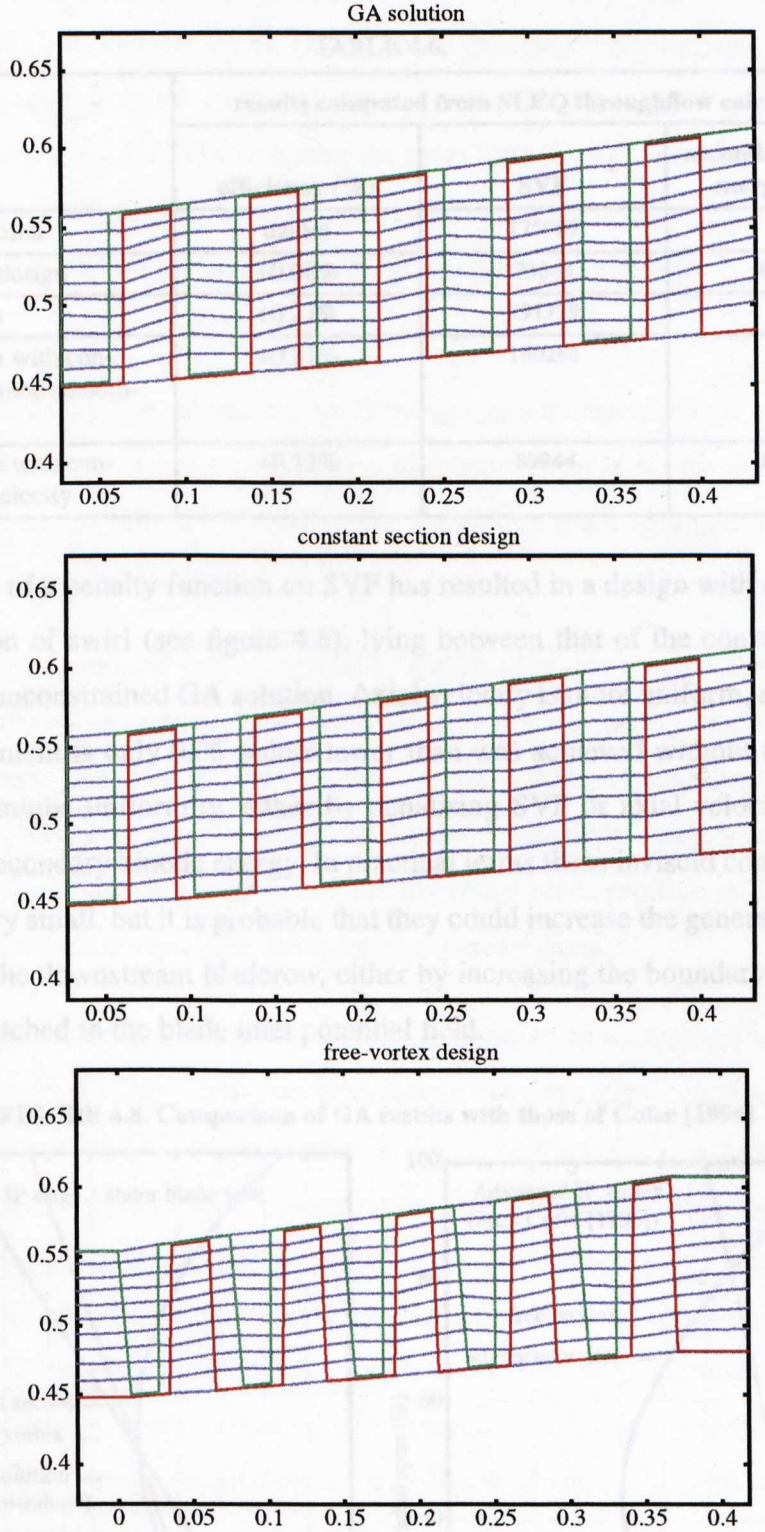

A large value of SVF indicated significant streamtube migration, and a small value described a smooth distribution. The SVF was computed for the constant section, free vortex, and GA solutions, and in the second experiment the GA attempted to hold the SVF below that calculated for the constant section design. Calculated efficiency, SVF, and values of inviscid secondary kinetic energy are compared in table 4.6, below.

TABLE 4.6.

	results computed from SLEQ throughflow calculation		
	efficiency (%)	**SVF**	**secondary kinetic energy (J/kg)**
(1) constant section	datum	175969	2.93
(2) free-vortex design	+0.08%	73363	0.045
(3) GA solution	+0.27%	291729	5.31
(4) GA solution with constrained streamtube smoothness	+0.21%	160264	2.64
(5) GA solution with constrained axial velocity	+0.12%	89944	0.520

The application of a penalty function on SVF has resulted in a design with a more uniform distribution of swirl (see figure 4.6), lying between that of the constant section design and the unconstrained GA solution. Axial velocity is more uniform, and the efficiency improvement is only 0.06 points lower than was achieved without the penalty. Increased streamtube uniformity, either by penalising SVF or axial velocity, reduces the stator exit secondary kinetic energy. In practical terms these inviscid components of vorticity are very small, but it is probable that they could increase the generation of secondary loss in the downstream bladerow, either by increasing the boundary layer skew or by being stretched in the blade inlet potential field.

FIGURE 4.8. Comparison of GA results with those of Cofer [1996]

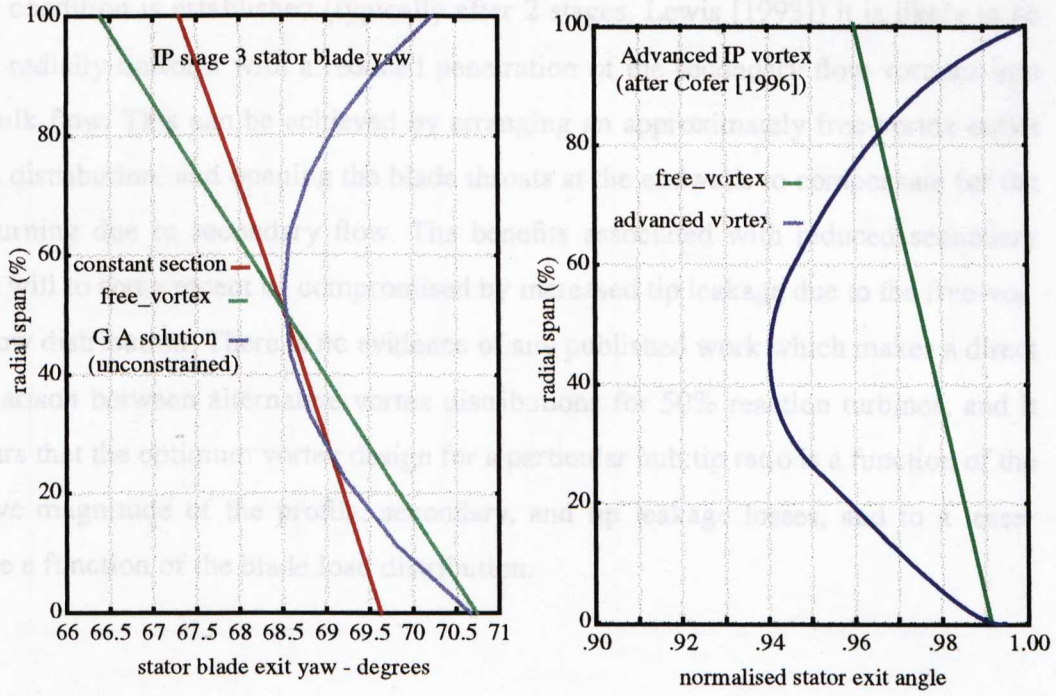

Several other workers (Cofer [1996], Dorman et. al. [1968], Schlegel et. al. [1976], Singh et. al. [1995], Kawagishi et. al. [1991]) have reported improvements in turbine efficiency by tightening stator angles at the endwalls. This is argued to reduce the strength of the secondary flows by reducing the mass flow through the relatively inefficient endwall regions. These workers have all considered low reaction blading, and the only published work on twisted blading for 50% reaction steam turbines is due to Denton et. al. [1996].

Figure 4.8 compares the GA solutions with IP turbine results reported by Cofer [1996] working at GE. He shows a stator outlet angle distribution that is comparable in shape to the optimised unconstrained GA results, but the neither the magnitude of the twist nor the aspect ratio can be deduced.

All of the published work reports an increase in efficiency, but in each case it is not possible to determine the origins of the improvements nor the quality of the reference design. For instance Singh et al [1995] report a small efficiency improvement using stators that are tightened at the endwalls in conjunction with some compound lean, yet it appears that some of the gain originates from improved blade profiles, and it is speculated that the reference design had relatively poor performance.

In the multistage environment at least, efficiency is likely to be maximised by increasing the uniformity of the flow from one bladerow to the next. Thus when a repeating stage condition is established (typically after 2 stages, Lewis [1993]) it is likely to be more radially uniform with a reduced penetration of the secondary flow vortices into the bulk flow. This can be achieved by arranging an approximately free-vortex outlet angle distribution, and opening the blade throats at the endwalls to compensate for the overturning due to secondary flow. The benefits associated with reduced secondary flows will to some extent be compromised by increased tip leakage due to the free-vortex flow distribution. There is no evidence of any published work which makes a direct comparison between alternative vortex distributions for 50% reaction turbines, and it appears that the optimum vortex design for a particular hub:tip ratio is a function of the relative magnitude of the profile, secondary, and tip leakage losses, and to a lesser degree a function of the blade load distribution.

4.6 HP turbine vortex design.

The calculation procedure outlined in section 1.5 was repeated for five stages of HP reaction blading, typical of the first group of a 250 MW HP turbine, with an aspect ratio of 0.7 and a hub:tip ratio of 0.93.

In this instance the GA has dramatically opened the stator hub angles and tightened the casing angles. At very low aspect ratio the efficiency becomes dominated by leakage loss and this reversal of the stator twist increases hub reaction with a lesser effect on the tip reaction, reducing tip leakage loss.

TABLE 4.7. Calculated SLEQ efficiency.

	efficiency (points)
constant section design	datum
free-vortex	+0.25
GA solution	+0.42

Figure 4.10, overleaf, compares the radial distribution of stator exit yaw, axial velocity, and stage reaction for stage 3. Once again, the solution has moved closer to constant absolute stator velocity which also serves to reduce the overall loss by reducing the span-wise averaged stator dynamic enthalpy. Figure 4.9 shows a comparative change in HP vortex distribution reported by Cofer [1996] with a low reaction HP steam turbine stage. Unfortunately normalised angles are plotted and hub:tip and aspect ratios are not given so a quantitative comparison is not possible.

FIGURE 4.9. Comparison of GA results with those of Cofer[1996].

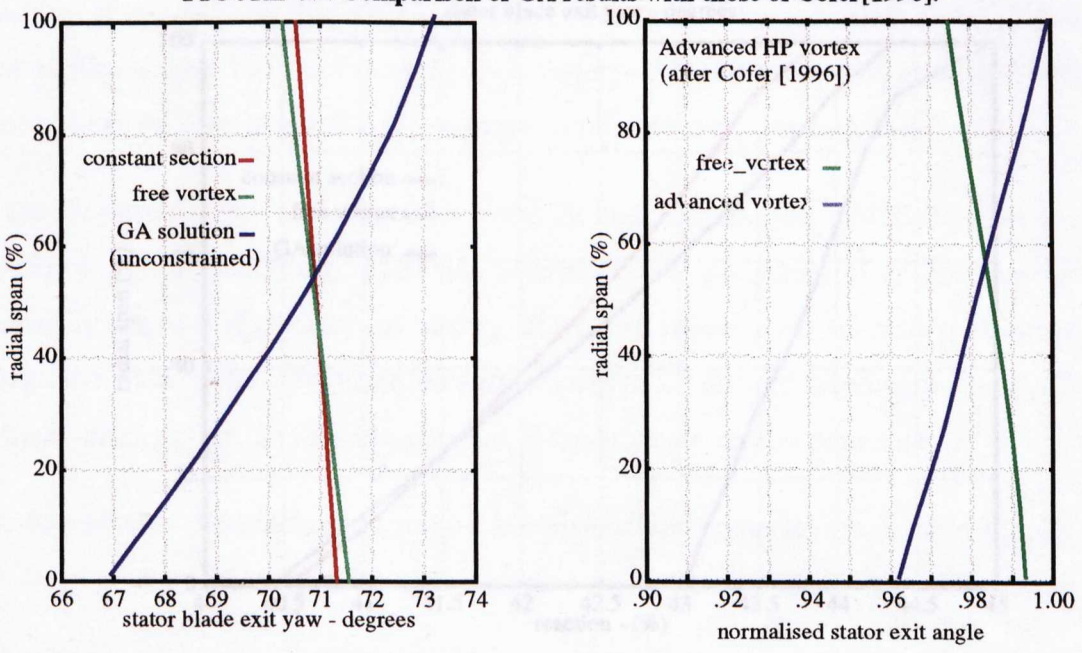

FIGURE 4.10. Stage 3 - radial variation of axial velocity, stator yaw, and reaction.

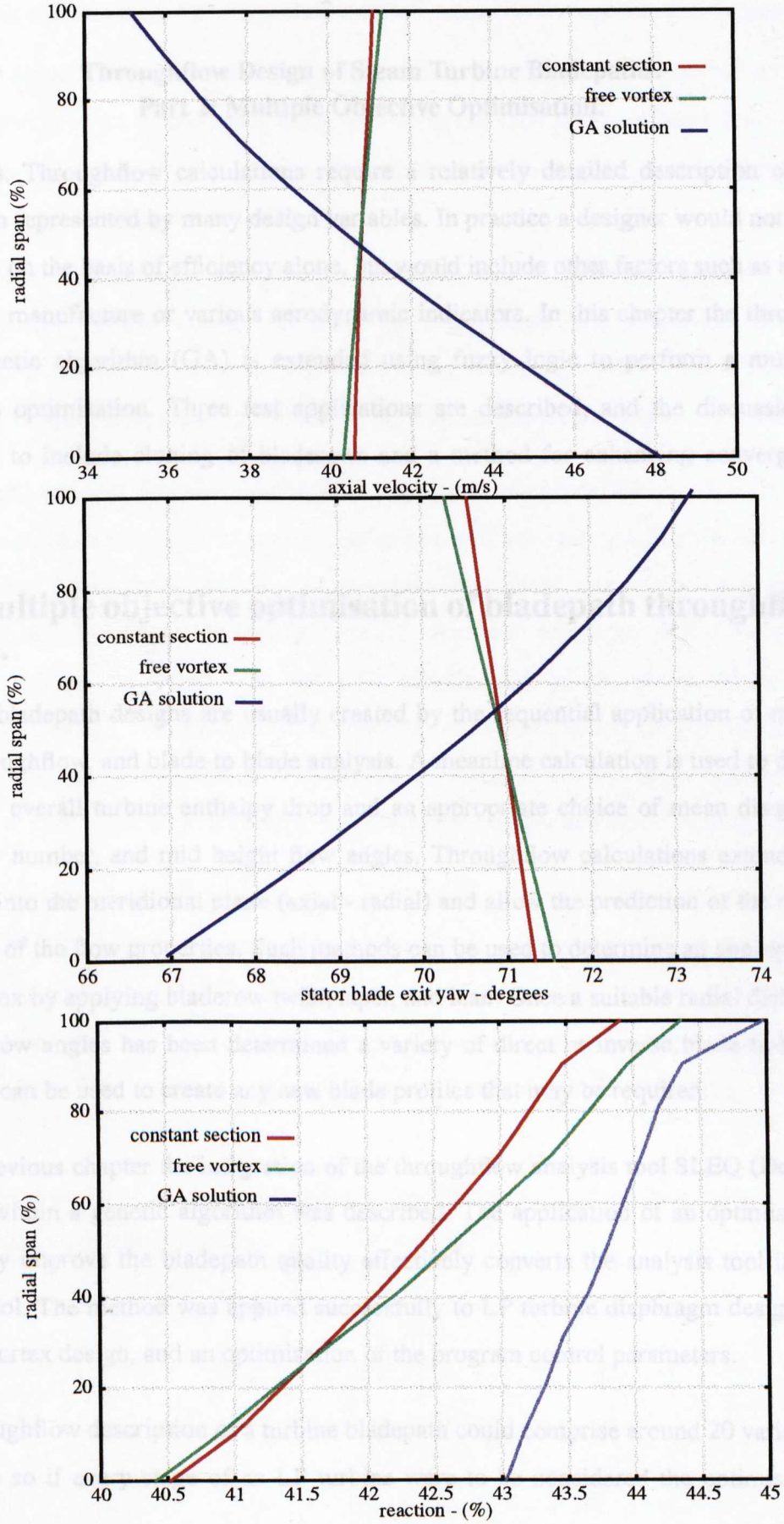

Chapter Five

Throughflow Design of Steam Turbine Bladepaths.
Part 2: Multiple Objective Optimisation.

Synopsis. Throughflow calculations require a relatively detailed description of the bladepath represented by many design variables. In practice a designer would not rank solutions on the basis of efficiency alone, but would include other factors such as suitability for manufacture or various aerodynamic indicators. In this chapter the throughflow genetic algorithm (GA) is extended using fuzzy logic to perform a multiple objective optimisation. Three test applications are described, and the discussion is extended to include cloning of bladerows and a method for enhancing convergence times.

5.0 Multiple objective optimisation of bladepath throughflow design.

Turbine bladepath designs are usually created by the sequential application of meanline, throughflow, and blade to blade analysis. A meanline calculation is used to determine the overall turbine enthalpy drop and an appropriate choice of mean diameter, bladerow number, and mid height flow angles. Throughflow calculations extend this analysis into the meridional plane (axial - radial) and allow the prediction of the radial variation of the flow properties. Such methods can be used to determine an appropriate flow vortex by applying bladerow twist, taper, and lean. Once a suitable radial distribution of flow angles has been determined a variety of direct or inverse blade-to-blade methods can be used to create any new blade profiles that may be required.

In the previous chapter the integration of the throughflow analysis tool SLEQ (Denton [1978]) within a genetic algorithm was described. The application of an optimiser to iteratively improve the bladepath quality effectively converts the analysis tool into a design tool. The method was applied successfully to LP turbine diaphragm design, IP turbine vortex design, and an optimisation of the program control parameters.

The throughflow description of a turbine bladepath could comprise around 20 variables per stage so if every stage of an LP turbine were to be considered the optimisation

problem might comprise 140 variables. The design problem is therefore of relatively large order and this causes two significant complications in the optimisation procedure:

1. In this application each of the variables is a blade metal angle. If the overall solution is judged in terms of efficiency alone the fitness can only be a very weak function of any one of the flow angles; that is a blade angle must change by a significant amount before the efficiency is influenced.
2. It is observed that most design engineers would not judge design quality by efficiency alone. Whilst turbine efficiency should obviously be an important criterion, other more subjective rankings might be applied. An example of this might be 'solution X is better than solution Y because moving blade Mach numbers are lower'.

These complications increase convergence time and can reduce the quality of the fitness evaluation, resulting in 'optimised' solutions which are not practical for manufacture or that suffer from obvious shortcomings that could not be detected by the optimiser. Application of the throughflow GA described in chapter 4 to a variety of design problems has shown that whilst the singular aim of improving efficiency is invariably achieved, solutions can have obvious deficiencies which are not fully represented by the throughflow loss models but are immediately obvious to the designer. An example of this might be a large value of flow Mach number at a blade leading edge.

A series of numerical experiments were performed to develop a strategy for robust multiple objective optimisation of the throughflow design work in an attempt to improve the performance of the optimiser in heavily constrained design spaces. Other code developments were undertaken to improve the performance and user-friendliness of the method. The main areas of improvement, described in the following sections, are:

1. The application of fuzzy logic within a GA fitness function to resolve constraints and multiple design objectives.
2. Use of identical blade profiles for two or more bladerows by cloning.
3. Development of a graphical user interface.
4. Accelerated convergence using a variable population size.

5.1 Resolving constraints and multiple design objectives.

In chapter 4 the optimisation of LP turbine design has been investigated using SLEQ and a genetic algorithm (GA). The optimisation problem was posed as 'maximise the calculated throughflow efficiency subject to a number of constraints'. Constraints were posed as penalty functions, and were of the form 'if hub reaction is less than 10% penalise efficiency'.

In reality, however, a designer will probably consider very many more factors than just efficiency when judging possible throughflow solutions. For instance, decisions are often influenced by incidence angles, flow mach numbers, or the radial distribution of flow variables. The number of features which distinguish a good design from a bad design is probably quite large, and it is not really practical to rigidly code firm rules or constraints against which to rank solutions. Equally, when two design requirements are in direct conflict (e.g. large blade height and low blade stress) the optimiser must be able to robustly exploit the trade-off.

The fundamental problem is that the evaluation of a design (in terms of *usefulness* or *value*) is not an absolute parameter but must somehow be gauged in terms of certain requirements (see for instance discussion in Pahl and Beitz [1996], chapter 4, page 71 et seq.). This evaluation must therefore embody all aspects of the design in the appropriate balance whilst remaining sufficiently robust to work well over the entire range of possible turbine bladepaths.

To obtain a fairly comprehensive list of design requirements for an LP turbine throughflow design a survey was made of the design engineers within the Turbine Design Department of Parsons Power Generation Systems Ltd.. The engineers were simply asked to list those features for which they would look when examining a throughflow design. The following list has been divided into requirements that were regarded as essential (MUST) and additional design features which were preferred but do not necessarily occur in all machines (WISH).

FIGURE 5.1. Design requirements for LP turbine throughflow design.

1.	Rotor inlet mach number less than unity.	WISH
2.	Stage reaction greater than 10% over span.	MUST
3.	Rotor and stator incidence angles less than 10 degrees over span.	WISH
4.	Final stage exit flow is axial or slightly underturned.	WISH
5.	Leaving energy is minimised.	WISH
6.	Exit yaw is uniform.	WISH
7.	Correct massflow is swallowed. (+/- 1%)	MUST
8.	Correct inlet pressure is achieved.(+/- 1%)	MUST
9.	Extraction pressures are achieved.(+/- 5%)	MUST
10.	Streamline curvature is minimised.	WISH
11.	Uniform spanwise massflow distribution.	WISH
12.	Uniform spanwise work.	WISH
13.	Uniform spanwise axial velocity - free vortex.	WISH
14.	Calculation is fully converged.	MUST
15.	Standard aerofoil profiles are used.	WISH

As might be expected, the list does not give fifteen independent design objectives, but instead expresses a much smaller number of requirements in alternative forms, e.g. statements 4,5, and 6 are all features of a moderately loaded exhaust, and statements 7 and 8 both result from correctly sizing the turbine swallowing capacity.

During the code development period a recently constructed 250 MW LP turbine was considered as a test case. The bladepath had seven stages, the first four of which were of standard 50% reaction design and had been sized to achieve the required turbine swallowing capacity and feedheater extraction pressures. The final three stages comprised a standard bladeset of highly tapered and twisted rotor bladerows, for which stator blades were to be designed to suit. The objective of the optimisation was to increase

the turbine efficiency by adjusting the stator inlet and outlet angles for the final three LP stages within the constraints of a fixed meridional layout.

The GA paradigm is centred around the notion of 'fitness'; a fitness function is used to rank the population prior to the selection process. For the range of turbine bladepath problems discussed this function generates data for the throughflow solver, runs the solver, and interprets the results to determine a value of fitness for each member of the population. For this test case three experimental fitness functions were applied, as described in the following sections.

5.1.1 Fitness function A - maximise efficiency and penalise stage reaction.

All optimisation procedures ultimately rely upon the maximisation or minimisation of one objective variable, and if a multiple objective problem is to be attempted the additional design requirements must be represented in the definition of solution fitness. This can be achieved using penalty functions.

FIGURE 5.2. Alternative forms of penalty function

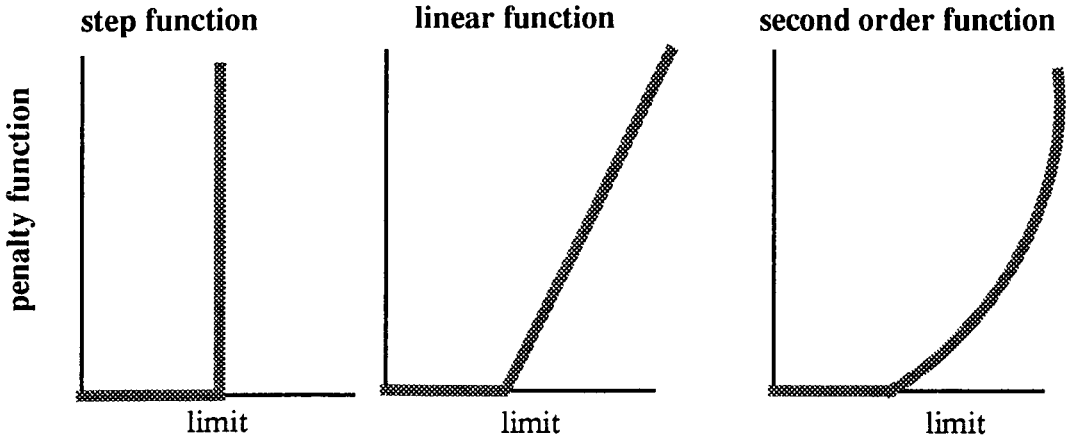

Figure 5.2 shows three alternative forms of penalty function. In each case the solution fitness is penalised when the design parameter, perhaps blade stress, exceeds a predefined limit. If the constraint is 'hard' and must be satisfied the step penalty function will be effective at excluding solutions that have blade stress in excess of the limit. Invariably the optimiser will then work on one side of the constraint boundary and favour designs that are distant from it, and the constraint will be easily satisfied but it

will be more difficult to achieve other design objectives (e.g. improve efficiency) as the constraint can dominate the selection pressure. The linear and second order penalty functions impose a less rigid constraint on the optimisation procedure (directly related to the degree of violation), and allow the GA to exploit the 'trades and balances' between constraints. Although this approach is simple to implement it is often not sufficiently robust for complex design problems. Often it is necessary to vary the influence of the penalty function during the search such that it has little effect during the early phase and allows a wide space to be explored, but imposes a tighter adherence to the constraints as the search progresses. Additionally, the constraints and objective function need to be appropriately balanced such that increased fitness is not traded-off against increased constraint violation. In this way an improved solution can be found but only with penalty functions that are tuned to the problem.

For this example the optimiser attempts to maximise turbine efficiency, and applies a simple linear penalty function if the stage reaction level falls below 10% on any streamline. The definition of fitness is as follows:

minimise

$$f(n) = (1 - \eta) + \frac{(10 - reaction)}{100} \qquad \text{for reaction} < 10\%$$

$$f(n) = (100 - \eta) \qquad \text{for reaction} > 10\%$$

A fitness function of this sort was used in chapter 3 to constrain the meanline inlet pressure and in chapter 4 to constrain the LP stage reaction.

5.1.2. Fitness function B - maximise efficiency and minimise constraint violation.

In the list of design requirements, given in figure 5.1 above, the most significant aerodynamic indicators are items 1 - rotor relative inlet mach number, 2 - stage reaction, and 3 - stator and rotor incidence angles. When a design engineer manually ranks solutions he or she might often reject a solution due to large areas of high mach number or severe incidence angles.

To include these design requirements within the optimisation an acceptance band was defined for each of the these criteria:

$$-10° < incidence_{(i,j)} < 10°$$

$$0.10 < reaction_{(i,j)} < 1.00$$

$$0.00 < \quad Mach_{(i,j)}^{rotor} < 0.70$$

where the subscripts i and j denote the axial and radial directions respectively. A '*C*' function was written to count the number of violations of these acceptance bands over each streamline / quasi-orthogonal intersection. The optimisation problem was then posed to maximise the calculated turbine efficiency with a linear penalty function imposed on the number of violations.

5.1.3 Fitness function C - use fuzzy logic to resolve constraint violations.

Fuzzy logic is a well publicised means by which 'engineering judgement' can be utilised within decision making processes. The mathematical concept of fuzzy sets was first proposed by Zadeh [1965] and is based on the principle that real-life decisions generally involve some uncertainty, and are best represented in linguistic rather than rigorous mathematical terms. As a simple example, in response to the impolite question 'are you human?' one could only sensibly reply 'yes' or 'no'. In this context one is either human or inhuman and therefore either a member of the set of human beings or the set of other species. Most real decisions are much less certain: in response to the question 'is it hot today?' one might expect responses like 'quite hot', 'not really', or 'a little'. Such responses are naturally subjective as they are relative to the respondents' notion of a hot day.

In conventional set theory an element either *is* or *is not* a member of a certain set (human or inhuman) and no other outcome is permitted. In fuzzy set theory an element may be a partial member of any number of fuzzy sets, in such a way that the membership function summed over all the fuzzy sets is equal to unity. A linguistic or fuzzy approach to decision making is arguably similar to the way in which humans make decisions. An obvious and often quoted example occurs when learning to drive a car: when a junction is approached an instructor would be unlikely to say 'start to brake 20

metres from the line' and more likely to say 'start to brake pretty soon'. Even though the instruction to apply the brakes is by nature fuzzy, the student must somehow interpret this into a definite, crisp instant in time at which the event must take place, taking into account road conditions and his interpretation of 'pretty soon'. This process is central to the concept of fuzzy logic: fuzzy information is received, judgement is applied, and a definite outcome is deduced.

Fuzzy logic uses fuzzy set theory to decide the outcome of a decision and it is often argued that a fuzzy representation of design rules can go some way towards encapsulating 'engineering judgement' that could not be robustly encoded as fixed rules (e.g. discussion in Bezdek [1993]).

The fuzzy decision making process can be divided into three distinct steps, as shown schematically in figure 5.3 below:

FIGURE 5.3. Fuzzy decision making.

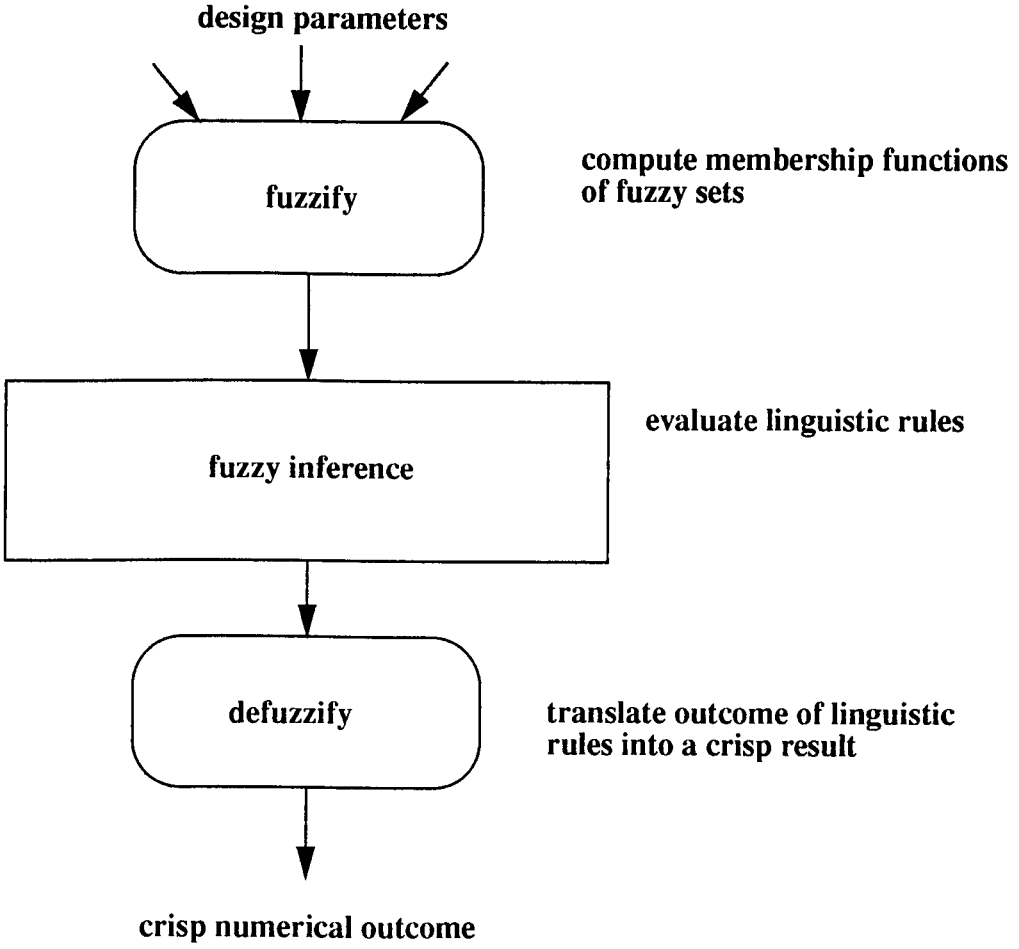

1. **Fuzzification**. The candidate design is evaluated and the design parameters are translated into fuzzy membership functions. For instance, if we consider turbine efficiency we might define three fuzzy sets good, ok, and bad as shown graphically below:

FIGURE 5.4. Fuzzy membership function for efficiency.

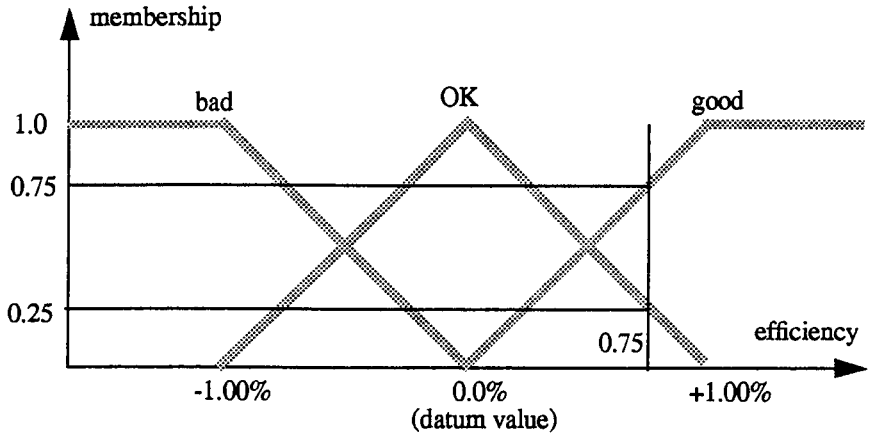

If the throughflow efficiency is increased by 1.00% the design is judged as good, and similarly if it is decreased by 1.00% it is judged as bad. Thus for a predicted efficiency of 0.75% compared to the datum value the design would have a fuzzy membership function of OK(0.25) and GOOD(0.75). Similar fuzzy membership functions are applied to the number of constraint violations detected in the design, with fuzzy set limits determined by the quality of the starting point.

2. **Fuzzy inference**. The second step in the fuzzy decision making process is to apply linguistic rules to judge the solution fitness. Rules are of the form:

if (efficiency = good) and (reaction = good) then solution = excellent

if (efficiency = OK) and (reaction = bad) then solution = bad

Since a design can be a member of a number fuzzy sets to different degrees many fuzzy rules can be true to varying degrees, and the process of defuzzification is needed to translate the outcome of the fuzzy rules into a crisp number upon which the optimisation can proceed.

The outcome of the fuzzy 'and' operator is the product of the membership values. Considering the rules given above, if efficiency has a membership function of GOOD(0.75), OK(0.25) and reaction has a membership function GOOD(0.6), OK(0.4) then

if (efficiency = good) and (reaction = good) then solution = excellent

is true to degree 0.6x0.75 = 0.45.

3. **Defuzzification**. The outcome of the fuzzy rules must be translated into a crisp numerical value to be of use in an optimisation process, and this is performed by the process of defuzzification. From the fuzzy rules a number of fuzzy outcomes will be true to varying degrees, as shown schematically in figure 5.5 below. In this implementation simple centroid defuzzification was used, and the solution fitness was taken as the centroid of the fuzzy set trapezia about the origin. The centroid position is therefore a measure of the degree to which efficiency is improved and violations are minimised, and the GA is used to increase the solution fitness by displacing the centroid to the right of the diagram.

FIGURE 5.5. Centroid defuzzification

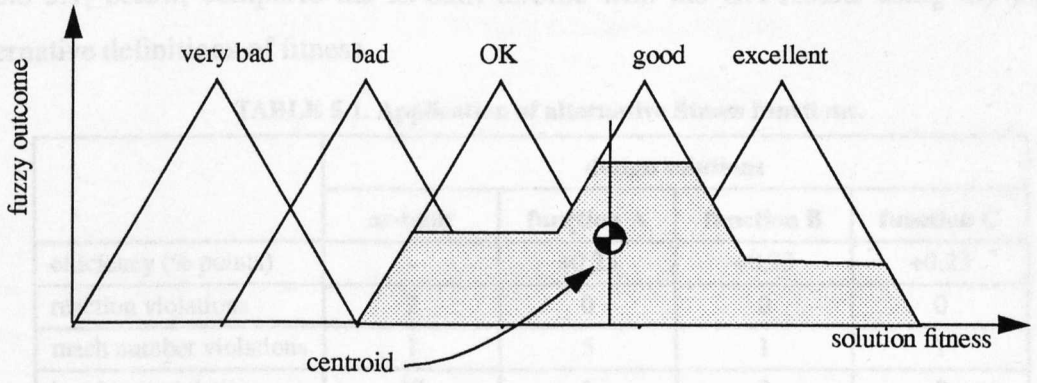

The fuzzy decision making process is described in more detail by Pearce and Cowley [1995].

The three fitness functions described in the previous sections were applied to the optimisation of a recently constructed 250MW LP turbine. The design objective was to

maximise efficiency by adjusting only the stator blades of the final three stages. Each stator was defined by a distribution of five inlet angles and five outlet angles. The problem therefore had thirty design variables, and was run for 200 generations with a population of 60 designs.

FIGURE 5.1. Meridional view through LP turbine.

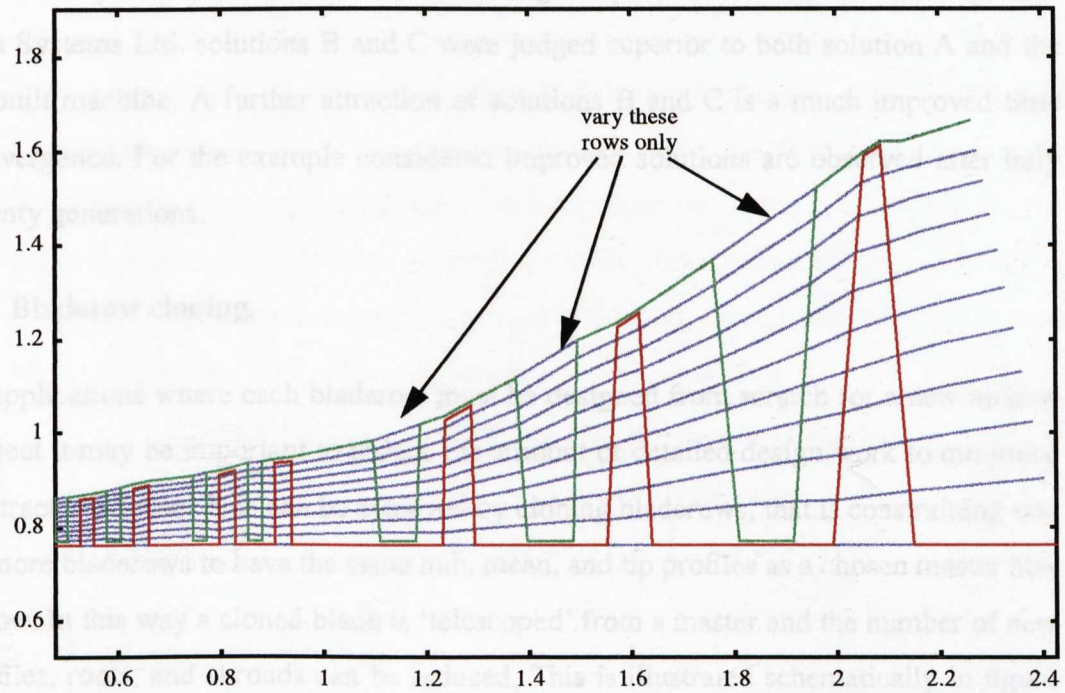

Table 5.1, below, compares the as-built turbine with the GA results using the three alternative definitions of fitness.

TABLE 5.1. Application of alternative fitness functions.

	design solutions			
	as-built	**function A**	**function B**	**function C**
efficiency (% points)	-	+0.25	+0.23	+0.23
reaction violations	2	0	0	0
mach number violations	1	5	1	1
incidence violations	17	1	3	2

In each case the GA has increased the cylinder efficiency by around one quarter of a percentage point. This was achieved by adjusting the stator inlet angles to reduce stator incidence angles, and adjusting stator throat angles to reduce rotor incidence and control the flow vortex, in particular by increasing root reaction and reducing tip reaction to reduce leakage losses. Given that the performance gain was achieved by adjusting

only 3 out of 14 bladerows it is likely to be cost effective as relatively little profile design work is required.

Although each of the fitness functions has given a broadly similar efficiency gain functions B and C (which both check for constraint violations) have also been able to reduce the occurrence of undesirable flow features as identified in figure 5.1. In a blind 'taste test' performed within the Turbine Design Department of Parsons Power Generation Systems Ltd. solutions B and C were judged superior to both solution A and the as-built machine. A further attraction of solutions B and C is a much improved time convergence. For the example considered improved solutions are observed after only twenty generations.

5.2 Bladerow cloning.

In applications where each bladerow must be designed from scratch for a new turbine project it may be important to reduce the amount of detailed design work to minimise contract lead-time. This can be achieved by cloning bladerows, that is constraining one or more bladerows to have the same hub, mean, and tip profiles as a chosen master bladerow. In this way a cloned blade is 'telescoped' from a master and the number of new profiles, roots, and shrouds can be reduced. This is illustrated schematically in figure 5.7 below:

FIGURE 5.7. Simple bladerow cloning.

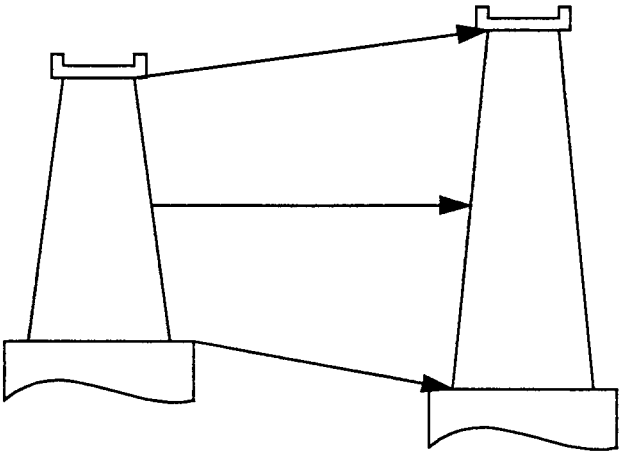

The process of cloning reduces the number of design variables in the optimisation problem, since the same distribution of inlet and outlet angle is used for both the master

and the cloned row. This reduction in the order of the problem, however, is associated with an increased number of constraints, since the a certain choice of inlet angle and outlet angle must provide good efficiency (and incidence etc.) in all rows where it is applied. It is acknowledged that there are other ways of cloning bladerows, for instance by scaling an appropriate section from a reference aerofoil on the basis of pitch to chord ratio, as described by Denton and Wallis [1996].

The cloning procedure was applied to the design of a six stage low reaction LP turbine, which comprised three low reaction stages of 'disk-and-diaphragm' construction, and three variable reaction stages. The twisted rotor blades for the final three stages were already designed for a prior application, and the objective of the optimisation was to select appropriate inlet and outlet angles for the six stator rows, and also to devise a cloned aerofoil which could be applied to each of the first, second, and third rotor rows; this was to allow common root and shroud geometries to be used.

TABLE 5.2. SLEQ results for six stage low reaction LP turbine

	bladepath configuration	
	starting point	optimised
efficiency improvement	-	+0.30%
incidence violations	8	2
reaction violations	6	0
mach number violations	2	1

Table 5.2 compares the results for the original and optimised bladepaths. The GA has achieved an improvement of 0.30% points over the starting point configuration, whilst ensuring that each stage has a reaction above 10%. Additionally occurrences of incidences greater than 10 degrees have been reduced from 8 to 2, and occurrences of inlet relative Mach numbers greater than 0.7 have been reduced from 2 to 1. Thus the optimised solution, when inspected by a design engineer, has improved performance and conforms much more closely with the list of good design features given in figure 5.1, and benefits from common root and shroud details in the first three rotor rows.

5.3 Graphical User Interface (GUI).

An important aspect of any computer based design tool is the interface with which it interacts with the engineer. Modern software is often controlled by pull-down menus

and 'point-and-click' mouse actions rather than keystrokes at a text terminal. An attempt was made to create an integrated control panel for the throughflow optimisation tool using Silicon Graphics ViewKit. The interface is shown in figure 5.8 overleaf.

The interface has three functional areas as described below:

1. A combined text field and drop pocket at the top of the panel which allows the user to type the name of the starting point SLEQ dataset or to 'drag-and-drop' it from a file manager.

2. Controls that govern the operation of the fitness function are provided to give the user some control over the search. Check-boxes are provided for yes/no decisions, and sliders are provided to set limits. The user can choose a bladepath definition on three or five radial sections, and ask the tool to include constraints on reaction, incidence, or mach number as well as optimising efficiency. When acceptance bands have been defined using the sliders the tool will inspect the starting point dataset and construct appropriate fuzzy sets based upon the quality of the solution.

3. Four control knobs are provided to allow adjustment of some of the GA control parameters, in this case crossover and mutation rates, population size, and the number of generations. When each field has been specified the calculation can be started by clicking the 'do_it' button. This writes the necessary configuration files, re-makes the GA software, and starts the calculation. On-line convergence plotting is provided using OpenGL.

FIGURE 5.8. Graphical User Interface for throughflow optimisation tool.

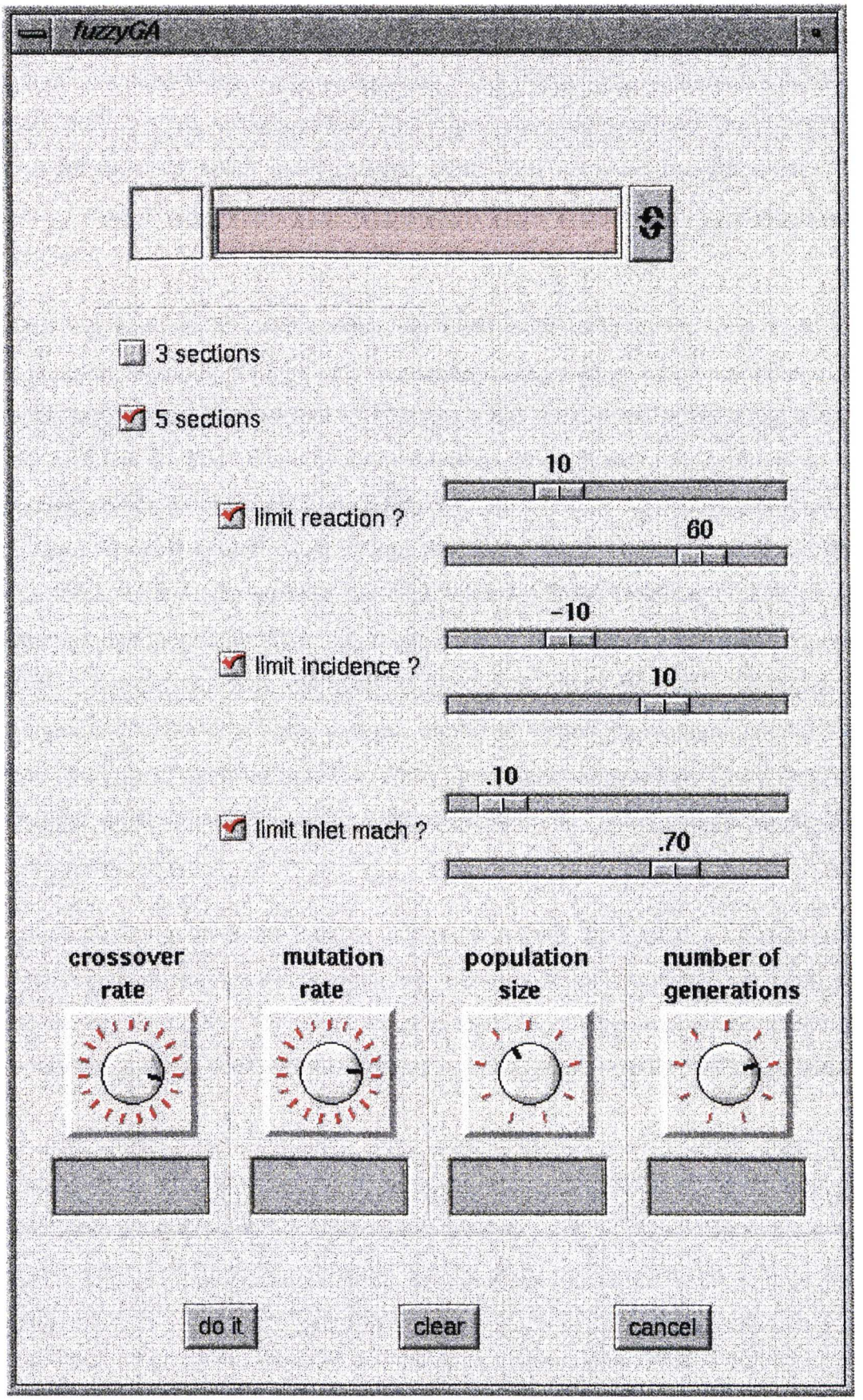

5.4 A simple method for improving convergence time.

An inescapable feature of heuristic search techniques such as genetic algorithms is the length of time taken to solve a given problem. A GA search commences from a pseudo-random starting point, and since there is a probabilistic element in each genetic operation it follows that much computational effort (and therefore run-time) must be expended evaluating poor solutions to stand a reasonable chance of identifying good solutions.

The convergence time for most practical problems is linked to the run-time of the fitness function, which in the case of a throughflow optimisation is between 10 and 30 seconds depending on the number of bladerows and the number of iterations within each evaluation. On this basis only a few thousand fitness function evaluations can be performed during an overnight run, and the user must decide whether to run a small population for many generations or a large population for few generations. This question is addressed by many workers (e.g. Greffenstette [1986], Goldberg [1989]) and it is observed that there is likely to be an optimum combination of population size and generation number that will minimise the number of fitness function evaluations to convergence. Greffenstette notes that this choice of control parameters depends not only on the type of problem but also on the fitness function parameters, and demonstrates that an additional GA can be used to optimise the control parameters for the main problem.

For practical design problems there is unlikely to be any opportunity to optimise the GA control parameters as the optimisation will only be run once, and as a rule of thumb the population size has been chosen to equal the number of problem variables. This 'square' problem configuration appears to converge well for all problems considered.

If a large population size is chosen the genetic diversity is maintained but the time to evaluate each generation will be increased. Conversely a small population size allows each generation to be evaluated quickly but the gene pool remains small. Since the appropriate compromise between population size and number of generations can vary from problem to problem a variable population size was implemented as follows: For the first generation a population of five times the number of variables is evaluated.

Thus a diversity of genetic material is created, and on the second and subsequent generations the population size shrinks to become equal to the number of variables.

FIGURE 5.9. Program convergence plots.

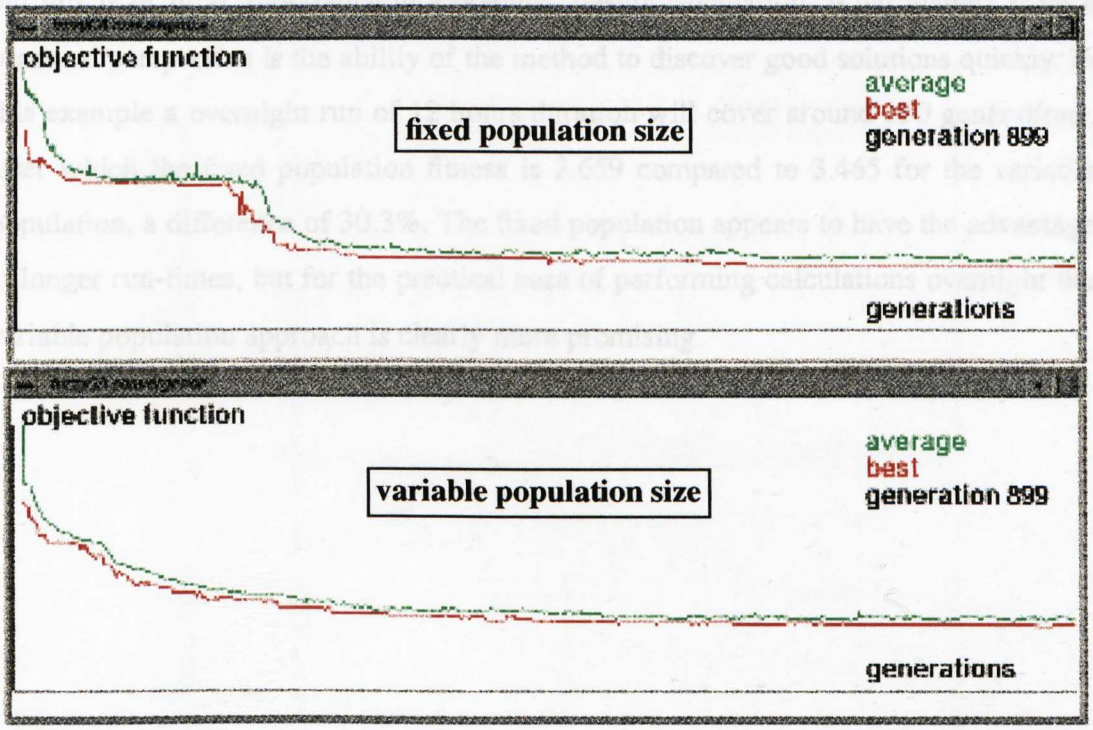

Figure 5.9, compares the program convergence output for the seven stage LP turbine considered in section 1.1 above. The upper plot shows a calculation performed with a fixed population size of 30, and the lower plot was produced with an initial population of 150 and subsequent populations of 30. Both the fixed and variable populations exhibit rapid initial convergence, since the initial population is randomly generated and therefore of poor fitness. However after twenty generations the fixed population calculation stagnates, and shows little improvement in fitness until 200 generations have been evaluated, whereas the variable population continues to converge steadily.

The variable population calculation maintains steady convergence because the initial population is more diverse. In other words, at the start of the run there is potentially a larger number of good design features present in the gene pool. Figure 5.10, shows the overall convergence of fitness, and also compares efficiency and number of incidence violations. The fixed population shows a larger increase in efficiency early in the calculation, but the variable population has quickly learned that convergence can be main-

tained by striving to reduce the number of incidence violations (number of grid points upon which the incidence angle exceeds 10 degrees)

Clearly after 900 generations the fixed population has achieved a slightly greater fitness but this is of little importance in a practical design calculation. What matters from a practical perspective is the ability of the method to discover good solutions quickly. In this example a overnight run of 12 hours duration will cover around 150 generations, after which the fixed population fitness is 2.659 compared to 3.465 for the variable population, a difference of 30.3%. The fixed population appears to have the advantage at longer run-times, but for the practical case of performing calculations overnight the variable population approach is clearly more promising.

FIGURE 5.10. Fitness, efficiency, and incidence angle convergence.

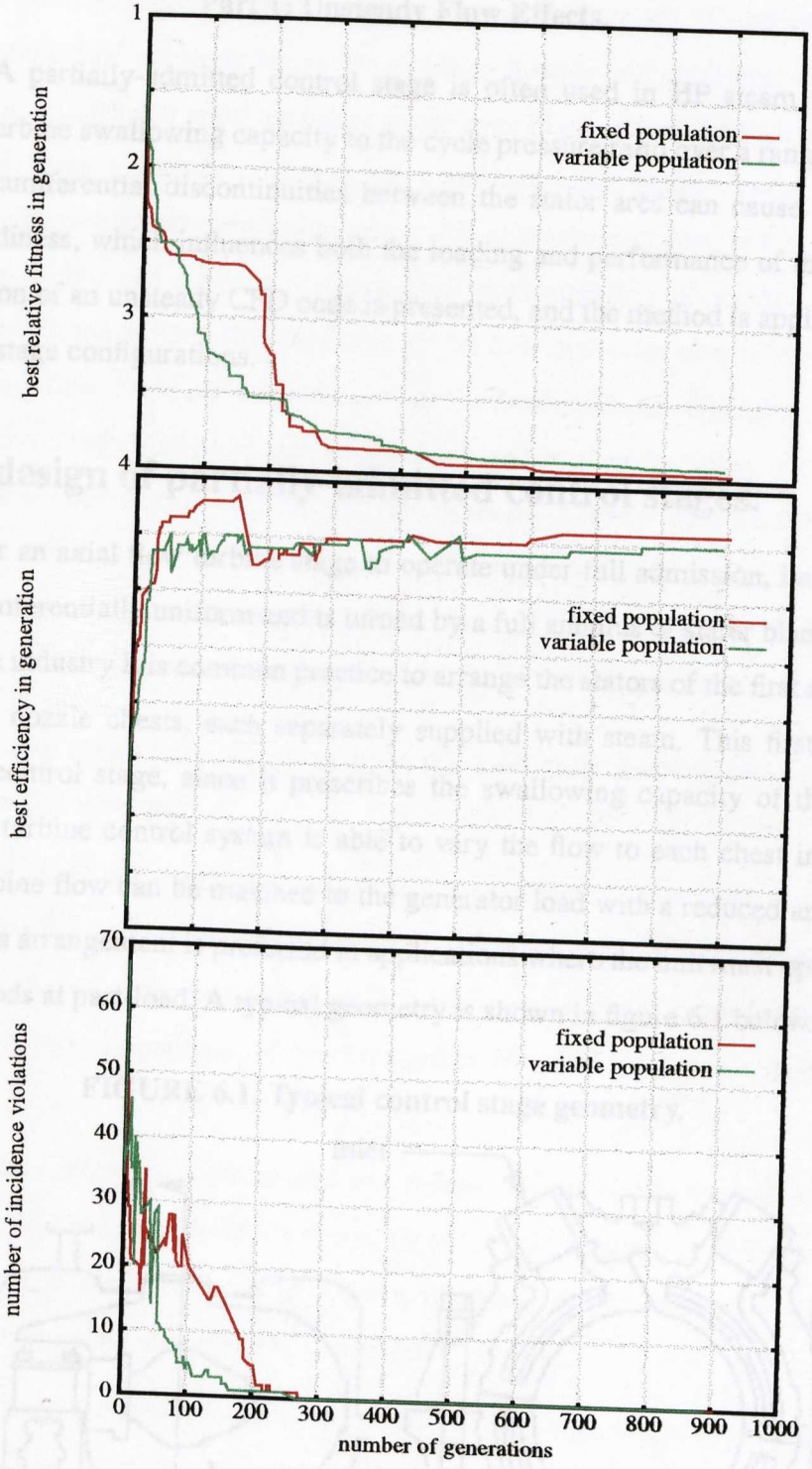

Chapter Six

Control Stage Design.
Part 1: Unsteady Flow Effects.

Synopsis. A partially-admitted control stage is often used in HP steam turbines to match the turbine swallowing capacity to the cycle pressure ratio over a range of power output. Circumferential discontinuities between the stator arcs can cause significant flow unsteadiness, which influences both the loading and performance of the blading. The validation of an unsteady CFD code is presented, and the method is applied to typical control stage configurations.

6.0 The design of partially-admitted control stages.

It is usual for an axial flow turbine stage to operate under full admission, i.e. the inlet flow is circumferentially uniform and is turned by a full annulus of stator blades. In the steam turbine industry it is common practice to arrange the stators of the first stage into three or four nozzle chests, each separately supplied with steam. This first stage is known as a control stage, since it prescribes the swallowing capacity of the whole machine: the turbine control system is able to vary the flow to each chest independently, and turbine flow can be matched to the generator load with a reduced amount of throttling. This arrangement is preferred in applications where the unit must operate for extended periods at part-load. A typical geometry is shown in figure 6.1 below.

FIGURE 6.1. Typical control stage geometry.

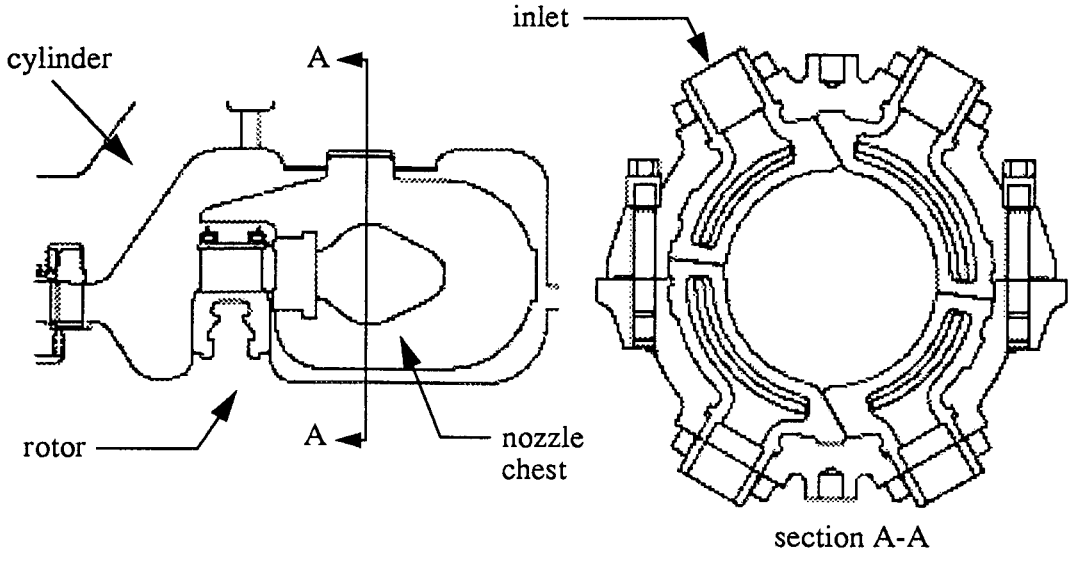

It is well known that the flow in a control stage is highly unsteady. When a rotor blade is well within the stator arc the passage flow is similar to the flow at full admission, but there is little throughflow between the stator arcs. It therefore follows that there must be a strong flow deceleration as the rotor passage leaves the arc of admission, and an equivalent period of acceleration as the passage flow is re-established at arc entry. There is also a significant windage effect as the rotor blades move through areas of low throughflow. These unsteady effects cause significant aerodynamic losses which can drastically reduce stage efficiency, and also create alternating stresses in the blade aerofoils.Turbine design and analysis methods such as throughflow or steady-state blade-to-blade calculations assume that the stator outlet flow possesses circumferential symmetry. Throughflow calculations solve for the circumferentially averaged meridional flow, whereas a steady blade-to-blade solution is based on the assumption that the flow-field comprises a number of identical passage domains. Clearly these assumptions are justifiable for a fully admitted stage, but when the stage is partially admitted there are significant circumferential variations and the flow is time-dependent. An unsteady multi-passage viscous calculation is therefore essential to fully predict the flow-field.

In the design of a steam turbine control stage there are three fundamental engineering issues that must be resolved:

1. The turbine swallowing capacity effectively prescribes the first stage stator throat area, and the designer must maximise stage efficiency by selecting an appropriate compromise between admission ratio and aspect ratio. A quantitative assessment of this effect requires knowledge of the relationship between efficiency and admission ratio.

2. The magnitude of the rotor blade unsteady forces must be known to predict the aerofoil fatigue life and size the blade chord. Generally the magnitude of these stresses is uncertain, and blades are conservatively sized and therefore operate with relatively low steady-state steam bending stresses.

3. Partial admission reduces the efficiency of the control stage, and also presents a circumferentially distorted inlet flow to the downstream blading. To enable a performance prediction to be made for the entire HP turbine the engineer must estimate the number of downstream stages required before the flow can be regarded as circumferentially uniform, and also predict a loss for this mixing process.

If a representative meanline optimisation of the HP turbine is to be attempted the importance of these effects must be known to engineering accuracy. There is relatively little information published on the subject of partial admission, and a review of the available literature indicates the phenomena are not fully understood. Roelke [1973] stated that a partial admission stage, considered in isolation, has three additional loss components due to:

- 'sucking' action at the end of the stator arc to reduce the rotor passage throughflow
- windage losses as rotating flows become established in the rotor passages as they move between the admitted arcs, and
- 'pumping' at the entry to the stator arc when the rotor passage flow is rapidly accelerated.

The majority of the published work, summarised in table 6.1, addresses either unsteady loadings or stage efficiency. Kroon [1947] and Pigott [1980] used a simple control volume analysis to estimate unsteady forces and stresses under conditions of resonance, and Kovats [1981] measured unsteady forces in a blow-down test facility. Boulbin et al [1992] measured unsteady blade forces on a water table using the hydraulic analogy between free-surface water flow and 2D gas flow, and demonstrated good agreement with an approximate prediction based upon the method of characteristics.

Stenning [1953], Ohlsson [1962], and Korematsu et al [1979] each produced analytical expressions for the variation in stage efficiency with velocity ratio and admission ratio. The relationships quoted are based around a meanline velocity triangle calculation with semi-empirical allowances made for windage and pumping losses, and although the results undoubtedly illustrate important trends they are too general for direct application to the steam turbine environment.

From a practical design perspective there is a clear need for a consistent prediction of both losses and unsteady forces at partial admission conditions. This information, whether obtained experimentally or from CFD analysis, can then be correlated for use within a simple control stage meanline design method.

TABLE 6.1. Comparison of published control stage partial admission investigations.

author(s)	organisation	summary of experimental or analytical methods used		
		stage configuration	procedure	results
Kroon [1947]	Westinghouse Electric Corp.	single impulse row	calculation of dynamic stress due to partial admission	simplified blade response
Stenning [1953] reviewed by Horlock [1966]	M.I.T.	single impulse row	momentum-based analysis of single blade row, including windage effects	curves of approximate stage efficiency versus velocity ratio and admission ratio
Ohlsson [1962]	de Laval - Ljungstrom	single stage	as Stenning, but including the effect of compressibility	efficiency and unsteady forces for small air-turbine
Korematsu and Hirayama [1979]	Tokyo University	single stage	meanline calculation following Ohlsson	Contours of efficiency with loading and flow coefficients (partial admission 'Smith Chart')
Pigott[1980]	Westinghouse Electric Corp.	single stage	extended Kroon's work to include nozzle wake loading	blade response and dynamic stresses
Kovats [1981]	Westinghouse Electric Corp.	single stage experimental turbine (blow-down)	Mach-Zender interferometer	instantaneous pressure distribution
Galatsan et al [1985]	Kharkov Turbine Works	1.5 stage experimental turbine	circumferential pressure traverses	variation of brake efficiency with flow coefficient, and mixing of non-uniform flow over downstream stator row
Boulbin et al [1992]	Conservatoire National des Artes et Métiers, Paris	single stage water table	experimental measurement of instantaneous pressure distribution, and calculation of forces using method of characteristics	time variation of aerofoil forces

In the following sections an unsteady CFD code is applied to the steam turbine partial admission problem. The method is validated against published test data, and predictions of both unsteady forces and stage efficiencies are presented for a number of steam turbine geometries. The discussion is extended to include the influence of stage reaction on circumferential non-uniformity.

6.1 Validation of an unsteady CFD solver for partial admission calculations.

The aerodynamic design of the control stage has previously been approached as a steady flow problem. The inviscid flow through both stator and rotor have been predicted using steady time marching codes, with an assumption of circumferential symmetry at the intra-stage mixing plane. The effects of the discontinuous stator grouping and very close axial spacing are beyond the scope of the previous analyses, although some allowance is made for them in the overall estimation of performance. At primary valve point flow may be admitted to only 20% of the arc, and strong disturbances with long length scales are created as blade passage flows are repeatedly accelerated and stagnated as the nozzle chests are traversed. An unsteady multi-row, multi-passage method is necessary to investigate the sources of loss under partial admission.

The CFD code used is a multistage, multipassage, unsteady, 2D Navier Stokes solver [He, 1994a], known as VIB2D. Unlike steady stage calculations, there is no circumferential averaging of the flow variables between bladerows; instead information is interpolated between nodal points at the grid interface. A structural dynamic model is included, which controls the deflection of each blade under the instantaneous aerodynamic loading. The method has found application across a range of rotor-stator interaction problems, such as the capture of rotating stall and stall flutter interactions in multistage compressors [He, 1994b].

6.1.1 Unsteady blade forces determined using a water table.

A published experiment (Boulbin et al [1992]) reports unsteady forces on a control stage blade at 50% admission, deduced from measurements taken on a radial flow water table (Fig 6.2). The hydraulic analogy between free-surface water flow and 2D gas-dynamic flow can be applied, under certain circumstances, to translate between

water depths and velocities recorded on the water table and the pressures and velocities present in the analogue turbine flow.

FIGURE 6.1. Water table *(courtesy Prof. M Pluviose).*

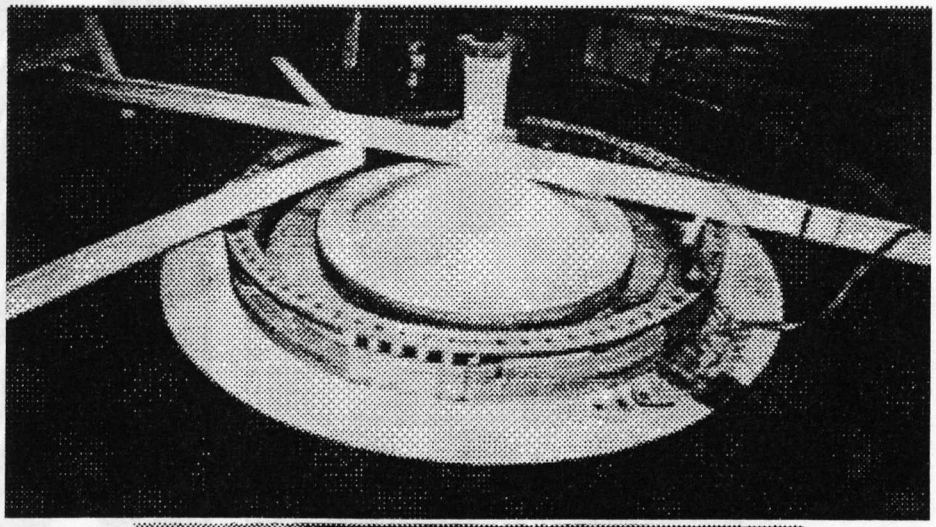

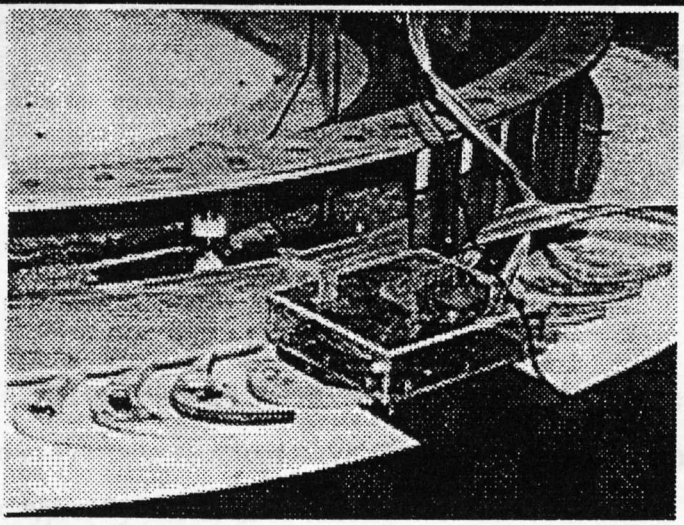

detail of blade passage

The published results are for an arc of ten stators with five passages blocked. Although the profiles are not explicitly given, the blade shape appears to be of arcs and flats construction: in the following calculations similar profiles have been used. The computational domain consists of 5 inlet ducts, ten stator passages, and 10 blade passages. Flow is admitted to five of the stator passages, and the lower two and upper three have a solid inlet boundary. A total of 47000 nodes were used to define the 2D grid; details are shown in figure 6.3. The flow conditions used were as follows: nozzle exit Mach number = 0.950, blade velocity ratio = 0.450. The nozzle opening coefficient used was 0.23.

FIGURE 6.3. Detail of computational grid.

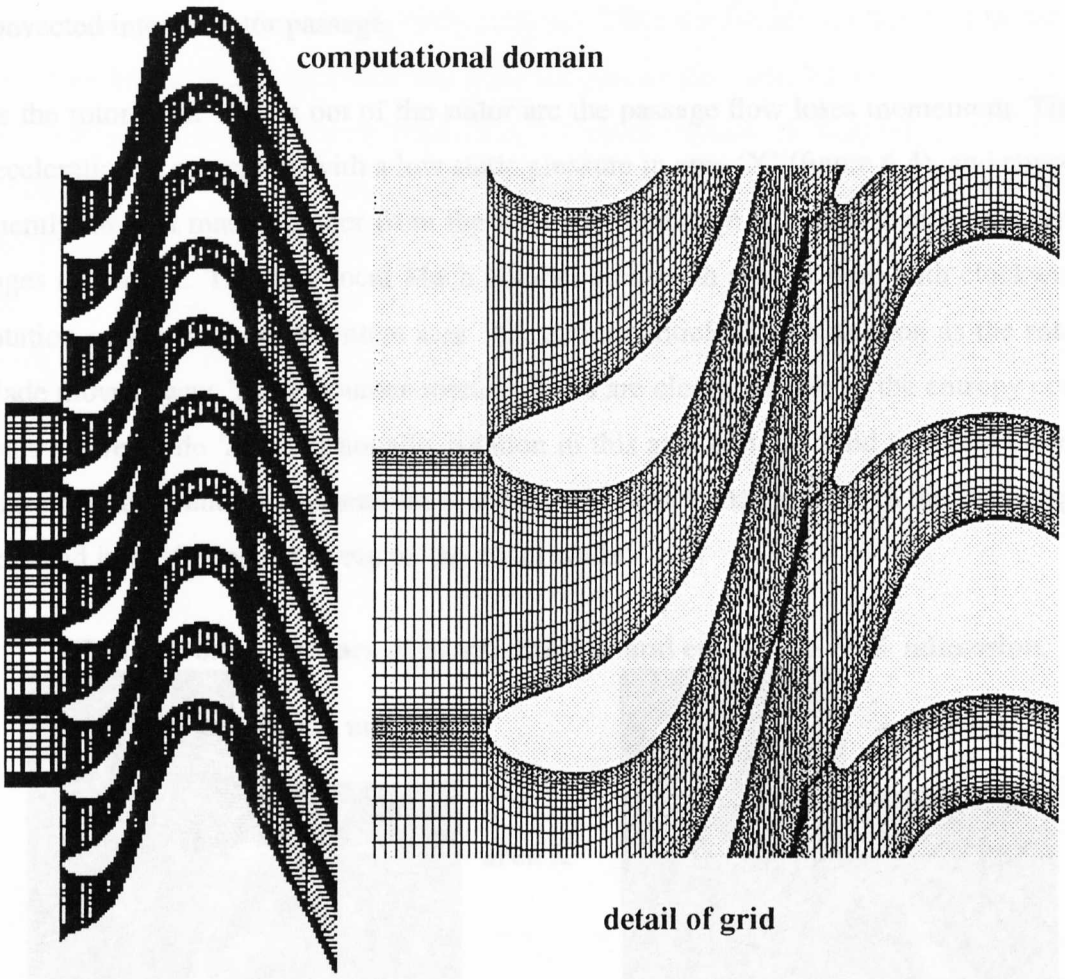

The code was run on a Silicon Graphics R8000 64 bit workstation, completing around 1000 timesteps per hour. Periodic solutions were obtained when each rotor blade had traversed the stator arc typically two or three times.

Figure 6.4 shows the instantaneous distribution of absolute Mach number and entropy at 24000 timesteps. As the moving blade enters the arc of admission (blade 'B' in figure 6.4) the suction surface is supplied with fluid whilst the pressure surface flow is relatively stagnant. An area of higher static pressure is formed around the inlet to the blade passage as the stagnant fluid is accelerated by the stator jet. Consequently the leading stator outlet Mach number is lower than for the other passages, and the passage outlet mass flow appears to fluctuate at the moving blade passing frequency. As the rotor blade moves further into the stator jet the high entropy stagnant fluid is expelled and the rotor passage flow becomes established. The wake from the first stator is very thick as the jet is sheared against low velocity fluid. A significant proportion of the sec-

tor loss appears to be generated by this mechanism, and high entropy fluid is seen to be convected into the rotor passage.

As the rotor blade moves out of the stator arc the passage flow loses momentum. This deceleration is associated with a low static pressure in area 'X' (figure 6.4), and consequently the exit mach number from the final stator passage is higher than for the passages in mid arc. The high local Mach number creates an area of fluid with clockwise rotation as the rotor blade enters area 'X', and an anticlockwise rotation as the rotor blade moves away. These counter-rotating flows are clearly visible in the entropy contours above blade 'A'. Additionally, rotation in this area entrains fluid from the closed stator passages, and loss generation is apparent in both the shear layer in the intra-stage gap, and in the boundary layers on the stator walls.

FIGURE 6.4. Contours of Mach number and entropy at 50% admission.

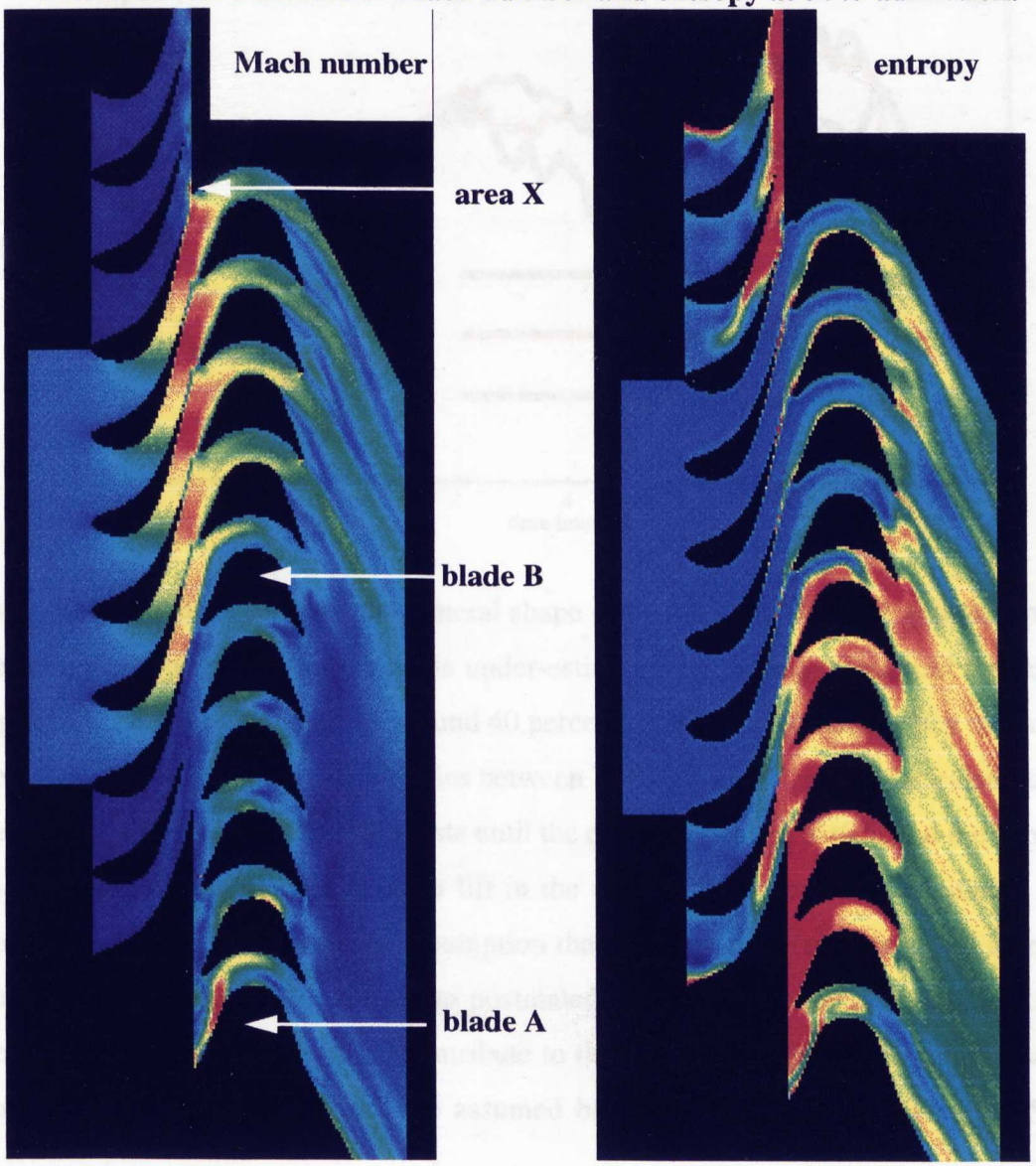

When a rotor blade enters the stator arc fluid is supplied to the suction surface whilst the pressure surface flow is relatively stagnant. Thus the blade experiences a negative lift at the beginning of the stator arc. Equivalently, as the blade leaves the arc the pressure surface is supplied with fluid as the suction surface is stagnating, and a net increase in lift is experienced. Figure 6.5 compares the measured rotor lift reported in the water table experiment with predictions from VIB2D. The plots show the instantaneous lift in an arbitrary rotor blade as it traverses the complete stator arc. Calculations were performed with both rigid blades and flexible blades, including the effect of fluid - structure interaction.

FIGURE 6.5. Comparison of experimental and calculated lift coefficient.

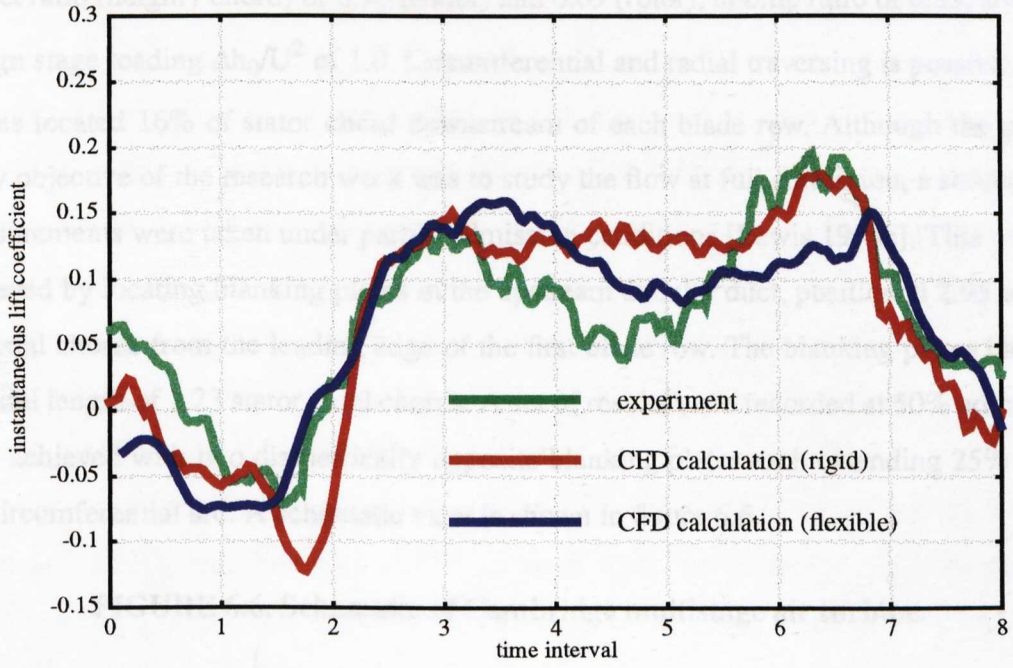

The rigid calculation captures the general shape of the unsteady loading with acceptable accuracy. The peak positive lift is under-estimated by eight percent, and the peak negative lift is over-estimated by around 40 percent. A significant discrepancy between the experimental and calculated lift lies between T=3 and T=5.5, where the calculation predicts a quasi-steady lift which exists until the exit load peak at T=6.5, and the experiment shows a dramatic reduction in lift in the middle of the arc. The calculated lift would appear consistent with the assumption that a steady flow (similar to full admission) exists within the stator arc. It was postulated that fluid-structure interaction within the experimental apparatus could contribute to this discrepancy, and a calculation was performed with flexible blades. The assumed blade resonant frequencies were 3500

Hz. flexural and 1200 Hz. torsional. Figure 7 compares the flexible calculation to the experimental results, and it is clear that the inclusion of the structural calculation improves the agreement between the curves. However, since the mechanical properties of the experimental blades are not known the comparison can only be regarded as conjectural.

6.1.2 Circumferential flow redistribution.

Results published by Lewis [1993, 1994b] describe an experimental air turbine at the Whittle Laboratory in the University of Cambridge constructed to model the flow in a high pressure steam turbine. The four repeating stages of 50% reaction blading have an aspect ratio (height / chord) of 0.76 (stator) and 0.69 (rotor), hub:tip ratio of 0.85, and a design stage loading $\Delta h_0/U^2$ of 1.0. Circumferential and radial traversing is possible in planes located 16% of stator chord downstream of each blade row. Although the primary objective of the research work was to study the flow at full admission, a series of measurements were taken under partial admission conditions [Lewis 1994a]. This was achieved by locating blanking plates in the upstream annular duct, positioned 2.95 stator axial chords from the leading edge of the first blade row. The blanking plates have an axial length of 1.23 stator axial chords. A set of results were recorded at 50% admission, achieved with two diametrically opposite blanking plates each extending 25% of the circumferential arc. A schematic view is shown in figure 6.6.

FIGURE 6.6. Schematic of Cambridge multistage air turbine.

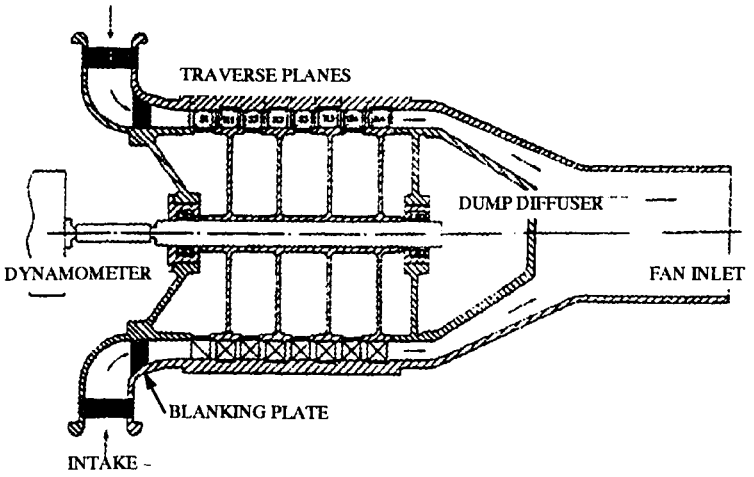

A VIB2D calculation was performed for this arrangement. Shaft speed was 640 rpm, and Reynolds number based on stator chord and midspan exit velocity was

$3.3x10^5$.Two stages were modelled for half of the annulus (62 blade passages) using an H-type grid of 164486 nodes. Periodically converged solutions were achieved in a run-time of around 48 hours on a Silicon Graphics R8000 workstation.

Contours of calculated Mach number and entropy at an isentropic velocity ratio of 0.36 are shown in figure 6.7, overleaf. The isentropic velocity ratio is defined as the mid-span blade speed factored by the isentropic jet speed based on the stagnation pressure drop over the whole turbine. The upper and lower extents of the computational domain are periodic boundaries, and the complete annulus comprises two such domains. Flow is admitted to the blading through the duct located in the centre of the domain. The most upstream surfaces of the upper and lower extents of the domain are a solid boundary.

Significant circumferential flow redistribution is apparent upstream of the first stator row. This is because the circumferential pressure gradient can only balance the axial pressure gradient with some curvature of the inlet jet. Consequently areas of lower static pressure occur upstream of the blanking plates, and the local mass flow increases from the centre of the inlet duct to the corner of the blockage. Since there is a strong velocity gradient normal to the curving jet boundary the generation of entropy is apparent in this region, and there is evidence of flow recirculation in the blanked area. The jet boundary curvature causes incidence angles of approximately +/- 45 degrees onto the stators which are circumferentially removed from the centre of the inlet duct. Velocity vectors (figure 6.8) show significant negative incidence onto blade 'A', which is located near the top of the domain. The leading edge stagnation point is on the suction surface at around 11% of axial chord, and the overspeed onto the pressure surface causes a gross flow separation. Equally, the velocity vectors around blade 'B' show strong positive incidence and an associated suction surface separation. In both cases there is little evidence of flow re-attachment, and the entropy contours show large losses within the passage and a thick wake.

Further circumferential flow distribution occurs in the intra-stage gap between the first stator and rotor due to the pressure drop associated with the 50% reaction design. However, the thick stator wakes at the extremes of the domain create additional rotor incidence, and the wakes are stretched and distorted by the rotor passage pressure field. An

area of increased loss is still apparent after both the first and the final stage, and this fluid is displaced circumferentially with the shaft rotation.

FIGURE 6.7. Contours of Mach number and entropy at 50% admission.

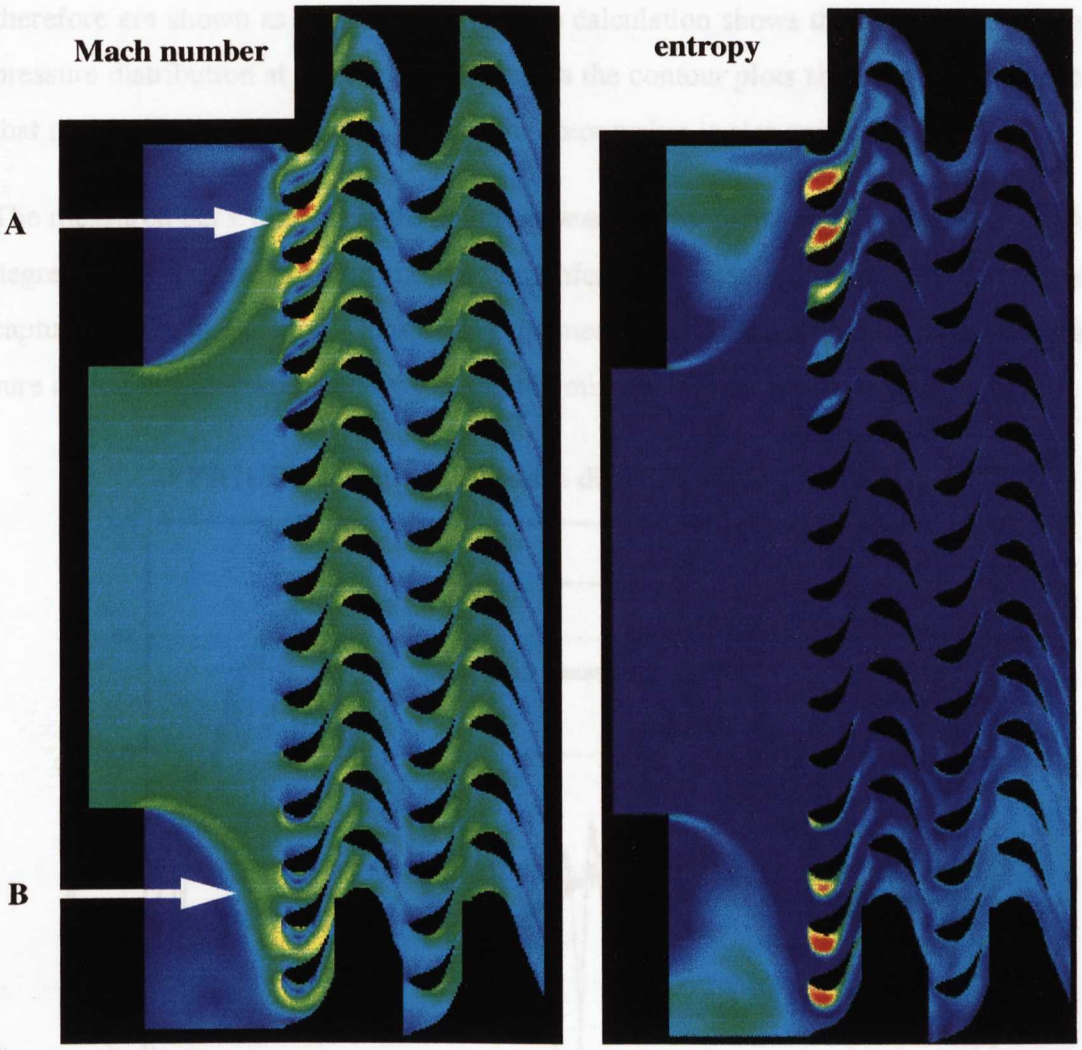

FIGURE 6.8. Predicted velocity vectors at blade 'A' and 'B'.

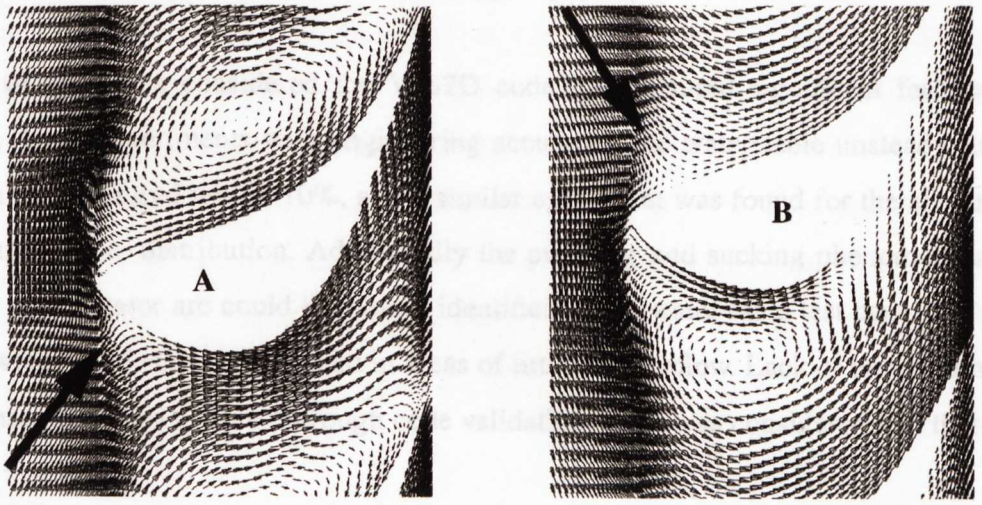

Figure 6.9 compares the measured and calculated total pressure distribution downstream of stage 1. The results are expressed as a total pressure coefficient, which is defined as the difference between the inlet and local total pressures non-dimensionalised by the turbine total pressure drop. The experimental results are time averaged and therefore are shown as a smooth curve. The calculation shows the instantaneous total pressure distribution at the same time-step as the contour plots shown in figure 6.7, so that the total pressure deficit in each of the rotor wakes is also apparent.

The measured peak total pressure deficit appears at approximately 55 degrees and 245 degrees, and both the position and the circumferential extent of this distribution is well captured in the calculation. Considering the mean of the calculated data, the peak pressure deficit is underestimated by 9% and the minimum is underestimated by 7%.

FIGURE 6.9. Total pressure distribution at stage 1 exit.

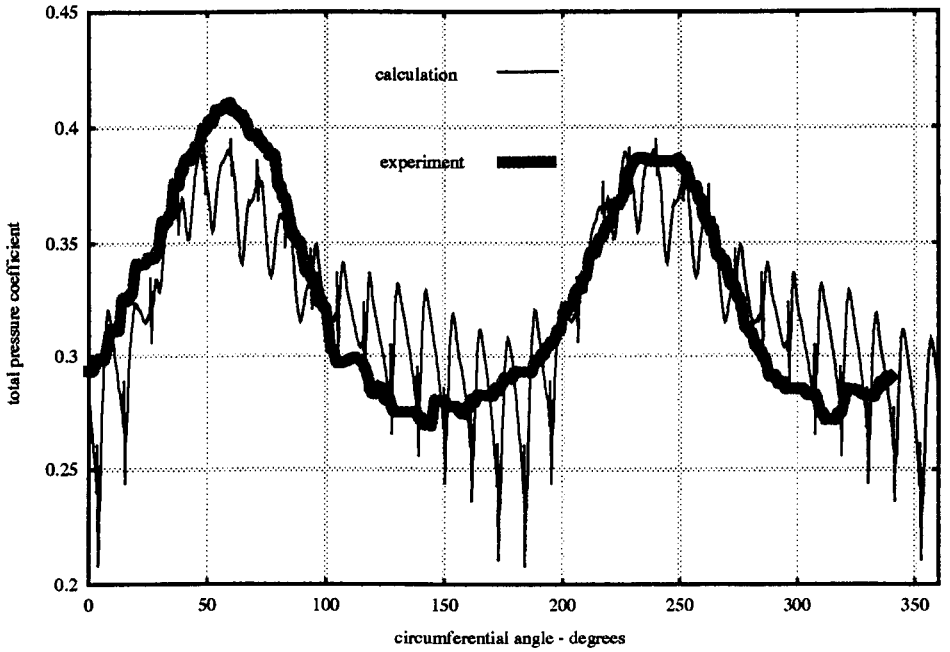

In both of the cases considered the VIB2D code has captured significant features reported in the experiments with engineering accuracy. The water table unsteady lift variation was captured within 10%, and a similar agreement was found for the air turbine total pressure distribution. Additionally the pumping and sucking phenomena at the ends of the stator arc could be clearly identified in the water table test case, and a chaotic windage effect was predicted in areas of little throughflow. Lack of experimental data has prevented a more thorough code validation, yet it was considered that there

was sufficient confidence in the method to attempt an analysis of a number of representative steam turbine arrangements.

6.2 Analysis of a production HP turbine control stage.

Partial admission is achieved by arranging the first stage stators into discrete nozzle chests, each separately supplied with steam. In a conventional nozzle controlled HP turbine for reheat application four nozzle chests are used, as shown in figure 6.10 below,

FIGURE 6.10. Typical arrangement of nozzle chests.

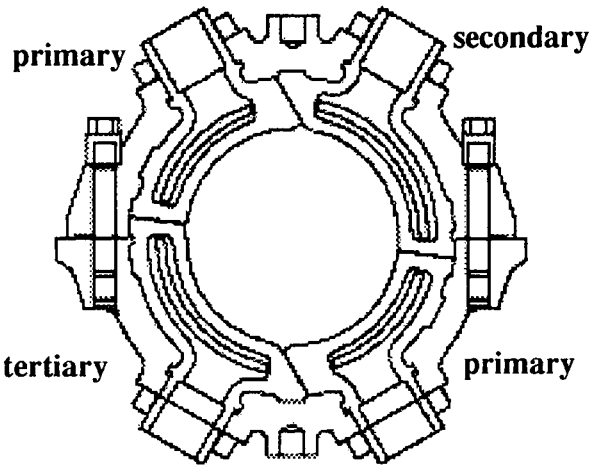

At valves wide open (VWO) conditions all four chests are supplied with steam and the turbine operates at maximum load (tertiary valve point). Two part-load valve points can be achieved, primary valve point at which only the primary chests are in operation, and secondary valve point at which the secondary and primary chests are used. These valve points might typically correspond to 60% and 80% of full load respectively.

A typical production turbine might comprise around 60 stator blades and 50 rotor blades, and a full annulus calculation was not possible within the available computer memory. Instead a fraction of the annulus comprising 8 stators and 7 rotors was modelled. Small adjustments in both stator and rotor aerofoil pitch were necessary to ensure that the circumferential extent of each row was identical. The overall error in blade count ratio was less than 1% and considered negligible in the subsequent analysis.

Calculations have been performed at pressure ratios corresponding to primary, secondary, and tertiary valve points, at admission ratios of 100%, 75%, 50%, and 25%. The results are arranged in two sections; the first discusses stage efficiency, and the second extends the analysis to consider unsteady forces.

6.2.1 Production HP turbine stage efficiency.

Unsteady calculations were performed for a typical production control stage over a range of admission ratios and stage loading. Figure 6.11, overleaf, shows a typical snapshot of the flow-field at secondary valve point with an admission ratio of 50%. As a rotor passage leaves the admitted stator arc an area of high Mach number (and low static pressure) is visible, and this feature is associated with the sucking action that decelerates the passage flow. Equivalently, the first stator in the arc has a somewhat reduced exit Mach number (and increased local static pressure) which serves to re-energise the rotor passage flow.

Each of these features is associated with loss generation. The final stator jet shears against stagnant fluid at the end of the arc, and the rotor blades appear to 'scrape' fluid across the trailing edges of the blanked stators creating rotating bodies of fluid which slowly move through the rotor passages when throughflow is low.

The rotor flow appears to be almost fully established in the passage labelled 'A'. Entropy is generated by both the shearing of the stator wakes in the blade leading edge potential field, and in the suction surface separation due to positive incidence. Each of these features appears to be considerably less lossy than the sucking, pumping, and windage effects and it is therefore clear that partial admission will drastically reduce the efficiency of the stage.

TABLE 6.2. Calculated stage efficiency (time-averaged).

stage velocity ratio (U/C_o)	stage admission ratio			
	100%	75%	50%	25%
0.458 (tertiary)	77.56	75.04	67.17	67.42
0.296 (secondary)	74.85	66.76	64.08	60.16
0.220 (primary)	62.82	60.23	59.36	49.46

The variation of stage efficiency with velocity ratio (U/C_o) and admission ratio is compared in table 6.2 above and figure 6.12.

FIGURE 6.11. Contours of Mach number and entropy at secondary valve point

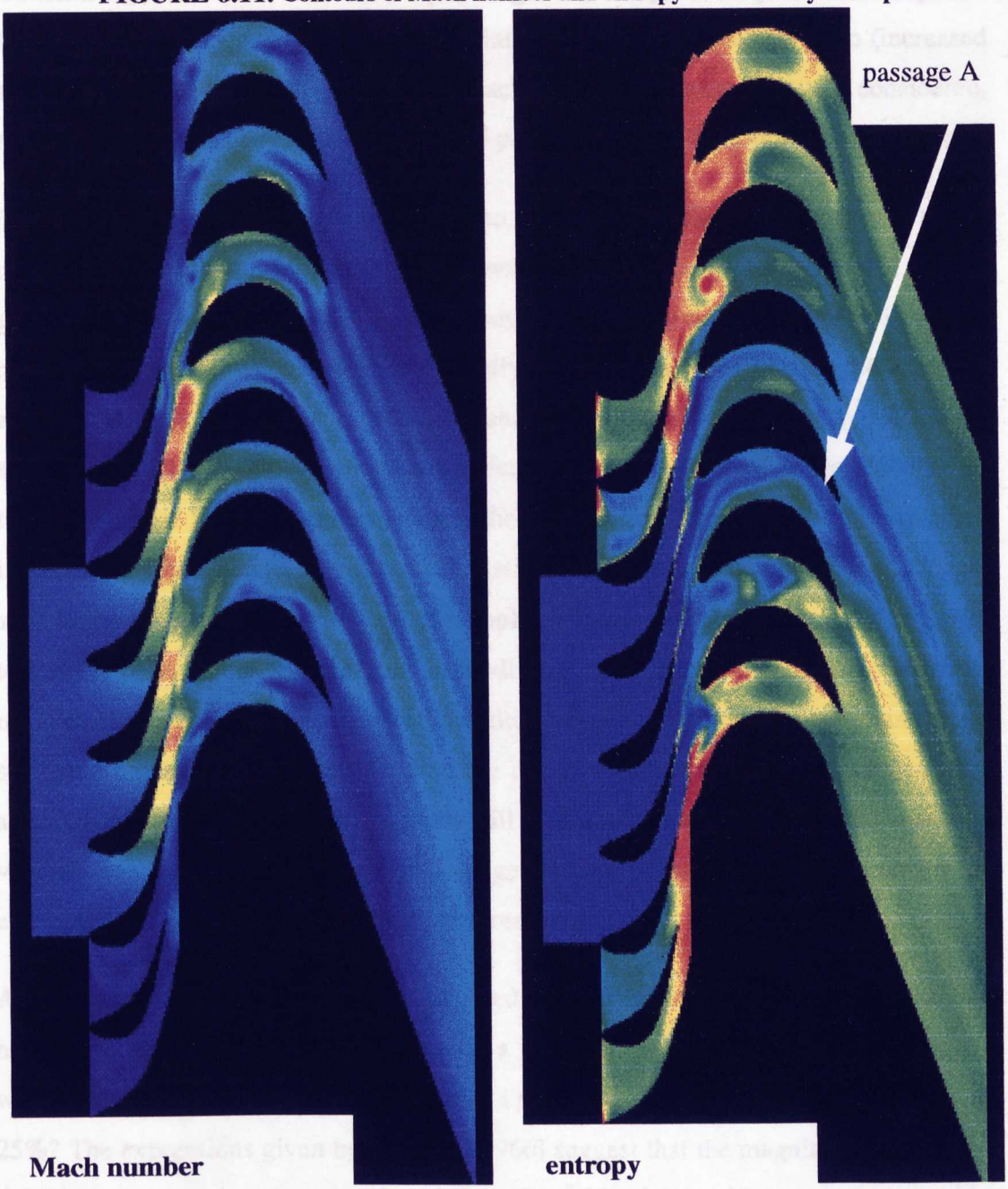

FIGURE 6.12. Calculated stage efficiency.

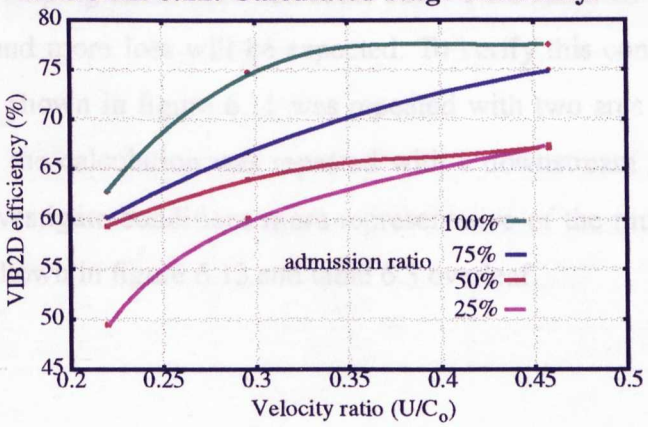

Considering the 100% admission case, stage efficiency falls by around 15 points between the tertiary and primary valve points due to reduced velocity ratio (increased stage loading). Additionally, comparing each of the three velocity ratios considered, stage efficiency falls by between 10 and 15 points between 100% and 25% admission.

The application of a 2D analysis method to a 3D flow problem will obviously fail to capture some of the physics of the real flow. In particular, control stage aspect ratio is generally small (0.3-0.6) and the strong endwall secondary flow structures will not be represented in a 2D calculation. Additionally, the rotor passages outside the admitted arc are relatively stagnant, and the highly unsteady windage losses directly reduce the shaft work output. The 2D analysis predicts strong circumferential recirculation in these regions of low throughflow: clearly the real 3D flow would also exhibit rotation in the radial plane. Unsteady viscous calculations are extremely computationally intensive, firstly because many iterations of complex solution procedures are often required to achieve periodic convergence, and secondly because many grid points are needed to mesh multipassage domains. A fully 3D multi-passage calculation for more than five or six blade passages is currently beyond the capability of most desktop workstations, although it is probable that such methods will eventually be able to predict the unsteady viscous flow through a complete multistage turbine. Such developments remain an extremely exciting area of turbomachinery research.

A further practical design issue not addressed in the literature is the significance of the number of admitted arcs. For instance, if a 50% admission turbine was considered, would better performance be achieved with a single arc of 50% or two admitted arcs of 25%? The expressions given by Horlock [1966] suggest that the magnitude of the partial admission loss is proportional to the number of 'ends', i.e. if two arcs are considered the sucking and pumping effect observed at the ends of the admitted arc will occur twice per revolution and more loss will be expected. To verify this concept the 50% admission calculation shown in figure 6.11 was repeated with two arcs of admission (2x25%). In addition, the calculation was repeated with a downstream stage of 50% reaction blading to investigate conditions more representative of the multistage environment. Results are shown in figure 6.13 and table 6.3 overleaf.

FIGURE 6.13. Entropy contours for one and two arc configurations.

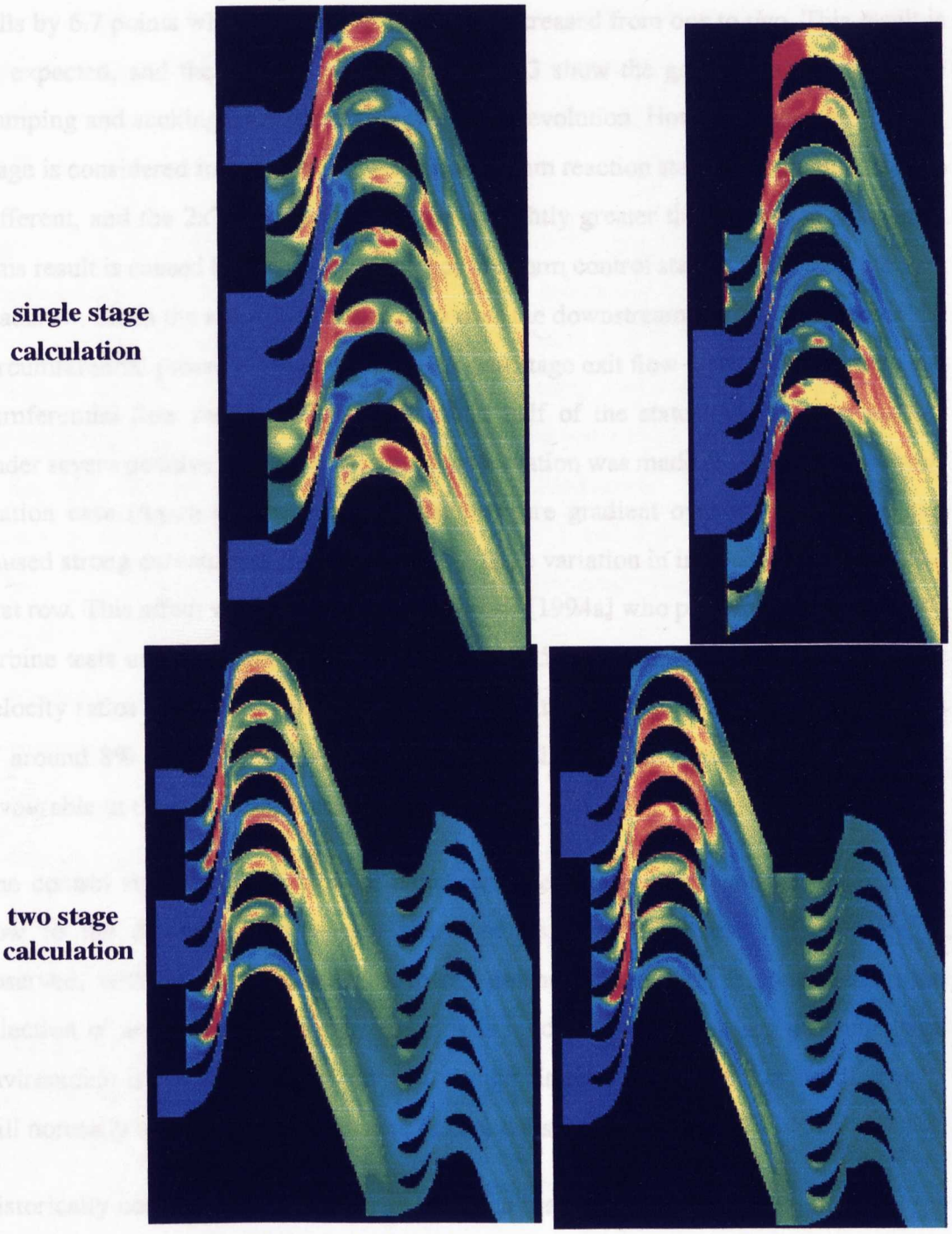

TABLE 6.3.Variation of stage efficiency with number of arcs.

admission configuration	stage efficiency (%)	
	control stage	two stages
single arc (1x50%)	64.08	78.50
double arc (2x25%)	57.34	78.60

When the control stage is considered in isolation the time-averaged stage efficiency falls by 6.7 points when the number of arcs is increased from one to two. This result is as expected, and the contour plots in figure 6.13 show the generation of loss in the pumping and sucking cycle occurring twice per revolution. However, when the control stage is considered in conjunction with downstream reaction stage the situation is quite different, and the 2x25% arrangement has a slightly greater time-averaged efficiency. This result is caused by the effect of the non-uniform control stage exit flow on the next bladerow. Since the average pressure drop over the downstream stators is similar to the circumferential pressure variation in the control stage exit flow there must be some circumferential flow redistribution, and around half of the stators are seen to operate under severe positive incidence. A similar observation was made for the air turbine validation case (figure 6.7) where the axial pressure gradient over the first blade row caused strong curvature of the inlet jet and a large variation in incidence angle over the first row. This effect was also observed by Lewis [1994a] who performed a series of air turbine tests using admission arrangements of 1x50% and 2x25%. Over the range of velocity ratios considered the two arc arrangement showed an efficiency improvement of around 8% for the four stage turbine, confirming that an increased arc number is favourable in the multistage environment.

The control stage with two arcs of admission presents a significantly more uniform flow to the downstream row and therefore less circumferential redistribution is observed, with reduced incidence onto the downstream stators. It appears then the selection of an appropriate number of arcs is much less critical when the multistage environment is considered: in a practical design situation the number of nozzle chests will normally be determined by mechanical or constructional issues.

Historically control stages appear to have been mainly impulse designs, arranged for nominally zero reaction at the tertiary valve point. Little mention of the effect of stage reaction is made in the literature, although Korematsu et al [1979] note that 50% reaction stages are likely to demonstrate higher efficiency when fully admitted but lower efficiency when partially admitted due to increased leakage flows. Both the calculation with two arcs of admission and the air turbine test case have shown that stage efficiency is strongly influenced by circumferential flow redistribution. It was postulated that increased stage reaction might promote some flow redistribution in the intra-stage gap

between stator and rotor, and reduce the partial admission losses. To test the validity of this assumption a test stage was created with nominally 20% reaction. The aerofoils used have been crudely created and no attempt has been made to design to the same section properties as the low reaction stage - this issue is addressed more fully in chapter 7.

Figure 6.14, overleaf, compares contours of Mach number and entropy for the original impulse stage and the 20% reaction stage at the secondary valve point. Significantly there is a much reduced loss due to pumping and sucking at the arc ends, and the windage losses are also reduced. This is due in part to some divergence of the stator jet into the intra-stage gap at the arc ends, and also because some reduced throughflow persists in the rotor passages which are not within the admitted sector. The 20% reaction design shows an increase in stage efficiency of between 7 and 8 percentage points at each valve point, although it is accepted that several important factors have been omitted from this brief analysis, including the following:

- moderate stage reaction will increase the rotor blade tip leakage flow and could also promote leakage between the nozzle chests into the exhaust space
- stresses in the reaction aerofoils have not been computed and an objective design comparison should be made on the basis of consistent aerofoil stress
- increased reaction will cause some rotor thrust which will ultimately have to reacted by a larger thrust balance piston.

The relative importance of these factors is evaluated in chapter 7, where an optimisation of the control stage configuration is considered using a genetic algorithm.

FIGURE 6.14. Comparison of impulse and moderate reaction stages.

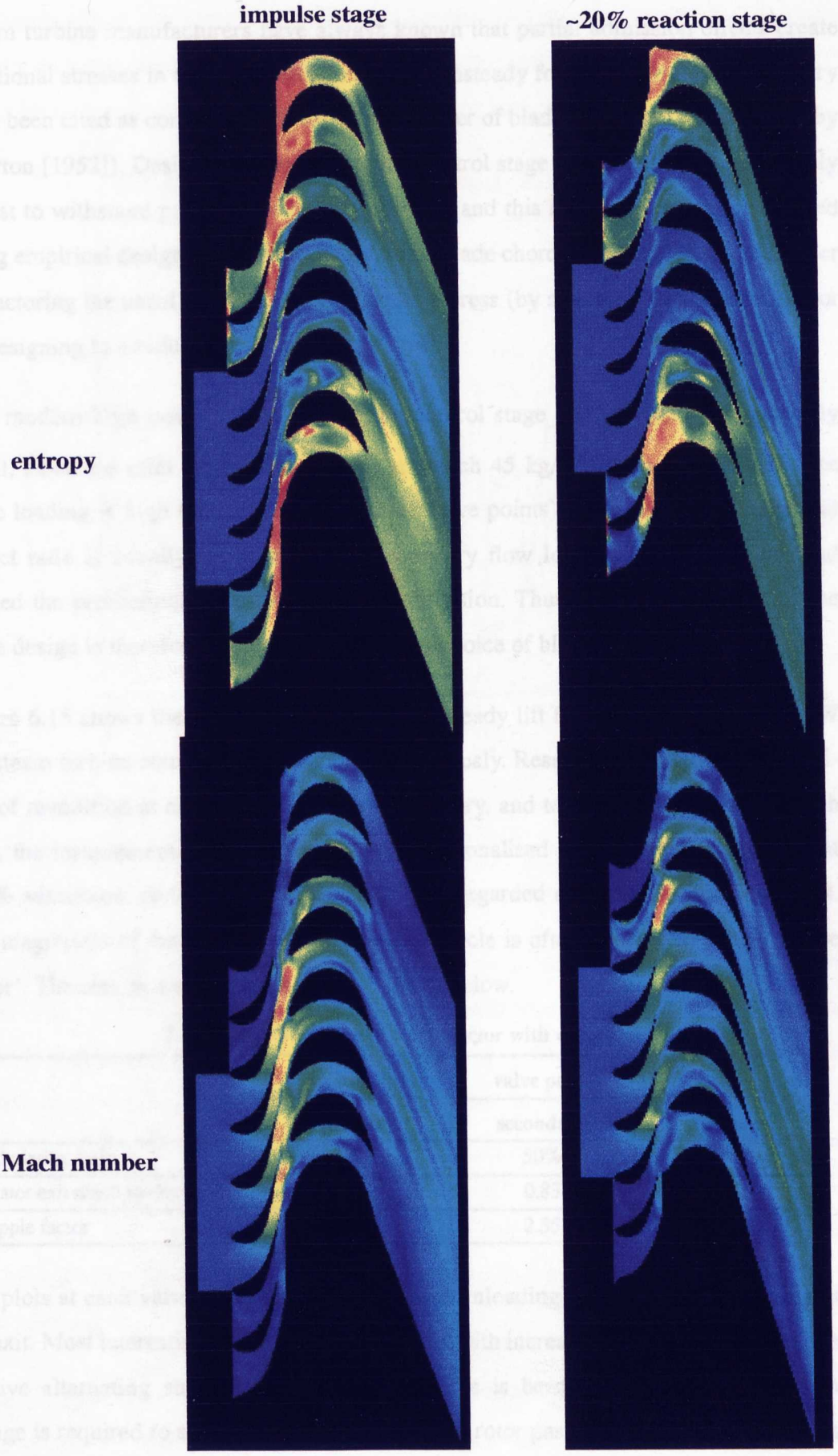

6.2.2 Unsteady forces in a production HP turbine.

Steam turbine manufacturers have always known that partial admission effects create additional stresses in the rotor blade aerofoils. Unsteady forces due to flow asymmetry have been cited as contributory factors in a number of blade (and disk) failures (e.g. by Kearton [1952]). Designers must ensure that control stage components are sufficiently robust to withstand prolonged unsteady loading, and this has been generally achieved using empirical design rules. Historically, rotor blade chord has been determined either by factoring the usual allowable steam bending stress (by a number less than unity), or by designing to a reduced reference stress level.

In a modern high power steam turbine the control stage blade heights are generally small, since the inlet steam density may approach 45 kg/m^3. Additionally, since the stage loading is high (and increases at lower valve points) blade chords are large and aspect ratio is usually less than unity. Secondary flow losses are considerable, and exceed the profile/incidence losses at full admission. Thus the overall success of the stage design is therefore highly sensitive to the choice of blade chord.

Figure 6.15 shows the variation in predicted unsteady lift for the production 250 MW HP steam turbine control stage considered previously. Results are plotted for two periods of revolution at each of the primary, secondary, and tertiary valve points. In each case, the instantaneous lift has been non-dimensionalised by the time-averaged lift at 100% admission, so the plotted quantity can be regarded as a relative bending stress. The magnitude of the non-dimensionalised lift cycle is often referred to as the 'ripple factor'. The results are summarised in table 6.4, below.

TABLE 6.4. Variation of ripple factor with valve point.

	valve point		
	primary	**secondary**	**tertiary**
admission ratio	25%	50%	75%
stator exit mach number	1.30	0.83	0.52
ripple factor	1.90	2.55	3.00

The plots at each valve point show the expected unloading at arc entry and loading at arc exit. Most interestingly, the ripple factor falls with increasing Mach number (i.e. the relative alternating stress cycle is reduced). This is because a smaller momentum change is required to stagnate and re-establish the rotor passage flow when the fluid is

more expanded. Therefore the unsteady proportion of the blade forces is reduced. This is clearly significant as the maximum flow turning (and therefore bending stress) occur at the primary valve point. The optimum blade chord (for a given reference stress) is therefore a function of Mach number as well as steady state loading.

FIGURE 6.15. Variation of unsteady lift with valve point.

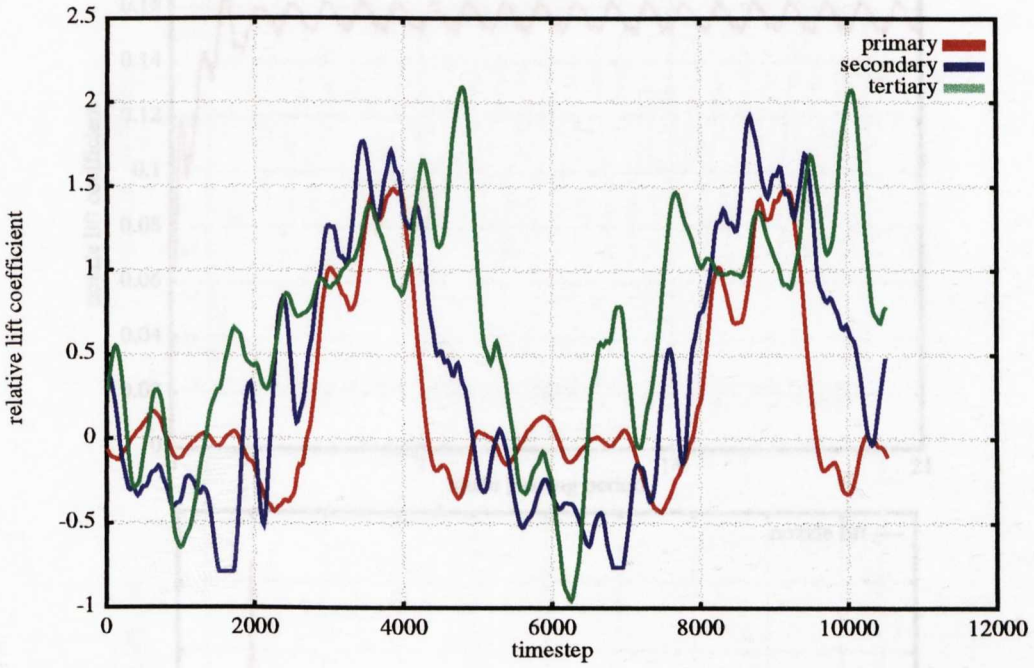

If the ripple factor is to be used in a prediction of the aerofoil fatigue endurance the frequency content of the unsteady loading must be determined. To attempt this a fast Fourier transform (FFT) was implemented using the C++ complex class.

The low reaction control stage at primary valve point was considered at 100% admission. The stator blade alternating lift was computed over 21 blade passing periods, and this is plotted in figure 6.16 overleaf. A periodic variation is achieved after 3 blade passings, and the unsteadiness in this case is due to the moving blade leading edge potential field interacting with the stator trailing edges. This effect is generally very strong in control stages, since the rotor blade pitch is large with respect to the intra-stage axial gap. The spectrum shows that the majority of the interaction occurs as expected at the moving blade passing frequency, but first and second harmonics are also present.

For the examples discussed above the computational domain is approximately one eighth of the complete annulus. This simplification reduces the range of frequencies

that can be captured in the unsteady calculation: if the full annulus is modelled the longest wavelength that could be detected is equal to the full circumference, and a reduced domain will not capture lower frequency interactions.

FIGURE 6.16. Stator blade lift variation and frequency spectrum.

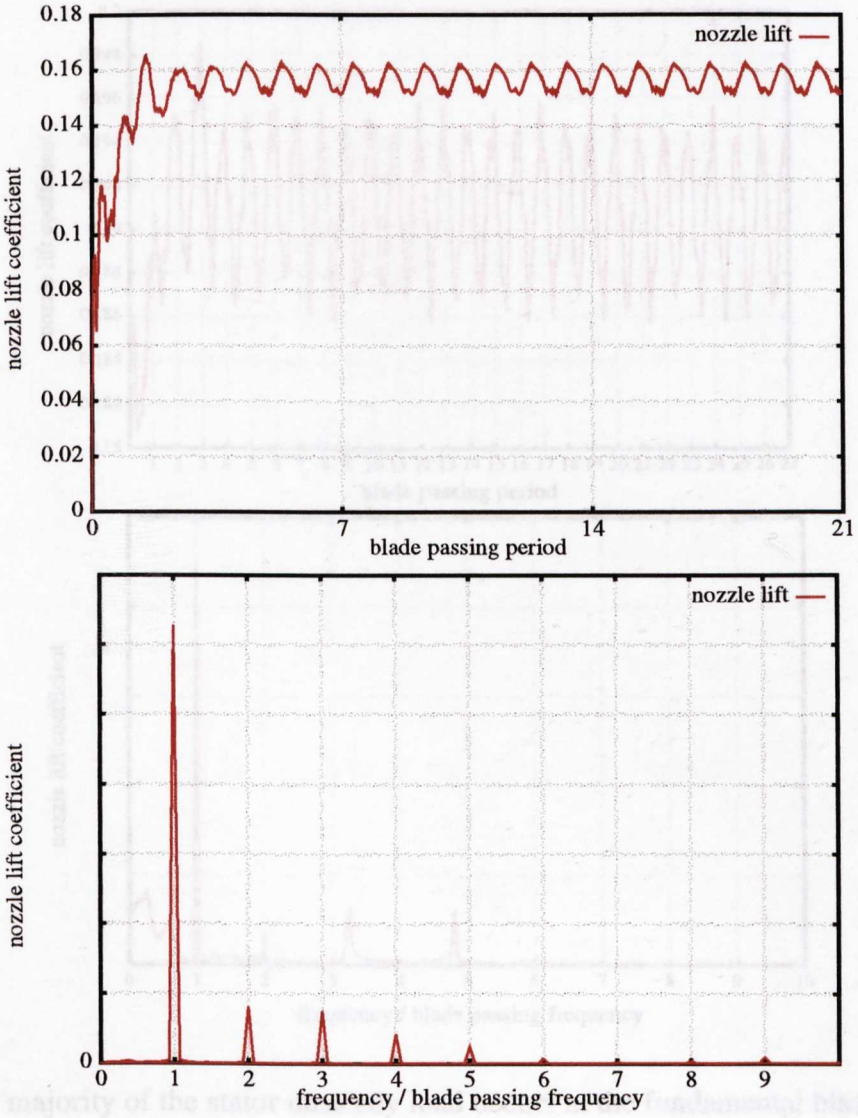

To test this hypothesis the calculation was repeated for a half-annulus domain of 30 stators and 27 rotors. This was the largest calculation possible within 128 Mb of RAM, with a run-time of seventy hours.

FIGURE 6.17. Computational domain for half annulus computation.

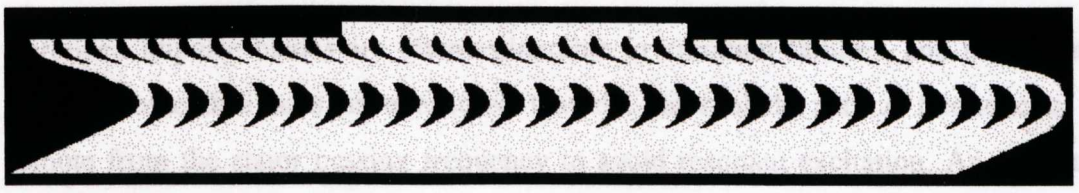

Eleven of the stator passages were admitted with flow, as shown in figure 6.17. The unsteady lift was recorded for the fifteenth stator blade which was located in the centre of the admitted arc.

FIGURE 6.18. Stator lift at primary valve point, 36.7% admission.

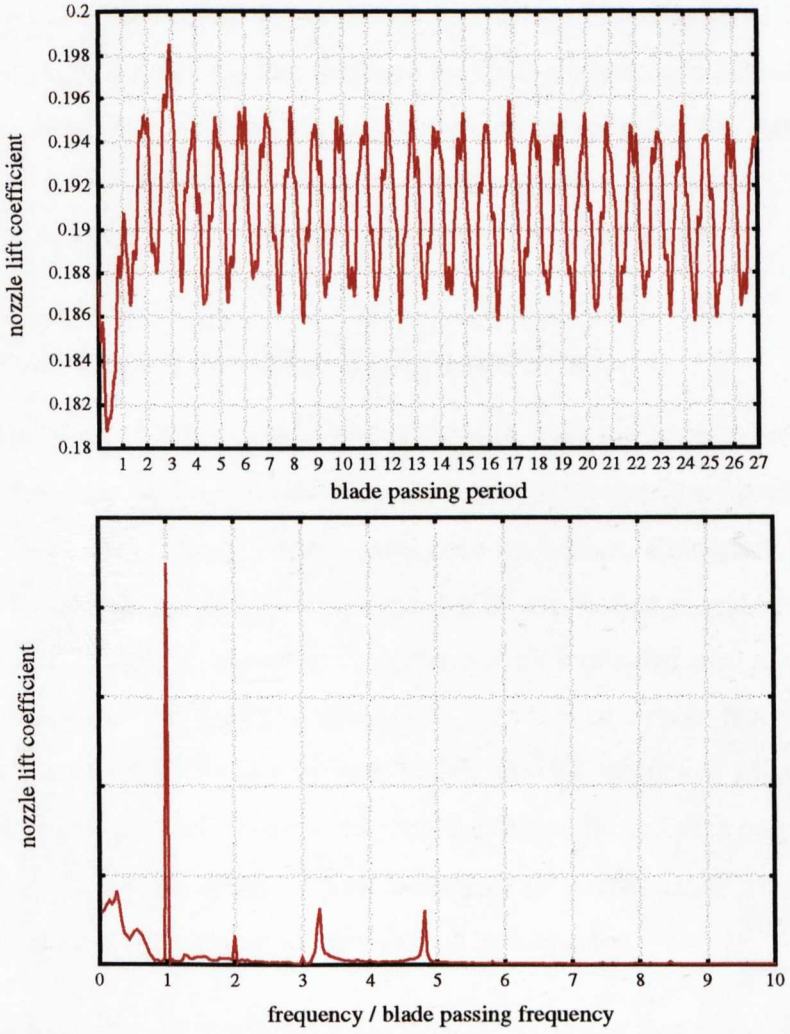

Again the majority of the stator unsteady load occurs at the fundamental blade passing frequency, with smaller responses at the first and second harmonic. There is an additional response between 0.2 and 0.6 times the blade passing frequency. The nozzle passing frequency is 3000 Hz, and the blade passing frequency is 2700 Hz, so it is possible that these low frequency responses are due to interaction (beating) between the blade and nozzle passing frequencies.

Shrouded impulse blades are often vulnerable to vibration failures, and traditionally steam turbine designers have ensured that the rotor blade natural frequencies are remote from the stator passing frequency to avoid resonant excitation. An important

observation from the unsteady CFD calculations is that the stator aerofoil must also endure an alternating loading, but at the blade passing frequency. Unsteady loadings determined from these calculations have now been used within Parsons Power Generation Systems Ltd. for the prediction of both stator and rotor fatigue life.

Chapter Seven

Control Stage Design.
Part 2: Stage Optimisation.

Synopsis. The previous chapter discussed the application of an unsteady CFD code to typical control stage geometries. Results from the CFD analyses and published aerodynamic loss correlations have been used to update an existing control stage meanline design method, which has been integrated within a genetic algorithm. Control stage optimisation is discussed, and a detailed design study is summarised.

7.0 Control stage meanline design method.

The application of the VIB2D code to typical control stage design problems has given some insight into the unsteady flow phenomena. In particular, the losses associated with the 'pumping and sucking' effect have been quantified, alternating forces have been predicted, and the significance of the number of arcs and stage reaction have been discussed. It is not realistic, however, to perform such a detailed analysis during the design timescale of a typical steam turbine project. This of course is a weakness of CFD methods: although CFD can give great insight into the physics of a flow-field considerable effort is required to assemble the data, run the code, and post-process the output. Furthermore, although areas of poor aerodynamic performance may be clearly identified, it is often not obvious how they should be corrected.

A recurrent theme throughout this work has been the assertion that simple methods are likely to be of more use during the design of a steam turbine. If run-times are short many more configurations can be examined during a fixed time scale, and fundamental design issues can be resolved without recourse to more complex methods. For instance, CFD codes might be applied late in the design process to produce new blade profiles, but it would clearly be inefficient to use a multistage CFD code to determine the optimum number of turbine stages.

To enable enhanced control stage designs to be generated, results from the VIB2D analyses were used in conjunction with published loss correlations to update an exist-

ing control stage meanline design method (Levitt [1986]). The modifications are not described in detail here, but are summarised below:

1. The correlations of Dunham and Came [1970] have been used to predict secondary flow losses.

2. Profile loss data reported by Traupel [1958] has been taken as representative of robust low reaction blading, and a correlation related to Ainley and Mathieson [1951] has been implemented to include the effect of incidence.

3. Partial admission losses have been correlated against stage velocity ratio and arc ratio by Levitt [1986], following a detailed review of model air and steam turbine tests performed by Parsons Power Generation Systems Ltd.

4. A leakage loss model has been implemented based on the diagram shown in figure 7.1 below. Three leakage paths are considered:

   - over the rotor blade tip
   - beneath the nozzle chests
   - between the nozzle chests

FIGURE 7.1. Control stage leakage paths.

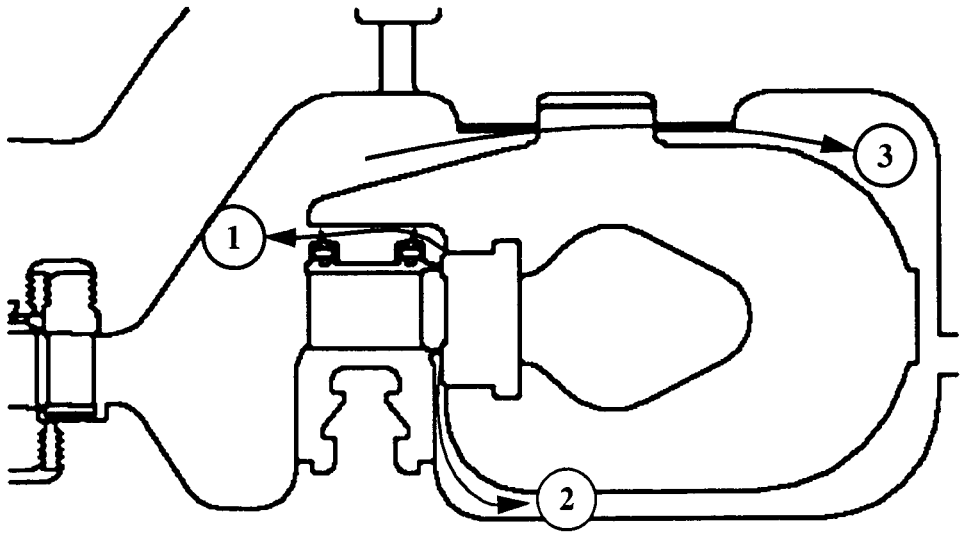

5. A stator arc divergence correlation has been implemented based on the results of the CFD analyses. The degree of divergence of the stator jet in the intrastage gap influences the rotor blade relative inlet flow angle, and this has been correlated against stage axial gap, stage reaction, and the number of stator arc ends.

The modified meanline design method has a run-time of only one or two seconds, and has been shown to predict the efficiency of existing steam turbine control stages with acceptable accuracy.

To investigate improved control stage configurations the meanline design tool was integrated within a genetic algorithm. As with earlier calculations, the *myGENEsys* GA was used, and the calculation was performed with a C shell 'wrapper'. The GA writes an input dataset to file for each candidate design, and runs the meanline design program as part of the fitness function evaluation. The output file is then searched to find the stage efficiencies and aerofoil bending stresses for use in the calculation of solution fitness. Running through the C shell in this manner sacrifices some computational efficiency since there are system overheads associated with reading and writing files, yet these effects are small and compensated for by an increase in portability and robustness.

The control stage optimisation tool has been combined with a graphical user interface (GUI) and run-time output plotting to create a user-friendly design tool. The following sections describe the optimisation procedure and present the results of some preliminary test cases.

7.1 Graphical User Interface (GUI).

In attempt to create 'point and click' functionality a graphical user interface was created using Silicon Graphics ViewKit 1.40 widgets. The interface, shown in figure 7.2, has been designed to resemble a blank 'form'; the appearance is similar to the HTML forms used on the internet for collecting subscription data etc.

Firstly the user enters steam conditions and shaft speed into a series of text fields. These items of data constrain the design space and remain fixed throughout the optimisation. In the present implementation the moving blade mean diameter also remains fixed to correspond with an existing modular product range. In each case the objective of the optimisation is to maximise efficiency without exceeding aerofoil reference stress levels. A number of constraints can be selected using tick-boxes:

1. Use existing range of modular stator and rotor profiles (denoted CN/CB)? If this option is selected aerofoil chords and angles are treated as discrete rather than continuous variables.

2. Include leakage loss? This option includes leakage effects in the calculation of stage efficiency, using a standard set of build clearances.

FIGURE 7.2. Control stage optimiser: Graphical User Interface.

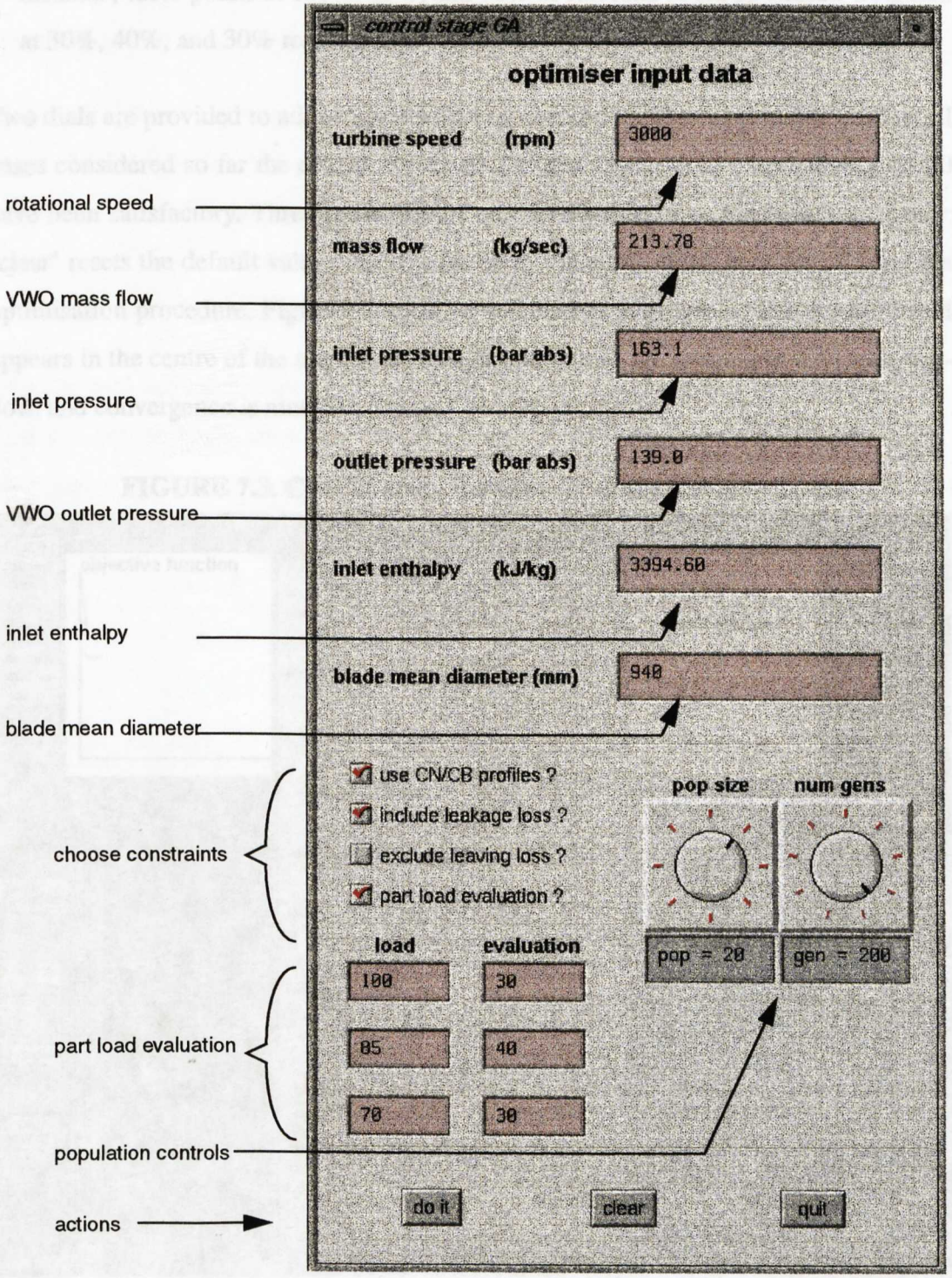

3. Exclude leaving loss? This allows the user to optimise on the basis of total-to-total or total-to-static efficiency.

4. Part load evaluation? If this option is chosen the stage will be optimised on the basis of a weighted efficiency calculated at each valve point. Otherwise the stage will be optimised on the basis of valves wide open efficiency only. The control panel allows the user to specify two valve points each with an associated weighting factor. For instance, valve points at 100%, 85%, and 70% of full load could be chosen weighted at 30%, 40%, and 30% respectively.

Two dials are provided to adjust the population size and number of generations. For all cases considered so far the default values of 200 generations, with a population of 20 have been satisfactory. Three push buttons are provided towards the bottom of panel: 'clear' resets the default values, 'quit' exits from the application, and 'do it' starts the optimisation procedure. Figure 7.3 shows a calculation in progress. The control panel appears in the centre of the screen, the design evaluations are running in the green window, and convergence is monitored in an OpenGL window.

FIGURE 7.3. Control stage optimiser: calculation in progress.

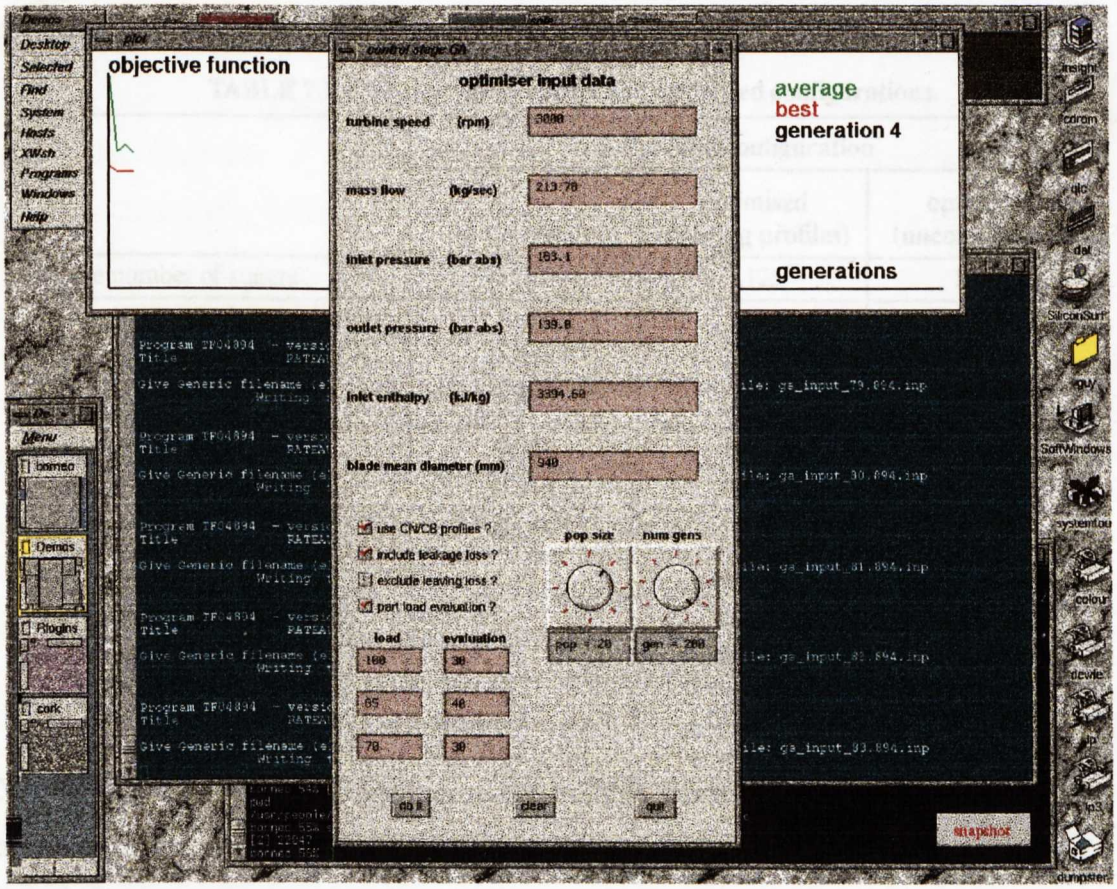

7.2 Control stage optimiser test cases.

A 250 MW HP turbine was considered as a test case for the optimiser. The stage has three valve points at 100%, 80%, and 60% of full load. Two optimisations were performed, firstly using a discrete range of existing blade profiles, and secondly allowing blade angles and chords to vary continuously. In both cases the objective of the optimisation was to maximise the weighted stage efficiency (using factors of 0.3, 0.4, and 0.3 at each valve point), with the addition of a penalty function to constrain the aerofoil stresses to within reference levels.

If the optimisation is performed using a library of existing control stage aerofoil profiles the design problem has five independent variables as follows: stator opening coefficient, stator chord, number of stators, rotor opening coefficient, and rotor chord. If aerofoil geometry is allowed to vary continuously three further variables are used to parametrize the stage: stator pitch, number of rotor blades, and rotor blade inlet angle.

Since the problem has relatively few variables and the objective function has a run-time of only a few seconds, improved blading configurations were identified rapidly, and convergence was observed in typically ten minutes. Table 7.1 below compares a datum stage design with the results of the optimisation.

TABLE 7.1. Comparison of datum and optimised configurations.

	blading configuration		
	datum stage	**optimised (existing profiles)**	**optimised (unconstrained)**
relative number of stators	1.000	1.125	1.375
relative stator opening coefficient	1.000	1.000	0.780
relative rotor opening coefficient	1.000	0.911	0.654
relative stator chord	1.000	1.000	0.916
admission ratio (tertiary)	0.664	0.747	0.837
admission ratio (secondary)	0.399	0.482	0.548
admission ratio (primary)	0.266	0.315	0.365
relative efficiency (tertiary)	-	+0.50%	+4.10%
relative efficiency (secondary)	-	+2.00%	+6.30%
relative efficiency (primary)	-	-0.40%	+2.70%
relative weighted efficiency		+0.83%	+4.56%

Considering firstly the optimisation using existing blade profiles, the optimiser has increased the weighted stage efficiency by 0.83%, primarily by exploiting the trade-off

between secondary loss and partial admission loss. The datum design used the smallest available stator opening coefficient, and efficiency has been increased by adding more stators and increasing the arc ratio at the expense of aspect ratio. Furthermore, a reduction in rotor opening coefficient has elevated the stage reaction by around three points. As the aerofoil stresses must remain beneath prescribed reference levels no reduction in stator chord has been possible, and the weighted efficiency improvement of 0.83% is modest.

A much larger efficiency improvement of 4.56% was observed when the variables were allowed to vary continuously. Again, partial admission losses have been reduced by increasing the arc of admission, but in this example the stator opening coefficient has been reduced and the stator throat area has been achieved without a reduction in aspect ratio. By designing close to the reference stress limit the stator chord has been reduced by a factor of 0.916 yielding a further reduction in aspect ratio and secondary loss. Stage reaction has also been increased by several points at each valve point.

7.3 CFD analysis of optimised control stage configuration.

The control stage optimisation method has indicated that improved stage efficiency can be achieved by exploiting the trade-off between secondary loss and partial admission loss, and also with moderate increases in stage reaction. In the previous chapter it was shown that increases in stage reaction also reduce the partial admission losses by reducing the severity of the pumping and sucking effect at the ends of the admitted arc. Increases in control stage reaction have generally been regarded as impractical (e.g. Korematsu et al [1979]) due to increased leakage losses, although an evaluation of such a design is not thought to have been published.

To investigate the role of moderate stage reaction in more detail a design study was performed using the unsteady CFD code VIB2D. Stator and rotor outlet angles were chosen to match the results of the unconstrained optimisation given in table 7.1, and replacement aerofoils were designed.

Figure 7.4, overleaf, shows the velocity distributions for the datum and moderate reaction stages at the tertiary valve point, calculated with a multistage Euler code (Denton [1992]). The increased reaction reduces the peak stator Mach number from 0.51 to 0.45 and increases the acceleration through the rotor row. The moderate reaction aerofoil

shapes are relatively crude and could be much improved: the intention was only to create typical aerofoil shapes.

FIGURE 7.4. Aerofoil velocity distributions at tertiary valve point.

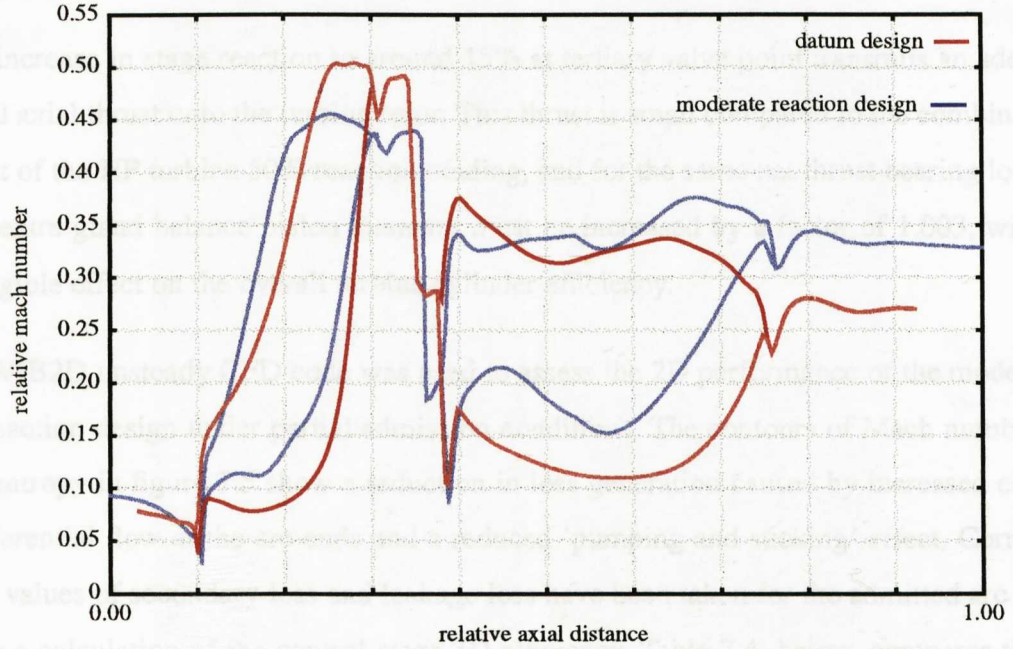

To allow a consistent comparison of the aerofoil stresses the moderate reaction stage has been designed with the same axial chords as the datum stage. Changes in blade stagger have therefore caused slight variation in aerofoil true chord. Table 7.2 compares the blade section properties non-dimensionalised by axial chord, and table 7.3 shows the changes in relative aerofoil bending stress.

TABLE 7.2. Comparison of aerofoil section properties.

	datum stage		moderate reaction	
	stator	**rotor**	**stator**	**rotor**
Area / C_x^2	0.341	0.308	0.439	0.343
Second moment of area I_{ss}/C_x^4 ($x10^2$)	5.368	1.964	6.416	2.732
Second moment of area I_{ww}/C_x^4 ($x10^3$)	4.556	6.407	6.236	6.565

TABLE 7.3. Comparison of relative aerofoil bending stresses.

	datum stage		moderate reaction	
valve point	**stator**	**rotor**	**stator**	**rotor**
tertiary	1.811	1.000	1.803	0.855
secondary	4.347	2.930	4.159	2.336
primary	7.142	4.701	6.925	3.827

The aerofoil bending stresses are expressed as maximum 2D section stresses non-dimensionalised by the datum stage rotor bending stress at the tertiary valve point. At the primary valve point, where the stage loading is highest, the stator and rotor stresses have been reduced by 3.0% and 18.6% respectively.

The increase in stage reaction to around 15% at tertiary valve point transmits an additional axial thrust onto the turbine rotor. This thrust is small compared to the combined thrust of the HP turbine 50% reaction blading, and for the same net thrust bearing load the centre gland balance piston diameter must be increased by a factor of 1.003, with negligible effect on the overall turbine cylinder efficiency.

The VIB2D unsteady CFD code was used to assess the 2D performance of the moderate reaction design under partial admission conditions. The contours of Mach number and entropy in figure 7.5 show a reduction in loss generation caused by increased circumferential flow at the arc ends and a reduced 'pumping and sucking' effect. Correlated values of secondary loss and leakage loss have been taken for the admitted arc to allow a calculation of the control stage 3D efficiency. Table 7.4, below, compares the control stage efficiency for the datum and moderate reaction designs at each of the three valve points, and expresses the improvements as changes in HP cylinder efficiency and an overall reduction in weighted heat-rate.

TABLE 7.4. Effect of control stage redesign on turbine heat-rate.

	tertiary valve point		**secondary valve point**		**primary valve point**	
	datum	**moderate reaction**	**datum**	**moderate reaction**	**datum**	**moderate reaction**
VIB2D efficiency	75.04	78.75	64.08	68.01	49.46	54.20
secondary loss	8.13	6.55	9.15	5.19	6.32	3.97
leakage loss	1.53	2.98	1.79	3.44	1.88	1.92
corrected stage efficiency	65.38	69.22	53.14	59.38	41.26	48.31
Δ HP cylinder efficiency (points)	+0.389		+1.483		+3.276	
Δ heat rate	-0.068		-0.261		-0.577	
heat rate weighting	0.30		0.40		0.30	
weighted Δ heat rate (%)	-0.288					

FIGURE 7.5. Entropy and Mach number contours at secondary valve point

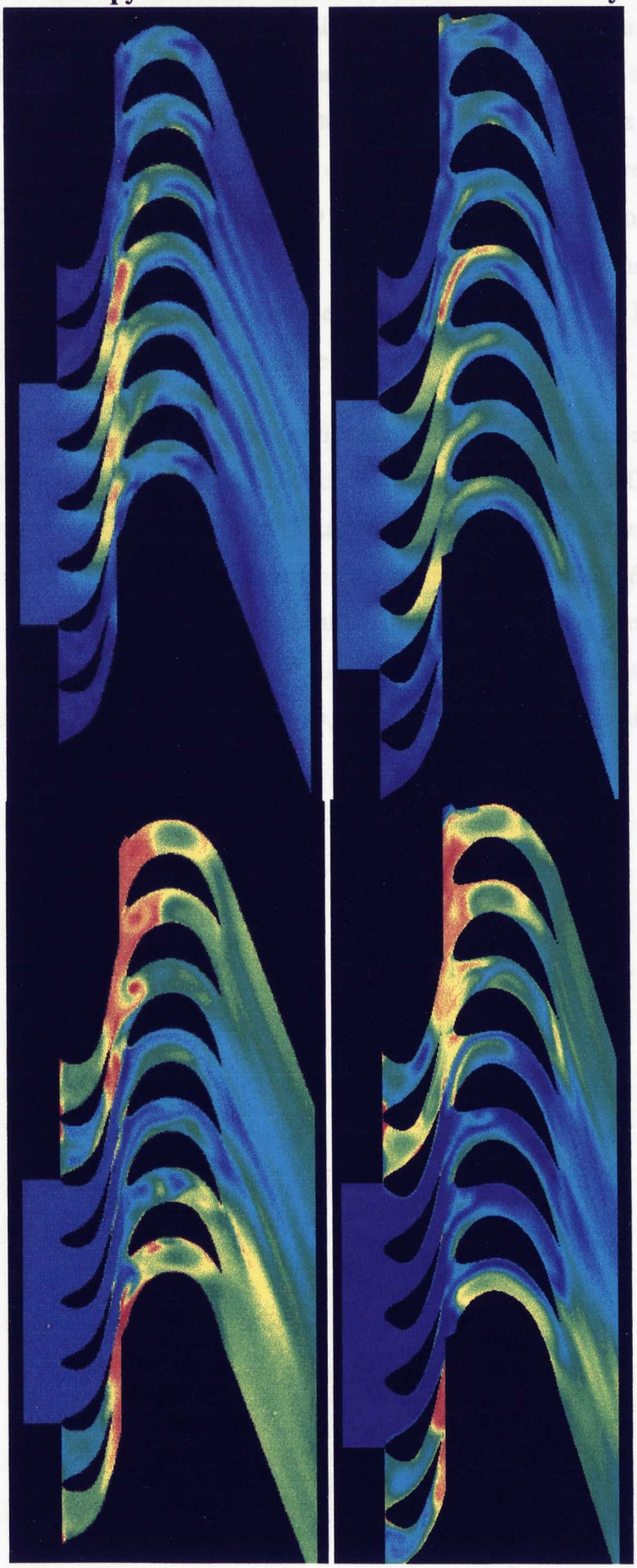

The VIB2D calculation shows that the moderate reaction design has an improved 2D efficiency of approximately 4 percentage points at each valve point. This difference includes the effects of partial admission loss and 2D aerofoil efficiency. Stage secondary losses have been calculated for the admitted arc using the correlations of Dunham and Came, and stage leakage loss has been evaluated. These losses were subtracted from the VIB2D efficiency to give a stage 3D efficiency. Whilst this approach is intuitive, it is acknowledged that in reality there will interactions between the secondary loss and partial admission loss mechanisms, and the assumption that the loss components are additive must be regarded with some suspicion.

Changes in HP turbine efficiency have been calculated, and a reduction in overall weighted heat-rate has been predicted based on weighting factors of 0.3, 0.4, and 0.3. A reduction in weighted heat-rate of 0.288% is predicted, which represents a considerable improvement in the cost-effectiveness of the entire machine. Significantly, this improvement is obtained by iterative application of a simple design method, at the same overall level of turbine technology. The improvements must be offset against the cost of developing new control stage aerofoils, but in practical cases this effect will be small.

Chapter Eight

Conclusions and Suggestions for Future Work.

8.1 Conclusions.

The primary objective of this period of research work has been to investigate the possible application of various optimising methods to the steam turbine design process. Attention has been focused on the meanline and throughflow definitions of the turbine bladepath, although the methodology discussed could have equal application to a much broader spectrum of turbomachinery design problems.

A sequential approach to the bladepath optimisation task has been adopted. If an approach of 'maximum rigour' were to be adopted the designer would attempt to model the turbine in as much detail as possible and analyse each design configuration with the most sophisticated methods available. Clearly such a 'global' optimisation could perform very well if the design lead-time is unlimited, but in all practical (i.e. manufacturing) scenarios time is severely restricted. Given a limited timescale the intuitive (and efficient) approach is to use the most basic representative model of the bladepath, and perform many iterations of simple design codes. In this way fundamental design features (such as the number of stages) can be established extremely quickly before more detailed analyses are performed.

Firstly a rule-based numerical optimisation framework was developed to perform a meanline design optimisation. The optimisation was based around an existing and fully validated meanline design code. Simple rules were employed to start the design search, and numerical optimisation was used to seek areas of good performance. Unlike other published methods the meanline search tool is fully sensitized to life-cycle cost, and allows the design space topology to be plotted as a financial evaluation. Rather than produce a single optimised configuration the software produces a gallery of 'legal' turbine bladepaths from which the designer can select a preferred design. This added transparency is essential if users are to have confidence in an optimisation procedure: they must be able to see what has been done.

The meanline design method was extended with the use of a genetic algorithm (GA). This heuristic technique allowed the meanline design space to be explored in more detail by varying the shape of the annulus boundaries. This produced a subset of optimised bladepath configurations derived from the optimum solutions identified by the meanline search tool.

Optimisation of the throughflow configuration was also attempted using a genetic algorithm. The objective of these calculations was to maximise turbine efficiency by varying aerofoil inlet and outlet angles along the span of an arbitrary number of bladerows. Such adjustments to the vortex design could be constrained by penalty functions, for instance to control changes in streamline curvature. This approach was extended to include a multi-objective optimisation of the throughflow design. A number of key design features were identified following a survey of a number of design engineers, and these were incorporated within a fuzzy logic fitness function. The purpose of this was to encapsulate engineering knowledge and rules-of-thumb to control the trade-offs between conflicting design requirements within the GA fitness evaluation. A blind 'taste test' showed that solutions optimised in this way were preferred by design engineers. A number of measures to reduce calculation run-times were implemented, including blade-row cloning, optimisation of program control parameters, and variable GA population size.

If an optimisation procedure relies on simple analysis methods containing correlated loss models the ultimate quality of the results is governed by the accuracy of the correlations. There is an inescapable contention in this approach: we must use correlated data to economically perform the optimisation, but if we have blind faith in the correlations the search may be misled. It is therefore crucial to re-assess the validity of correlated data each time a step-change in blading technology is made. In some areas, notably control stage partial admission, there is very little published data and it is therefore difficult to develop a representative meanline design method. A novel approach to this problem has been to apply an unsteady CFD solver to a variety of control stage problems, and use the results to develop new correlations as required. The integration of the new design method within a GA has yielded significant performance improvements, the consistency of which have been verified with a further application of the unsteady CFD code.

During the planning phase of the project it was speculated that the application of formal optimising strategies could confer three significant business advantages to a turbine manufacturer. In order of increasing importance, they were:

1. Integrating existing analysis methods within an optimising framework automates the design process and reduces the labour associated with manually creating datasets and processing output.
2. The automated approach can significantly reduce design lead-times, and since the software runs unattended the designer is free to perform other duties.
3. A systematic and more exhaustive search of the design space will often identify design configurations with improved evaluation.

It is felt that the software tools developed within this research are capable of conferring each of these advantages. The application of these methods to a relatively large number of ongoing design problems has shown that they can identify significant performance improvements, generally much more quickly than an experienced design engineer. A number of bladepaths wholly or partly designed with these methods are now committed for manufacture, and early test results from an LP turbine suggest that performance gains are already being achieved.

It is significant that all of the reported improvements in turbine evaluation have been achieved at the same level of turbine technology. Thus the improvements are free of cost in the sense that no further development or experimental work is necessary to implement them: there is only the expense of designing blade profiles if required, and preparing engineering drawings.

The 1990's has been a period of considerable development in the field of turbomachinery, and increasingly sophisticated analytical and experimental techniques are now yielding greater insight into complex phenomena such as secondary flow control, transition, fluid-structure interaction, and heat transfer. Many researchers throughout the world are to be applauded for their exciting contributions to this fascinating field. The key challenge for design engineers is to incorporate these new technologies within their products, and procedures for design optimisation can play an important part in the exploitation of new design features.

8.2 Suggestions for further work.

1. **Parallelisation**. All of the optimisation work described has been performed on single processor machines, although parallel processing was used for much of the CFD analysis. Both the rule-based and heuristic optimisation procedures are essentially design by repeated evaluation. Such problems are amenable to parallelised solution; for instance in the optimisation of a throughflow design the population could be evaluated simultaneously over a number of processors. Subramani [1995] showed that if the fitness function evaluation was relatively lengthy (i.e. minutes) the optimisation could be performed by farming out the evaluations to a network of workstations. This approach clearly has much potential in a manufacturing organisation, where there may be many CAD workstations etc. which are unused outside working hours.

2. **Blade section design**. The throughflow optimisation procedure produces new runs of blade angles and in some cases the design of new blade sections is necessary. It is often difficult to determine a radial distribution of blade sections that can be stacked to form a robust aerofoil with satisfactory vibration characteristics. Trigg et al [1997] have applied a GA to 2D blade section design using the Dawes [1992] code, and also report difficulty in determining an appropriate stack. The application of an optimising method to a coupled throughflow, mechanical, and blade-to-blade calculation would allow the vortex distribution and aerofoil stack to be evolved simultaneously, although this is approach is likely to be impractical with current workstations.

3. **3D control stage analysis**. The control stage CFD analyses have been performed with a 2D method and secondary flow losses were not predicted. Additionally the windage effects in areas of low throughflow are likely to be predominantly three-dimensional. A fully 3D control stage analysis would allow a more realistic prediction of control stage loss to be performed, and could also suggest potential performance improvement strategies (e.g. circumferential variations in stator blade outlet height).There is also a need to optimise the control stage geometry in conjunction with the wheelcase transition and downstream stage.

References

Ainley, D. G., and Mathieson, G. C. R., 1951, 'A Method of Performance Estimation for Axial-Flow Turbines', Aeronautical Research Council, Reports and Memoranda, 2974.

Baeck, T., 1992, 'A User's Guide to GENEsYs 1.0", University of Dortmund, Department of Computer Science.

Baines, N. C., and Japikse, D., 1994, 'Introduction to Turbomachinery', Oxford University Press.

Balje, O. E., and Binsley, R. L., 1968, 'Axial Turbine Performance Evaluation. Part A: Loss-Geometry Relationships', ASME Journal of Engineering for Power, Vol. 90, pp 341-348.

Balje, O. E., and Binsley, R. L., 1968, 'Axial Turbine Performance Evaluation. Part B: Optimisation With and Without Constraints', ASME Journal of Engineering for Power, Vol. 90, pp 349-360.

Bezdek, J. C., 1993, 'Fuzzy Models. What Are They and Why?', IEEE Transactions on Fuzzy Systems, Vol. 1, pp 1-6.

Birmingham, R., Cleland, G., Driver, R., and Maffin, M., 1997, 'Understanding Engineering Design', Prentice Hall.

Bolter, J. R., and Grant, J., 1990, 'A Unified Range of Steam Turbines', I.Mech.E. paper C386/039.

Boulbin, F., Penneron, N., Kermarec, J., Pluviose, M., 1992, 'Turbine Blade Forces due to Partial Admission', Revue Française de Méchanique 1992-1993, pp 203-208.

Cleland, G., 1994, 'A Generic Approach to Spatial Engineering Incorporating Knowledge-Based Systems', PhD Thesis, University of Newcastle upon Tyne.

Cofer IV, J. L., 'Advances in Steam Path Technology', ASME Journal of Engineering for Gas Turbines and Power, Vol. 118, pp 337-352.

Cohen, H., Rogers, G. F. C., and Saravanamuttoo, H. I. H, 1972, 'Gas Turbine Theory', second edition, Longman.

Craig, H. R. M., and Cox, H. J. A., 1971, 'Performance Estimation of Axial Flow Turbines', proceeding of I.Mech.E., Vol. 185, pp 407-424.

Cravero, C., and Dawes, W. N., 1997, 'Throughflow Design Using an Automatic Throughflow Optimisation Strategy', ASME paper 97-GT-294.

Davis, W., and Millar, D., 1976, 'Throughflow Calculation Based on Matrix Inversion', AGARD CP-195.

Dawes, W. N., 1992, 'Towards Improved Throughflow Capability: The Use of Three Dimensional Viscous Flow Solvers in a Multistage Environment', ASME Journal of Turbomachinery, Vol. 114, pp 8-17.

Denton, J. D., 1975, 'A Time-Marching Method for Two and Three Dimensional Blade to Blade Flow', Aeronautical Research Council, Reports and Memoranda, 3775.

Denton, J. D., 1976, 'A Survey and Comparison of Methods of Predicting the Profile Loss of Turbine Blades', I.Mech.E. paper C76/73.

Denton, J. D., 1978, 'Throughflow Calculations for Transonic Axial Flow Turbines', ASME Journal of Engineering for Power, Vol. 100, pp 212-218.

Denton, J. D., 1992, 'The Calculation of Three-Dimensional Viscous Flow Through Multistage Turbomachines', ASME Journal of Turbomachinery, Vol. 114, pp 18-26.

Denton, J. D., 1993, 'Loss Mechanisms in Turbomachines', 1993 IGTI Scholar Lecture, ASME Journal of Turbomachinery, Vol. 115, pp 621-656.

Denton, J. D., Wallis, A. M., Borthwick, D., Grant, J., and Ritchey, I., 1996, 'The Three-dimensional Design of Low Aspect Ratio 50% Reaction Turbines', I.Mech.E. paper S461/008/96.

Dixon, S. L., 1978, 'Fluid Mechanics and Thermodynamics of Turbomachinery', Pergamon.

Dollin, F., and Brown, W. S., 1937, 'The Flow of Fluids Through Opening in Series', The Engineer, August 27 1937, pp 223 et seq.

Dollin, F.,1963, 'Some Design Problems Arising in the Development of Very Large High-speed Turbines', Proc. Institution of Mechanical Engineers, 1963, Vol. 177, no. 9, pp221-267.

Dorman, T. E., Welna, H., and Lindlauf, R. W., 1968, 'The Application of Controlled-Vortex Blading to Advanced Axial Flow Turbines', ASME Journal of Engineering for Power, Vol. 90, pp 245-250.

Dunham, J., and Came, P. M., 1970, 'Improvements to the Ainley-Mathieson Method of Turbine Performance Prediction', ASME Journal of Engineering for Power, 1970, pp 252-256.

Electrical Research Association, 1967, '1967 Steam Tables', Edward Arnold, London.

Ertas, A., and Jones, J. C., 1996, 'The Engineering Design Process', John Wiley and Sons.

Fogel, L. J., 1966, 'Artificial Intelligence through Simulated Evolution', Wiley.

Galatsan, V. N., Gol'man, V. I., Zarubin, L. A., and Relikh, B. H., 1985, 'An Investi-

gation of The Governing Stage of a Turbine Together with the Following Fixed Blade Row', Teploenergetika, Vol. 32, pp 61-63.

Garey, M. R., and Johnson, D. S., 1979, 'Computers and Intractability. A Guide to the Theory of NP-Completeness', Freeman.

Goldberg, D. E., 1989, 'Sizing Populations for Serial and Parallel Genetic Algorithms', Proceedings of 3rd International Conference on Genetic Algorithms, George Mason University, USA, June 4-7 1989.

Grant, J., Wood, N. B., Walters, P. T., 1991, 'Design and Site Test Evaluation of Some Blading Retrofit Packages for Improving the Efficiency of Low Pressure Turbines in UK Power Stations', I.Mech.E. conference paper C423/63.

Greffenstette, J. J., 1986, 'Optimisation of Control Parameters for Genetic Algorithms', IEEE Transactions, Systems and Cybernetics, Vol. 16, pp 122-128.

Hart, M. and Whitehead, D. S., 1987, 'A Design Method for Two-Dimensional Cascades of Turbomachinery Blades', International Journal of Numerical Methods in Fluids, Vol. 7, pp 1363-1381.

Hart, M., Hall, D. M., and Singh, G., 1991, 'Computational Methods for the Development of Large Steam Turbines', I.Mech.E. paper C423/009.

He, L., 1994a, "Integration of 2D flow-structure coupled system for calculation of turbomachinery aerodynamic / aeroelastic instabilities". International Journal of Computational Fluid Dynamics, Vol. 3, pp. 217-231.

He, L., 1994b, "Rotating stall / stall-flutter predictions using a fluid / structure coupled method", 7th International Symposium on Unsteady Aerodynamics, Fukouka, Japan.

Holland, J. H., 1976. 'Adaptation in Natural and Artificial Systems', University of Michigan Press.

Horlock, J. H., 1966, 'Axial Flow Turbines', Butterworth, London.

Horlock, J. H., 1978, 'Actuator Disk Theory. Discontinuities in thermo-fluid dynamics', McGraw-Hill.

Horlock, J. H., 1987, 'Cogeneration: Combined Heat and Power. Thermodynamics and Economics', Pergamon.

Horowitz, E., 1984, 'Fundamentals of Computer Algorithms', Computer Science Press.

Jenkins, R. M., 1991, 'A Direct Optimisation Procedure for Spanwise Work Distribution in Non-free Vortex Turbine Stages', ASME paper 91-GT-204.

Kacker, S. C., and Okapuu, U., 1982, 'A Mean Line Prediction Method for Axial flow Turbine Efficiency', ASME Journal of Engineering for Power, Vol.104, pp 111-119.

Kalderon, D., 1979, 'Design Aspects of Large Steam Turbines for Worldwide Application in Fossil and Nuclear Power Stations', I.Mech.E. paper C197/79.

Keane, A. J., 1996, 'Experiences with Optimizers' I.Mech.E. Seminar Genetic Algorithms in Design Optimisation, 1996.

Kearton, W. J., 1951, 'Steam Turbine Theory and Practice', 6th edition, Pitman.

Kearton, W. J., 1952, 'Steam Turbine Operation', 6th edition, Pitman, chap 9.

Kirkpatrick, S., Gellat, C. D., and Vecchi, M. P., 1983, 'Optimization by Simulated Annealing', Science, Vol. 220, pp 671-680.

Kobayashi, K., Honjo, M., Tashiro, H., and Nagayama, T., 1991, "Verification of flow pattern for three-dimensional-designed blades", I.Mech.E paper C423/015

Koch, C. C., 1981, 'Stalling Pressure Rise Capability of Axial Flow Compressor Stages', ASME Journal of Engineering for Power, Vol. 103, pp 645-656.

Korematsu, K., and Hirayama, N., 1979, 'Performance Estimation of Partial Admission Turbines', ASME conference paper 79-GT-123.

Koza, J.R, 1993, 'Genetic Programming', MIT Press.

Kroon, R. P., 1940, 'Turbine Blade Vibration due to Partial Admission', ASME Journal of Applied Mechanics, pp A161-A165.

Levitt, A., 1986, 'Rateau Control Stage Analysis using Soderberg's Correlation', NEI Parsons Engineering Memorandum 86.339.138.

Lewis, K. L., 1993, 'The Aerodynamics of Shrouded Multistage Turbines', PhD Thesis, University of Cambridge.

Lewis, K. L., 1994a, "The Influence of Partial Admission on the Performance of a Multistage Turbine", Whittle Laboratory internal report, University of Cambridge, UK.

Lewis, K. L., 1994b, "Spanwise Transport in Axial-flow Turbines: part1 - the Multistage Environment", ASME Journal of Turbomachinery, Vol. 116, pp. 179-186.

Lewis, R. I., 1997, 'Turbomachinery Performance Analysis', Arnold.

Macchi, E., and Perdichizzi, A., 1981, 'Efficiency Prediction for Axial-Flow Turbines Operating with Nonconventional Fluids', ASME Journal of Engineering for Power, Vol. 103, pp 718-724.

Marsh, H., 1968, 'A Digital Computer Program for the Through Flow Fluid Mechanics in an Arbitrary Turbomachine, using a Matrix Method', Aeronautical Research Council, Reports and Memoranda, 3509.

Massardo, A., and Satta, A., 1990a, 'Industrial Design Optimization of Small and Large Size Axial Turbines', ASME Paper 90-GT-220.

Massardo, A., and Satta, A., 1990b, 'Axial Flow Compressor Design Optimization: Part I - Pitchline Analysis and Multivariable Objective Function Influence', ASME Journal of Turbomachinery, Vol. 112, pp 399-404.

Massardo, A., Satta, A., and Marini, M., 1990c, 'Axial Flow Compressor Design Optimisation: Part II - Throughflow Analysis', ASME Journal of Turbomachinery, Vol. 112, pp 405-410.

Mitchell, J. M., 1979, 'Design of Large Reheat Steam Turbines for U.K. and Overseas Markets', I.Mech.E. paper C184/79.

Oeynhausen, H., Drozdiok, A., and Deckers, M., 1997, 'Advanced Steam Turbines for Modern Power Plants', I.Mech.E. paper C522/032/97.

Ohlsson, G. O., 1962, 'Partial-Admission Turbines', Journal of the Aerospace Sciences, Vol. 29, pp 1017-1028.

Optlaka, G., 1972, 'Economic Problems in the Design of Steam Power Stations', Brown Boveri Review, 1972, pp 36-41.

Pahl, G., and Beitz, W., 1988, 'Engineering Design: a Systematic Approach', The Design Council.

Parsons, Sir C. A., 1900, 'Motive Power - High Speed Navigation - Steam Turbines', address to the Royal Institution, 26 January 1900.

Parsons, Sir C. A., 1911a, 'The Steam Turbine', 1911 Rede Lecture, University of Cambridge, Cambridge University Press.

Parsons, Sir C. A., 1911b, 'The Marine Steam Turbine from 1894 to 1910', Institution of Naval Architects, Jubilee Meetings, 5 July 1911.

Parsons, Sir C. A., 1924, 'Steam Turbines', proc. The World Power Conference at the British Empire Exhibition, Wembley.

Pearce, R., and Cowley, P. H., 1995, 'Use of Fuzzy Logic to Overcome Constraint Problems in Genetic Algorithms', Genetic Algorithms in Engineering Systems: Innovations and Applications (GALESIA) Conference, University of Sheffield, September 1995.

Pigott, R., 1980, 'Turbine Blade Vibration due to Partial Admission', International Journal of Mechanical Science, Vol. 22, pp 247-267.

Pochabradsky, B., 1947, 'Effect of Centrifugal Force in Axial-Flow Turbines', Engineering, March 1947, pp 205-207.

Potts, I., 1987, 'The Importance of S-1 Stream Surface Twist in the Analysis of Inviscid Flow through Swept Linear Turbine Cascades', I.Mech.E paper C258/87.

Rao, S. S., and Gupta, R. S., 1980, 'Optimum Design of Axial Flow Gas Turbine Stage. Part 1: Formulation and Analysis of Optimisation Problem', ASME Journal of Engineering for Power, Vol. 102, pp 782-789.

Rao, S. S., and Gupta, R. S., 1980, 'Optimum Design of Axial Flow Gas Turbine Stage. Part 1: Solution of the Optimisation Problem and Numerical Results', ASME Journal of Engineering for Power, Vol. 102, pp 790-797.

Rayleigh, Lord, 1933, 'Some Personal Reminiscences of Sir Charles Parsons', from the introduction to 'Scientific Papers and Addresses of the Hon. Sir Charles A. Parsons', Cambridge University Press.

Richardson, A, 1911, 'The Evolution of the Parsons Steam Turbine', Engineering, London.

Roelke, R. J., 1973, 'Turbine Design and Application', NASA SP-290, A. J. Glassman ed., Vol. 2, chap. 8.

Ryzkov, V. K., 1979, 'Steam Turbine Building at the 'Leningradsky Metallichesky Zavod' Association', I.Mech.E. paper C201/79.

Schlegel, J. C., Liu, H. C., Waterman, W. F., 1976, 'Reduction of End-Wall Effects in a Small, Low-Aspect-Ratio Turbine by Radial Work Redistribution', ASME Journal of Engineering for Power, Vol. 98, pp 130-136.

Schnecke, V., and Vornberger, O., 1996, 'A Genetic Algorithm for VLSI Physical Design Automation', proceedings of ACEDC 1996, University of Plymouth.

Shigley, J. E., and Mischke, C. R., 1989, 'Mechanical Engineering Design', McGraw-Hill International.

Singh, G., Walker, P. J., and Haller, B. R., 1995, 'Development of Three-dimensionsal Time-marching Method for Optimisation of Short Height Stages', European Conference on Turbomachinery - Fluid Dynamics and Thermodynamic Aspects, Erlangen, March 1995.

Smith, A, 1970, 'Survey of Twisted Blading Development in Steam Turbines', proceedings of the I.Mech.E, Vol. 184, pp 449-474.

Smith, S. F., 1965, 'A Simple Correlation of Turbine Efficiency', Journal of the Royal Aeronautical Society, Vol. 69, pp 467-470.

Subramani, D., 1994, 'Structural Layout of myGENEsys', University of Newcastle upon Tyne Engineering Design Centre internal note.

Subramani, D., 1995, 'Ship Design for Safety and Survivability', PhD Thesis, University of Newcastle upon Tyne.

Tong, S. S., and Gregory, B. A., 1992, 'Turbine preliminary Design Using Artificial Intelligence and Numerical Optimisation Techniques', ASME Journal of Turbomachinery, Vol. 114, pp1-7.

Traupel, W., 1958, 'Thermische Turbomaschinen', Springer-Verlag, Berlin, PAMET-RADA translation 20.

Trigg, M. A., Tubby, G. R., and Sheard, A. G., 1997, 'Automatic Genetic Optimization Approach to 2D Blade Profile Design for Steam Turbines', ASME conference paper 97-GT-392.

Wakeley, G. R., and Grant, J., 'The Application of Formal Optimising Methods to the Design of Steam Turbine Reaction Bladepaths', I.Mech.E. paper S461/009/96.

Wakeley, G. R., 1997, 'Retrofit Steam Turbine Bladepaths for Performance Improvement and Life Extension', Conference Paper, C.E.A. 1997.

Whittle, Sir F., 1953, 'Jet - The Story of a Pioneer', Muller, 1953.

Wilkinson, D. H., 1970, 'Stability, Convergence, and Accuracy of Two-dimensional Streamline Curvature Methods Using Quasi Orthogonals', I.Mech.E. Fluid Dynamics paper 34.

Wu, C. H., 1952, 'Matrix and Relaxation Solutions that Determine Subsonic Flow through an Axial Gas Turbine', NACA note 2750.

Zadeh, L. A., 1965, 'Fuzzy Sets', Journal of Information and Control, Vol. 8, pp 338-353.

Zwiefel, O., 1945, 'the Spacing of Turbo-Machine Blading, Especially with Large Angular Deflection', Brown Boveri Review, 1945, pp 436-444.